BİLİMSEL MADENCİLİK DERGİSİ
SCIENTIFIC MINING JOURNAL

TMMOB Maden Mühendisleri Odası Yayını / The Publication of the Chamber of Mining Engineers of Turkey

ISSN 2564-7024
e-ISSN 2587-2613
Cilt / *Vol:* 61
Sayı / *No:* 1
Mart / *March*
2022

TMMOB MADEN MÜHENDİSLERİ ODASI
UCTEA CHAMBER OF MINING ENGINEERS

BİLİMSEL MADENCİLİK DERGİSİ
Scientific Mining Journal

Cilt / Vol: 61, Sayı / No: 1, Mart / March, *2022*

TMMOB Maden Mühendisleri Odası'nın hakemli dergisidir.
A peer-reviewed quarterly journal of the Chamber of Mining Engineers of Turkey

Baş Editör / *Editor-in-Chief*
Dr. Nejat Tamzok, Türkiye Kömür İşletmeleri / *Turkish Coal Enterprises*

Editörler / *Editors*
Dr. Bülent Toka, Maden Tetkik ve Arama Genel Müdürlüğü */ General Directorate of Mineral Research and Exploration*
Dr. İlkay Bengü Can, Hacettepe Üniversitesi */ Hacettepe University*
Dr. Ümit Özer, İstanbul Üniversitesi - Cerrahpaşa / *Istanbul University - Cerrahpaşa*
Dr. Mehtap Gülsün Kılıç, Nadir Toprak Elementleri Araştırma Enstitüsü/ *Rare Earth Elements Research Institute*

Editör Yardımcıları */ Editor Assistants*
Dr. Emre Yılmazkaya, Hacettepe Üniversitesi */ Hacettepe University*
Dr. Ece Kundak, Eskişehir Osmangazi Üniversitesi */ Eskişehir Osmangazi University*

Dizgi-Tasarım Editörü / *Layout-Design Editör*
Sena Naz Gökdemir

AMAÇ VE KAPSAM

Bilimsel Madencilik Dergisi TMMOB Maden Mühendisleri Odası'nın açık erişimli elektronik ortamda ve basılı olarak yayımlanan süreli bilimsel yayınıdır. Dergi 1960 yılından itibaren yayımlanmaktadır. Derginin ismi 2016 yılı Haziran sayısına kadar "Madencilik" şeklindeyken, benzer isimli popüler dergilerle karıştırılabilmesi nedeniyle 2016 yılı Eylül sayısından itibaren "Bilimsel Madencilik Dergisi" olarak değiştirilmiş ve o tarihe kadar 0024-9416 olan ISSN numarası da 2564-7024 olarak güncellenmiştir.

Yılda 4 kez (Mart-Haziran-Eylül-Aralık) yayımlanan Bilimsel Madencilik Dergisi (ISSN: 2564-7024), maden mühendisliği ve mineral endüstrisi alanında ulusal ve uluslararası düzeyde yapılan, bilimsel normlara ve yayın etiğine uygun, özgün bilimsel çalışmaları bilim insanlarına, maden mühendislerine ve kamuoyuna duyurmayı ve bu yolla bilimsel bilgiyi toplumla paylaşmayı amaçlamaktadır. Derginin yayın dili Türkçe ve İngilizce'dir.

Dergi, maden mühendisliği alanında özgün bir araştırmayı bulgu ve sonuçları ile yansıtan kuramsal, deneysel ve uygulamalı araştırma makalelerine; yeterli sayıda bilimsel makaleyi tarayıp konuyu bugünkü bilgi ve teknoloji düzeyinde özetleyen, değerlendirme yapan ve bu bulguları karşılaştırarak yorumlayan tarama makalelerine; özgün bir yöntem veya tekniği tarif eden kısa makale olarak tanımlanabilecek teknik notlara; ve gerçek ya da kuramsal bir mesleki uygulamayı temel alan, sistematik veri toplama ve veri analizi içeren vaka çalışmalarına yer vermektedir.

Dergide, yenilenemeyen maden kaynakların sürdürülebilir madencilik ilkeleri doğrultusunda insanlığın hizmetine sunulması için gereken mevcut bilginin geliştirilmesini sağlayacak konularda eserlere öncelik verilmektedir. Bu kapsamda; maden arama, maden yatağı modelleme, topoğrafya, maden ekonomisi, jeoistatistik, kaya mekaniği ve jeoteknik, kazılabilirlik etüdü, yer altı ve açık maden işletme, maden tasarımı, madenlerde ve tünellerde tahkimat sistemleri, delme-patlatma tasarımı, madenlerde üretim planlaması ve optimizasyon, madenlerde iş sağlığı ve güvenliği yönetimi, maden havalandırma, yeraltı kömür madenlerinde metan gazı emisyonu ve metan drenajı, cevher hazırlama ve zenginleştirme, proses mineralojisi, analitik teknikler, öğütme, sınıflandırma ve ayırma, flotasyon/flokülasyon, katı/sıvı ayırımı, fiziksel zenginleştirme yöntemleri, hidro ve biyometalurji, üretim metalurjisi, modelleme ve simülasyon, enstrümantasyon ve proses kontrol, geri dönüşüm ve atıkların işlenmesi, maden hukuku, madenlerde çevre sağlığı ve yönetimi, madenlerde nakliyat, makina ve ekipman seçimi ve planlaması, kömür gazlaştırma, mermer teknolojisi, endüstriyel hammaddeler, uzay madenciliği, denizaltı madenciliği ve mekanizasyon ile ilgili konular dergi içeriğinde yer almaktadır.

Gönderilen yazılar editörler kurulu ve konusunda uzman hakemler tarafından bağımsız ve akademik yayıncılıkta en iyi uygulamalarla uyumlu şekilde değerlendirilmekte olup, değerlendirme süreci sonunda yayınlanması uygun görülen yazıların yayın hakları yazarlar tarafından telif sözleşmesi ile TMMOB Maden Mühendisleri Odası'na devredilir.

AIMS AND SCOPE

Scientific Mining Journal, which is published in open access electronic environment and in printed, is a periodical scientific journal of Union of Chambers of Turkish Engineers and Architects Chamber of Mining Engineers. The name of the journal was "Mining" until June 2016 and it has been changed to "Scientific Mining Journal" since September 2016 because it can be confused with popular journals with similar names and the ISSN number has been updated from 0024-9416 to 2564-7024.

Scientific Mining Journal, published four times a year (March-June-September-December), aims to disseminate original scientific studies which are conducted according to the scientific norms and publication ethics at national and international scale, to scientists, mining engineers, the public; and thus to share scientific knowledge with society. The journal is in both Turkish and English.

The journal covers theoretical, experimental, and applied research articles, which reflects the findings and results of an original research in the field of mining engineering; review articles, which assess, evaluates, and interprets the findings of a comprehensive review of sufficient number of scientific articles and summarize them at present information and technology level; technical notes, which may be defined as a short article that describes a novel methodology or technique; a case studies, which are based on the theoretical or real professional practice and involves systematic data collection and analysis.

The journal gives priority to works that will enable the advancement of current available information necessary to serve humanity with nonrenewable mineral resources with the perspective of sustainable mining principles. In this context, mine exploration, mineral resource modeling, surveying, mine economics and feasibility, geostatistics, rock mechanics and geotechnics, diggability studies, underground and surface mining, mine design, support design in underground mines and tunnels, rock penetration and rock fragmentation, mine production planning and pit optimization, mine health and safety management, mine ventilation, methane emission and drainage in underground coal mines, mineral processing and beneficiation, process mineralogy, analytical techniques, mineral comminution, mineral classification and separation, flotation/flocculation, solid/liquid separation, physical enrichment methods, hydro and biometallurgy, production metallurgy, modeling and simulation, instrumentation and process control, recycling and waste processing, mining law, environmental health and management, transportation, machinery and equipment selection and planning, coal gasification, marble technology, industrial minerals, space mining, submarine mining and mechanization are included in the journal content.

Submitted manuscripts are evaluated by the editorial board and expert referees independently in accordance with the best practices in academic publishing. The publishing rights of the manuscripts, approved for publication at the end of the evaluation process, are transferred to the Chamber of Mining Engineers by the authors.

BİLİMSEL MADENCİLİK DERGİSİ

Scientific Mining Journal

Bilimsel MADENCİLİK Dergisi makale dizin ve özlerinin yer aldığı veri tabanları:

Scientific MINING Journal is indexed or abstracted in:

SCOPUS

Google Scholar

ULAKBİM TR Dizin

GeoRef

OpenAIRE

Makale Yazım Kuralları, Yayın Danışma Kurulu, Hakem Değerlendirme Süreci ve Hakem Listelerine http://www.mining.org.tr adresinden erişilebilir.

Author Instructions, Editorial Advisory Board, the Peer Review Process and Reviewer Lists can be accessed from http://www.mining.org.tr

Etik Kurallar / *Publication Ethics*

Dergiye gönderilecek çalışmalarda, araştırma ve yayın etiğine uyulması tartışmasız bir ön koşul olarak kabul edilmektedir. Yayın Etik Kurallarına http://www.mining.org.tr adresinden erişilebilir.

Complying with the research and publication ethics is considered an indisputable precondition to be published. Publication Ethics can be accessed from http://www.mining.org.tr

BİLİMSEL MADENCİLİK DERGİSİ

Scientific Mining Journal

TMMOB Maden Mühendisleri Odası adına sahibi /

Owner on behalf of the Chamber of Mining Engineers of Turkey: Ayhan Yüksel

Sorumlu yazı işleri müdürü / R*esponsible editing manager: Mehmet Erşat Akyazılı*

Yönetim yeri ve yazışma adresi / *Correspondence address:*

Selanik Cad. No: 19/4 06650 Kızılay-Çankaya / ANKARA TURKEY

Tel: +90 312 425 10 80 / +90 312 418 36 57 • Fax: +90 312 417 52 90

e-mail: smj@maden.org.tr

web: http://www.mining.org.tr

Yayın türü / Publication type: Yerel süreli yayın, 3 ayda bir yayımlanır / *Local periodical, quarterly*

Tasarım / *Design*: Gülendem Gültekin

Baskı yeri / *Printed at: Ziraat Gurup Matbaacılık Ambalaj San. ve Tic. A.Ş.*

Baskı tarihi ve saati / *Printing date:* 01.03.2022 at 09:00

Basım adedi / *Number of printed copy:* 1500

BİLİMSEL MADENCİLİK DERGİSİ
SCIENTIFIC MINING JOURNAL

TMMOB Maden Mühendisleri Odası Yayını / The Publication of the Chamber of Mining Engineers of Turkey

ISSN 2564-7024
e-ISSN 2587-2613
Cilt / *Vol:* 61
Sayı / *No:* 1
Mart / *March*
2022

İÇİNDEKİLER / *CONTENTS*

ISSN 2564-7024
9 772564 702003

Madencilik - Mining, 2022, 61(1), 7-12

BİLİMSEL MADENCİLİK DERGİSİ
SCIENTIFIC MINING JOURNAL
TMMOB Maden Mühendisleri Odası Yayını / The Publication of the Chamber of Mining Engineers of Turkey

www.mining.org.tr

Original Research / Orijinal Araştırma

Studies on the effects of vessel nozzle parameters on the ore transportation efficiency in deep-sea mining

Yicong Zeng[a, *], Hailiang Xu[b, **], Bo Wu[b, ***]

[a] School of Electronic Information Engineering, Changsha Social Work College, Changsha, 410004, China
[b] School of Mechanical and Electrical Engineering, Central South University, Changsha, 410082, China

Geliş-Received: 8 Eylül-September 2021 • Accepted: 4 Ocak-January 2022

A B S T R A C T

As it is difficult to control the ore volume concentration of pump-vessel combined ore transporting equipment for deep-sea mining during the ore pulp conveying process and it can't remain continuous, stable and reliable in the process, the SIMPLE algorithm is adopted to calculate and analyze the rules of the vessel nozzle parameters effects on the ore transportation concentration and conveying efficiency based on the Euler-Euler model and standard $\kappa - \varepsilon$ turbulence model, and the conclusion is experimentally verified that ore transportation volume concentrations can be controlled and adjusted by controlling vessel nozzle parameters. Simulation results are drawn as follows: with the vessel nozzle diameter bigger, the ore transportation volume concentration becomes bigger and the water jet impacting force on ores becomes weaker so that the transporting process gets more stable. With the nozzle outlet height from the vessel bottom greater, the ore transportation volume concentration also becomes bigger, but the transporting process gets less stable. When the nozzle outlet height from the vessel bottom equals to 800 millimeters or 900 millimeters, it can ensure that the ore transportation volume concentration get bigger and the transporting process gets stable simultaneously.

Keywords: Deep-sea mining, Ore transportation, Vessel nozzle, Volume concentration, Solid-liquid two-phase flow.

Introduction

Manganese nodules lie widely on seabed deep about from 3000 meters to 6000 meters (Yang et al., 2020). One of key links in deep-sea mining research recently is how to transport ores from 6000 meters sea floor to the mining ship at sea level continuously, stably and efficiently and simultaneously ensure its transmission process reliable, economic and advance (Li et al., 2016). At the beginning of 20th century main developed countries in the world have all carried out much theoretical and experimental research (Cao et al., 2020). And it is widely recognized that the hydraulic transporting system has great potential for industrial appliance (Pang, 2020).

In the pump-vessel combined ore lifting equipment, as shown in Figure 1, the new ore lifting system is invented according to the hydraulic transportation principle, which has many advantages such as high transmission efficiency, long service life, safe and reliable transmission (Takano et al., 2020; Slade et al., 2020). It consists of a water pump, two vessels, transportation pipes and seven control valves. Each vessel is equipped with a nozzle. Before the mining system begins to work, the Valve 3 and 7 is turned on, whilst the other valves are turned off. When the water pump is turned on, sea water will be transported to sea level through the transportation pipe by the pump. After the mining crawler starts working, ores will flow into vessel 1 through valve 3, and some sea water in vessel 1 will be drained away through valve 3. When vessel 1 is filled with ores, turn off valve 3 and turn on valve 1, 2 and 6. Then ores in vessel 1 will flow into the flexible hose, and be transported to the mining ship. Since valve 3 is turned off, ores will flow into vessel 2 through valve 6. When ores in vessel 1 are carried over and vessel 2 is filled with ores, turning off valve 1, 2 and 6, meanwhile turning on valve 3, 4 and 5, ores in vessel 2 will flow into the transportation pipe and be transported to the mining ship, while ores flow into vessel 1 through valve 3. Repeating the above working steps, through turning on or off valves, ores in two vessels will be transported to the transportation pipes alternately, and then ores in the pipes will be lifted to the sea level continuously by the water pump (Xu et al., 2020; Leal Filho et al., 2021).

* Corresponding author / Sorumlu yazar: cszycong@qq.com. • https://orcid.org/0000-0001-5858-8116
** csuxhliang@aliyun.com. • https://orcid.org/0000-0001-8098-0640
*** csuwubo@aliyun.com. • https://orcid.org/0000-0001-9151-0425

https://doi.org/10.30797/madencilik.992728

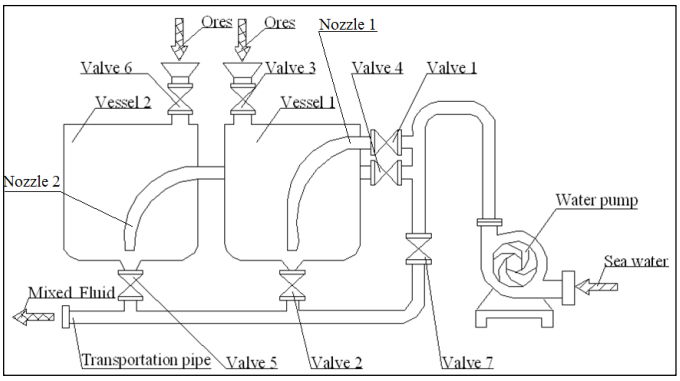

Figure 1. *Schematic diagram of pump-vessel combined ore lifting equipment*

In transporting ores, if the ore transportation concentration is too low, it may reduce conveying efficiency and economic benefits. If the concentration is too high, it may also affect the transmission reliability. So the ore transportation concentration should be controlled in a reasonable degree to make the whole transporting process efficient and reliable (Kotoky et al., 2018a; Hu et al., 2020). When the lifting equipment is working, ores in the vessel will flow from the vessel bottom into the transportation pipe under its own gravity and the pressure of the water jet out of a nozzle, and then it will be lifted to the mining ship at sea level. The vessel nozzle and the water jet out of the nozzle will affect the flow of ores in the vessel to the transportation pipe directly, and then the ore transportation volume concentration. So the key to raise ore conveying efficiency is to study the vessel nozzle parameters effects on the ore transportation concentration for deep-sea mining (McLoone and Quinlan, 2020).

For above problems, with a pump-vessel combined ore lifting equipment for a study object, with seawater for conveying medias, with manganese nodules for conveying materials, the SIMPLE algorithm will be used in this paper to calculate and analyze the vessel nozzle parameters effects on the ore transportation concentration when manganese nodules are lifted by the pump-vessel combined ore lifting equipment based on the Euler-Euler model of the Fluent software and the standard turbulence model. The mathematical model, calculation results and analysis, experimental study and conclusions are explained in the next section.

1. Mathematical model

1.1. Fundamental assumptions

In order to ensure calculations feasible and results reliable, some assumptions are made for the model as follows (Kotoky et al., 2018b):

The temperature of the flow field is equally distributed.

The solid-liquid two-phase flow is continuous and incompressible, whose physical property values are constant. The main phase flow is sea water. The second phase flow is ore particles of manganese nodules.

The particles of the particle phase are spherical and homogeneous. Take no account of the phase change of the flow. The maximum filling volume fraction of ore accumulation is 0.67.

There is dual-phase coupling between the particles and sea water. But the particle collision problem is ignored.

The mass of particles in the transportation pipe is conservational. The deposition effects of particles on the pipe wall are ignored.

1.2. Control equation

Because the volume percentage of the particle phase is greater than 10% and there is a strong interactive solid-liquid flow between the solid and liquid, the Dual-Euler model is used to perform simulation combined with particles dynamics theory. And also because the speeds of solid-liquid two phases are different and the initial ore particles in the vessel are stacked, the Euler-Euler model of the Fluent software is selected to perform calculations. Assuming the solid phase flow and liquid one are continuous filled with the whole flow field, their continuity equation and momentum equation can be obtained separately as follows (Eshghinejadfard et al., 2019; Jebakumar et al., 2018).

In the solid phase flow condition, a continuity equation and a momentum equation will be obtained as follows;

$$\frac{\partial C_V}{\partial t}+\frac{\partial C_V u_s}{\partial x}=0 \tag{1}$$

$$\frac{\partial}{\partial t}(C_V u_s)+\nabla\,(C_V u_s u_s)=-\frac{1}{\rho_s}\nabla\,(C_V P)+\frac{1}{\rho_s}\nabla\,(C_V \tau_s)+C_V F_s+\frac{M_s}{\rho_s} \tag{2}$$

In the liquid phase flow condition, a continuity equation and a momentum equation will be obtained as follows;

$$\frac{\partial(1-C_V)}{\partial t}+\frac{\partial\left[(1-C_V)u_l\right]}{\partial x}=0 \tag{3}$$

$$\frac{\partial}{\partial t}[(1-C_V)u_l]+\nabla\,[(1-C_V)u_l u_l]=-\frac{1}{\rho_l}\nabla\,[(1-C_V)P]+\frac{1}{\rho_l}\nabla\,[(1-C_V)\tau_l]+(1-C_V)F_l+\frac{M_l}{\rho_l} \tag{4}$$

Here C_v is the solid-phase volume concentration, u_l is the velocity of the liquid phase, u_s is the velocity of the solid phase, r_l is the density of the liquid phase, r_s is the density of the solid phase, P is the average pressure, t_l is the stress tensor sustained by the liquid phase, t_s is the stress tensor sustained by the solid phase, F_l is the external force per unit mass sustained by the liquid phase, F_s is the external force per unit mass sustained by the solid phase, M_l and M_s are the interaction forces between the two phases. In the two-phase flow of solid-liquid, the interaction forces belong to the internal forces, so

$$M_l+M_s=0 \tag{5}$$

The two phases of the Dual-Euler model are coupled by Equation 5, and then they can be solved.

1.3. Control equation Vessel computational model and grid of vessel model

Ore conveying equipments that work on seabed about 5000 meters deep are under very high pressure, so the vessel is designed into a container made up of a cylinder barrel, an upper hemisphere shell and a lower hemisphere shell, to improve its loading conditions. The vessel volume V and inside diameter D_i can be obtained by the formula as follow:

$$V=\frac{\pi}{6}D_i^3+\frac{\pi}{4}D_i^2 h \tag{6}$$

Here V is the vessel volume, D_i is the vessel inside diameter and h is the vessel barrel height.

Among ore conveying equipments, an ore relay warehouse connected between hard pipe and hose is joined at the bottom of the lift hard pipe, whose weight and volume have much effect on the lift pipe's loading conditions. The vessel is fixed in the relay warehouse, which occupies the largest proportion of weight and volume, so the

suitable vessel volume should be selected. According to Chinese sea general design requirements v5.0, the discharging capacity of the ore relay warehouse is the collection capacity of the collector for 10 minutes so the ore warehouse's volume is designed to 6m^3. The vessel inside diameter is designed to 1800mm. According to Equation 6, the vessel height can be calculated. So basic parameters of the vessel shown in Table 1 can be obtained.

Table 1. *Basic parameters of vessel*

Name	Volume(m^3)	Inside diamete (mm)	Height(mm)
Parameter	V	D_i	h
Value	6	1800	1158

In order to improve transmission efficiency, the ore conveying equipments adopt two vessels to transport ores alternately, so the two vessels have absolutely same structure and transmission way. So as to save computer resources, this paper only considers the effects of single vessel nozzle diameter and the height of the nozzle outlet from the vessel bottom on the ore transportation concentration. The ore particles outlet at the vessel bottom is designed into a venturi tube to strengthen roll suction and impact forces when the fluid flows in high speed so that ores in the vessel flow towards the transport pipe more smoothly. Simplifying the loading hopper and inlet valve, the computational model is obtained as shown in Figure 2. The computational model mainly consists of a vessel, a nozzle and transportation pipe. According to the computational model characteristic, the model is meshed into five parts using the Gambit software, which the grid unit size is size 8 or size 10. The vessel model grid is shown in Figure 3. The five parts are the vessel cavity, the vessel outlet part, the nozzle, the inlet and outlet part of transportation pipe.

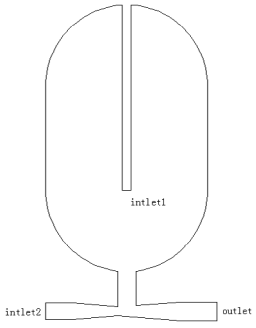

Figure 2. *Vessel computational model*

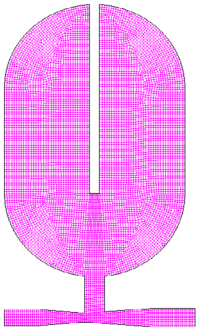

Figure 3. *Vessel model grid*

As different transmission condition parameters have much effect on the volume concentration of ore transportation, other main parameters of conveying equipments take fixed values so that it can prevent them from affecting calculation and analysis results of the vessel nozzle parameters (Dai et al., 2021). According to calculation and analysis results of the solid-liquid two-phase flow in the vessel, transmission condition parameters of ore conveying equipments are taken as shown in Table 2.

Table 2. *Vessel transmission condition parameters*

Parameters(Units)	Values
Stack height of ores(mm)	900
Grain size of ores(mm)	8
Diameter of transportation pipe's *outlet*(mm)	200
Diameter of transportation pipe's *inlet2*(mm)	160
Inlet velocity of nozzle's *inlet1*(m/s)	2.0
Inlet velocity of transportation pipe's *inlet2* (m/s)	5.0

1.4. Operating environment and boundary conditions setting Define the velocity entrance as an inlet boundary.

By using an inlet boundary that is homogeneous, stationary and has a given velocity along the axial direction, the entrance velocity is set according to different transmission working conditions such as valve openings, flow rates and etc.

Give the estimates of the turbulent kinetic energy and the dissipation rate.

Define the slurry outlet as a free flow boundary.

2. Calculation results and analysis

2.1. Analysis on vessel nozzle diameter effects on ore transportation concentration

When vessel basic parameters and transmission condition parameters are constant, with a nozzle diameter increment of 25mm, six sets of parameters are selected from 25mm to 150mm for simulation calculations. Then the simulation results are obtained as shown in Figure 4.

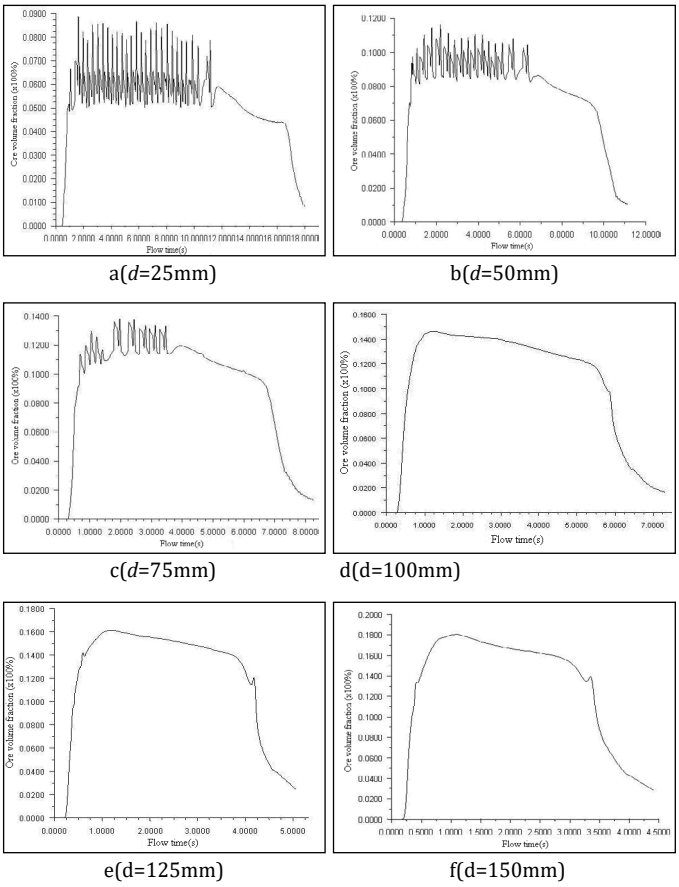

a(d=25mm) b(d=50mm)

c(d=75mm) d(d=100mm)

e(d=125mm) f(d=150mm)

Figure 4. *Ore volume fraction curves in different nozzle diameters*

As shown in Figure 4-a, Figure 4-b and Figure 4-c, the ore transportation volume concentration will present a zigzag wave along with the conveying time when the nozzle diameter is less than 75mm. And the smaller the nozzle diameter, the bigger the fluctuation amplitude is and the longer the fluctuation time is. It follows that when the nozzle diameter is smaller, the flow rates and impact forces become weaker and the ore outflow is not easy to control so that the ore volume concentration has an extraordinary change. As shown in Figure 4-d, Figure 4-e and Figure 4-f, when the nozzle diameter is bigger, the flow rates and impact forces

become larger, the stress area of the ore layer also increases, and the force condition of ore is relatively more balanced so that ores flow into the transportation pipe smoothly under the gravity and suction. So the ore transportation volume concentration has very small fluctuation or even no fluctuation.

2.2. Analysis on effects of height of nozzle outlet from vessel bottom on ore transportation concentration

According to the vessel nozzle diameter effects on the ore transportation concentration, as known, the bigger the nozzle diameter, the higher the ore conveying efficiency is, and the more stable the transportation process is. When the nozzle diameter takes 100mm, effects of the nozzle outlet height from the vessel bottom on the ore transportation concentration has been analyzed, which the height changes from 200mm to 1200mm with an increment of 200mm. By monitoring results of ore volume fraction in the outlet, ore volume fraction curves are obtained as shown in Figure 5.

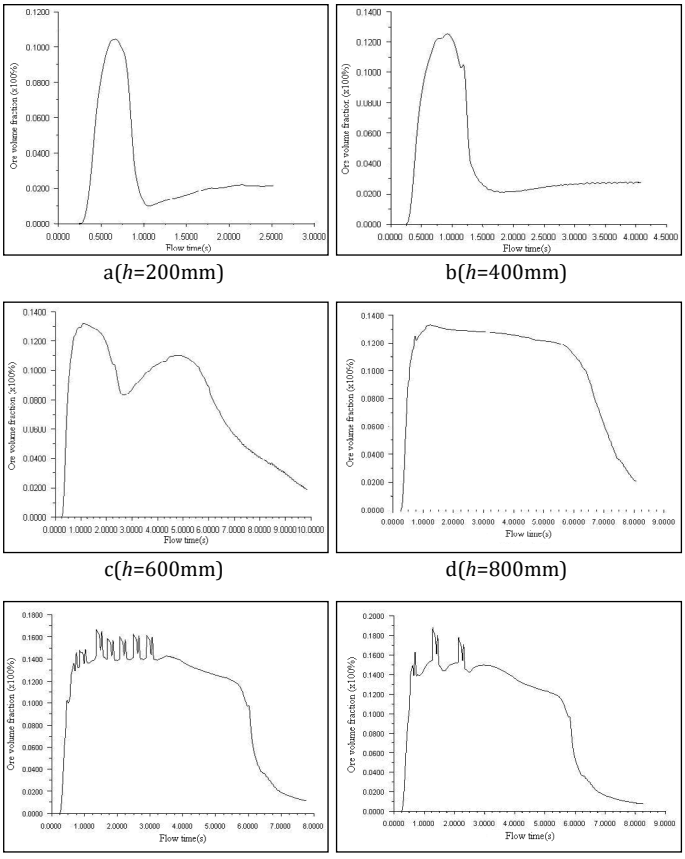

a(h=200mm) b(h=400mm)

c(h=600mm) d(h=800mm)

e(h=1000mm) f(h=1200mm)

Figure 5. *Ore volume fraction curves in different heights from nozzle to vessel bottom*

Based on analysis on Figure 5-a and Figure 5-b, when the nozzle outlet height from the vessel bottom is less than 600mm, the ore volume fraction in the outlet of transportation pipes will be in a higher state within a short time after the beginning of transportation, then decline dramatically, and finally in a stable stage of slow rise. By analysis on the ore volume fraction contour when h is equal to 200mm and 400mm shown in Figure 6, it is obtained that ores in the vessel almost doesn't change after conveying 2.0s. But from the impact situation of the nozzle jet on the ores, the greater the nozzle outlet height from the vessel bottom, the larger the impact area of the nozzle jet on the ores is, and the longer the time of ores in a highly efficient transporting state is.

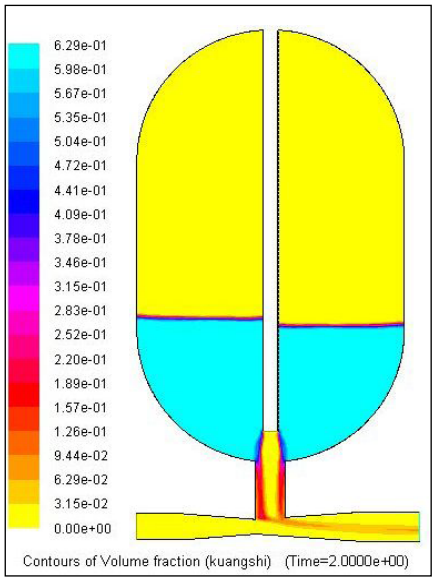

a(h=200mm, t=2.0s)

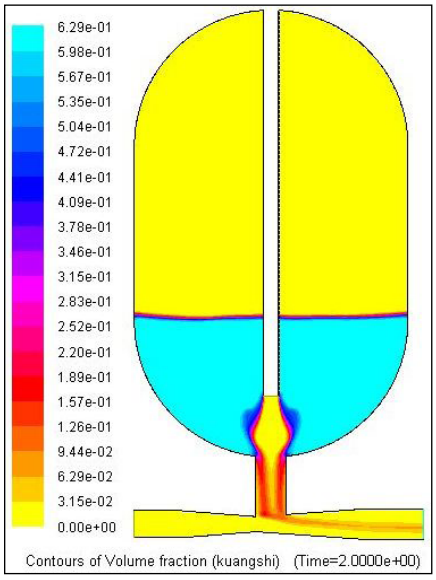

b(h=400mm, t=2.0s)

Figure 6. *Ore volume fraction contour of two different device parameters in the same flow time*

When the height of the nozzle outlet from the vessel bottom is equal to 600mm, as shown in Figure 5-c, the ore volume concentration in conveying will change in a hump shape with time, which it will increase firstly, decline dramatically again, and then also suddenly increase. This will affect the stability of the ore conveying seriously.

As shown in Figure 5-d, the ore conveying process is stable and highly efficient when the height of the nozzle outlet from the vessel bottom is equal to 800mm, which can be basically completed from 0.25s to 6.5s. The ore volume fraction curve looks smooth without fluctuations. The ore volume fraction basically keeps in a certain range and has a slightly declining trend.

When the height of the nozzle outlet from the vessel bottom is equal to1000mm or 1200mm, as shown in Figure 5-e and Figure 5-f, the whole ore conveying process looks fluent. The two ore volume fraction curves in the outlet keep good similarity, but the

ore transportation volume concentration in conveying will have a violent fluctuation that presents a zigzag wave, which shows that feeding is not uniform and the conveying process is not stable. The ore volume concentration fluctuation is of randomness and its rule is very difficult to control, so it is difficult to adopt an automatic way to control the transportation concentration consistency. This transmission scheme does not meet requirements that the ore conveying process keeps stable in the deep-sea mining.

All above analysis shows that the ore conveying process will be stable and highly efficient when the nozzle outlet height from the vessel bottom is 800mm or from 800mm to 900mm.

3. Experimental study

A single vessel lifting system as shown in Fig.ure 7a is designed according to the lifting principle of the equipment. A test equipment of ore lifting system as shown in Figure 7b is built in accordance with the experimental schematic (Figure 7a).

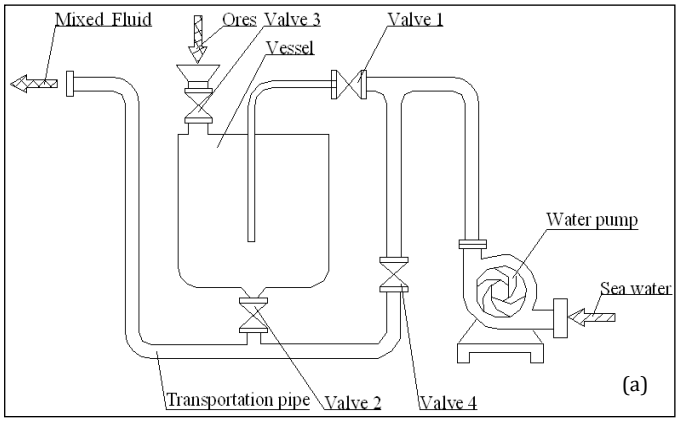

Figure 7. *Notation of experimental study*

When other parameters of the test equipment are kept constant, the equipment is installed with different diameter nozzles. When the required time of ore stable conveying process is taken as ore transmission time, the average volume fraction in stable ore transportation is taken as the ore transportation volume concentration, results can be obtained as shown in Table 3.

Table 3. *Ore volume concentration and transmission time in different nozzle diameters*

Nozzle diameter (mm)	25	50	75	100	125	150
Transmission time (s)	18	11	8	7	5	4.2
Ore volume concentration (%)	5.5	9.2	11.2	13.1	14.8	16.9

As shown in Table 3, when the nozzle diameter takes the minimum value of 25mm, the ore transportation volume concentration is smallest and only 5.5%, and the transmission time is longest and equal to 18s. When the nozzle diameter takes the maximum value of 150mm, the ore transportation volume concentration is equal to the maximum value of 16.9%, and the transmission time is relatively shortest and the whole process takes only 4.2s. So it can be seen that the nozzle diameter can affect the ore conveying efficiency when other conditions are same. The bigger the nozzle diameter, the higher the ore conveying efficiency is, the weaker the water jet impact force on ores becomes, and the more stable the transportation process is.

When other parameters of the test equipment are kept constant, the equipment is installed nozzles with different heights from the vessel bottom. When the required time of ore stable conveying process is taken as ore transmission time, the average volume fraction in stable ore transportation is taken as the ore transportation volume concentration, results can be obtained as shown in table 4. As shown in Table 4, the test results show that the ore volume concentration of the equipment increases with the height of the nozzle outlet increases.

Table 4. *Ore volume concentration and transmission time in different nozzle heights*

Nozzle height (mm)	200	400	600	800	1000	1200
Transmission time (s)	3	4	9	8	7	8
Ore volume concentration (%)	4.8	5.3	7.2	12.5	13.2	13.5

The lifting test shows that the bigger the nozzle diameter, the higher the ore conveying efficiency is. Similarly the ore lifting system is tested by adjusting the nozzle outlet height from the vessel bottom when other parameters of the equipment are kept constant. Test results show that the transport capacity of the equipment increases with the nozzle outlet height increases. The results are consistent with the above analysis, which also verifies the correctness of the simulation results. It further proves that it is feasible to control the ore transportation concentration by changing the nozzle diameter and the nozzle outlet height from the vessel bottom.

Conclusions

After numerical simulation analysis on the vessel nozzle diameter and the nozzle outlet height from the vessel bottom in this paper, which shows how they affect the ore conveying efficiency, some conclusions are obtained as follows:

The bigger the nozzle diameter when other vessel parameters are kept constant, the higher the ore conveying efficiency is, the weaker the water jet impact on ores becomes, and the more stable the transportation process is.

When the nozzle diameter takes 100mm and the nozzle outlet height from the vessel bottom is less than 600mm, the ore volume

fraction in the transportation pipes outlet will be in a higher state within a short time after the beginning of transportation, and then drop dramatically. When the height is more than or equal to 800mm, the ore conveying process is stable and highly efficient, at which ore volume fraction basically keeps in high range and has a slightly declining trend. But when the height is more than 1000mm, the ore volume fraction in conveying will has a violent fluctuation that presents a zigzag wave, which shows that feeding is not uniform and the conveying process is not stable. So the ore conveying process is stable and highly efficient when the height takes 800mm.

A single vessel lifting test equipment has been designed in accordance with the experimental schematic. The experiment verifies effects of the nozzle diameter and the nozzle outlet height from the vessel bottom on the ore conveying efficiency for deep-sea mining.

There are many factors affecting the ore conveying efficiency for deep-sea mining. The next step is to explore the optimal working parameters of conveying equipment such as conveying concentration, conveying speed, head, flow, etc. The influence on sensitivity of these parameters will be also studied in the future.

Acknowledgement

We express our gratitude to State Key Laboratory of High Performance Complex Manufacturing of Central South University for providing research condition and thanks to all members who help our field studies. This work is supported by a grant from the National Natural Science Foundation of China (No. 51375498).

References

Cao, Y., Du, X.G., Song, H.F., Lin, Q., Yang, B. 2020. Overall strength analysis and assessment of underwater buffer station in deep sea mining .Ship & Ocean Engineering, 49(3), 136-139.

Dai, Y., Li, X.Y., Yin, W.W., Huang, Z.H., Xie, Y. 2021. Dynamics analysis of deep-sea mining pipeline system considering both internal and external flow. Marine Georesources & Geotechnology, 39(4), 408-418. https://doi.org/10.1080/1064119X.2019.1708517

Eshghinejadfard, A., Hosseini, S.A., Thévenin, D. 2019. Effect of particle density in turbulent channel flows with resolved oblate spheroids. Computers and Fluids, 184, 29-39. https://doi.org/10.1016/j.compfluid.2019.01.027

Hu, Q., Zou, L., Lv, T., Guan, Y.J., Sun, T.Z. 2020. Experimental and Numerical Investigation on the Transport Characteristics of Particle-Fluid Mixture in Y-Shaped Elbow. Journal of Marine Science and Engineering, 8(9), 675. https://doi.org/10.3390/jmse8090675

Jebakumar, A.S., Magi, V., Abraham, J. 2018. Lattice-Boltzmann simulations of particle transport in a turbulent channel flow. International Journal of Heat and Mass Transfer, 127, 339-348. https://doi.org/10.1016/j.ijheatmasstransfer.2018.06.107

Kotoky, S., Dalal, A., Natarajan, G. 2018a. Effects of specularity and particle-particle restitution coefficients on the hydrodynamic behavior of dispersed gas-particle flows through horizontal channels. Advanced Powder Technology, 29(4), 874-889. https://doi.org/10.1016/j.apt.2018.01.004

Kotoky, S., Dalal, A., Natarajan, G. 2018b. A parametric study of dispersed laminar gas-particle flows through vertical and horizontal channels. Advanced Powder Technology, 29(5), 1072-1084. https://doi.org/10.1016/j.apt.2018.01.024

Leal Filho, W., Abubakar, I.R., Nunes, C., Platje, J.J., Ozuyar, P.G., Will, M., Nagy, G.J., Al-Amin, A.Q., Hunt, J.D., Li, C.L. 2021. Deep Seabed Mining: A Note on Some Potentials and Risks to the Sustainable Mineral Extraction from the Oceans. Journal of Marine Science and Engineering, 9(5), 521. https://doi.org/10.3390/jmse9050521

Li, J.H., Song, J.C., Luo, Y. 2016. Research progress and prospect of deep sea polymetallic sulfide mining. Ocean Development and Management, 36(11), 29-37.

McLoone, M., Quinlan, N.J. 2020. Particle transport velocity correction for the finite volume particle method for multi-resolution particle distributions and exact geometric boundaries. Engineering Analysis with Boundary Elements, 114, 114-126. https://doi.org/10.1016/j.enganabound.2020.02.003

Pang, J.P. (2020): Development of research on deep-sea polymetallic nodule mining vehicle in China. Mining & Processing Equipment, 48(3), 8-11. DOI: 10.16816/j.cnki.ksjx.2020.03.002

Slade, W.H., Peacock, T., Alford, M. 2020. Monitoring Deep-Sea Mining's Effects. Sea Technology, 61(9), 13-16.

Takano, S., ONO, M., Masanobu, S. 2020. Evaluation method of pipe wear for development of seafloor massive sulfides. Journal of JSCE, 8(1), 288-302. DOI: 10.2208/JOURNALOFJSCE.8.1_288

Xu, H.L., Peng, N., Yang, F.Q. 2020. Effect of slurry flow rate on cavitation characteristics of deep-sea mining pump. Journal of Drainage and Irrigation Machinery Engineering, 38(3), 217-223.

Yang, J.M., Liu L., Lyu, H.N., Lin, Z.Q. 2020. Deep-Sea Mining Equipment in China: Current Status and Prospect. Strategic Study of CAE, 22(6), 1-9.

BİLİMSEL MADENCİLİK DERGİSİ
SCIENTIFIC MINING JOURNAL
TMMOB Maden Mühendisleri Odası Yayını / The Publication of the Chamber of Mining Engineers of Turkey
www.mining.org.tr

Original Research / Orijinal Araştırma

A study on effects of modified calcite on filler retention and mechanical properties of fluting papers

Modifiye kalsitin dolgu tutunumu ve fluting kağıtların mekanik özellikleri üzerine etkileri

Tamer Sozbir[a,**], Mustafa Cicekler[b,*]

[a] *Kahramanmaras Paper Industry Incorp., Kahramanmaraş, TURKEY*
[b] *Kahramanmaraş Sütçü İmam University, Faculty of Forestry, Kahramanmaraş, TURKEY*

Geliş-Received: 16 Eylül-September 2021 • Kabul-Accepted: 12 Kasım-November 2021

A B S T R A C T

In this study, the use of modified calcite as a filler in fluting paper production was investigated and its effects on retention and some mechanical properties of the papers were determined. Ground calcium carbonate (GCC/calcite) and cationic starch were used for modification. Filler modification with alum effect of CPAM resulted in starch-calcite encapsulation. Produced modified calcite (MC) was used in fluting paper production at certain dosages as filler. Simultaneously, paper was made with unmodified calcite (UC), and the effects of modified calcite on the paper properties and filler retention were studied. The results of this study indicated that the use of 10% MC improved filler retention and provided approximately 23% more retention than the use of 10% UC. In addition, mechanical properties and air permeability values of MC-filled papers were higher than those of UC-filled papers. With the use of MC in fluting papers production, better filler retention was achieved, while the reduction in mechanical properties caused by the addition of filler can be minimized. Besides, impurities in white water can be minimized by reducing the filler dosage given during paper production.

Keywords: Calcite, Starch, Modification, Fluting paper, Retention, Mechanical properties

Introduction

Paper, which is one of the most produced and consumed substances in the world, and that the development in production and consumption in the countries affects other countries instantly, has an important strategic position. There is an increasing fiber deficit in the world and it is stated that cellulose investment is required in various sources and large pine forests are needed. However, high capital cost is required in cellulose production (Laftah and Wan Abdul Rahman, 2016).

Cellulose is not produced in Turkey and imported cellulose costs are overmuch (Cicekler and Tutus, 2021). Paper makers are seeking for alternative solutions to minimize cellulose-related costs, whether in paper or paper packaging. The fillers used to improve the paper properties are therefore of great importance. (Lourenço et al., 2019; Nikkhah Dafchahi et al., 2021; Tutus et al., 2020; Zhang et al., 2013). Since these non-fiber inorganic materials are much cheaper compared to fiber materials, they are highly preferred because they reduce production costs and provide faster drying compared to fiber raw materials, thus increasing production (Karademir et al., 2013; Lee et al., 2021).

Many industrial raw materials are evaluated in paper production and used for two different purposes as filling and coating. Some minerals are used only in filling or coating, while others can be used in both areas (Beazley, 1991). According to the type of paper produced, approximately 25% filling mineral is used. Fillers improve some paper properties such as opacity, whiteness, ink absorption, surface smoothness, dimensional stability, printing quality, softness and durability properties. Features required from an ideal filler; high whiteness, proper refractive index and grain distribution, high degree of retention, insolubility in water, or very little dissolution, low density, chemically reactive, low abrasion and cheap (Gigac et al., 1995; Kim et al., 2011; Tutus et al., 2018).

While the market share of calcite ($CaCO_3$) was less than 1% in the European paper industry 25 years ago, it now has more than 40% of the market. The use of calcite has increased in the past decade and has been approved in alkali papermaking process, especially in Europe (Hubbe and Gill, 2016; Shen et al., 2009). It has an important position in the filling and white pigment markets. Calcite can be prepared with lower cost, preserves the mechanical characteristics of the paper, provides to use more filler in paper

* Corresponding author / Sorumlu yazar: mcicekler87@gmail.com • https://orcid.org/0000-0001-5793-2827
** First author: tamersozbir@kmkaper • https://orcid.org/0000-0001-9035-8214

https://doi.org/10.30797/madencilik.994264

structure and improves whiteness, opacity and air permeability of papers without losing the brightness (Shen et al., 2010; Tutus et al., 2020). Calcite filled papers can keep their whiteness longer than filler-free papers. Because it is used in alkaline environment, it provides an advantage in terms of preventing environmental pollution (Geng et al., 2021; Shen et al., 2009).

Loss of binding due to increased mineral fillers leads to retention problems, as the fillers are more difficult to retention and more retention aids is required; this leads to formation and printing problems such as sheet delamination, picking, linting, dusting (Cadotte et al., 2007; Yang et al., 2013; Yoon and Deng, 2006). Therefore, the filler content in paper is rarely limited to values higher than 30% (Hubbe and Gill, 2016; Shen et al., 2009). For a paper mill producing 1800 tons/day, if it was possible to increase the filler content of a paper with an average of 30% filler content by 5%, a significant amount of fiber (90 tons/day) gain could be achieved.

Quality papers imported from foreign markets are at higher price and these prices reduce purchasing power and limit the use of quality papers such as carbonless paper, printing paper, copy paper, special thin papers. Although enough industrial raw materials are available for quality paper production in Turkey, it is still expected to be implemented. The technology required for the use of industrial raw materials has not been provided yet in paper industry. High-cost strength-enhancing chemicals are used to achieve high strength properties, which increases production costs (Strand et al., 2017). Considering the waste paper and cellulose costs, the use of low-cost fillers has gained importance. Beside, fillers are not fibrous, so they can cause decreases in strength properties of the papers. Some authors have investigated the modification of filler particles by starch or its derivatives or by filler particle encapsulation with a starch gel. Both techniques are very effective in improving the mechanical properties of the paper, such as the tensile, burst, and tear indices, without sacrificing optical properties (Cao et al., 2011; Kuusisto and Maloney, 2016; Shen et al., 2009; Xie et al., 2019). The purpose of the current study was to increase the filler retention and to prevent the decrease in mechanical properties due to the increase in the filler rate.

1. Materials and methods

1.1. Materials

Calcite (D50=2,8 µm) as filler taken from OMYA Mining Inc. was modified and used in this study. Technical properties of the calcite were given in Table 1.

Table 1. *Calcite properties used in the study*

Calcite Properties	Values
45 mesh screen (ISO 787-7), %	0.01
Top cut (D98, Malvern Mastersizer 2000), µm	13.0
< 2 µm (Malvern Mastersizer 2000), %	37.1
Average (D50, Malvern Mastersizer 2000), µm	2.8
Brightness CIELAB (ISO 11664-4), L*, a*, b*	98.5, -0.03, 0.8
Brightness RY (C/2º, DIN 53163), Ry	96.2
Moisture content, %	0.1
$CaCO_3$, %	98
$MgCO_3$, %	1.7
F_e2O_3, %	0.05
HCl insoluble content, %	0.2

Starch, retention aids and cationic polyacrylamide (cPAM) were purchased from the market. Fluting papers were produced by recycling old corrugated cardboards (OCC).

1.2. Calcite modification

Modified calcite production was carried out with the preparation steps of starch and calcite shown in Figure 1. Calcite was transferred to a beaker with distilled water to be 8% dry matter and mixed continuously to provide homogeneous slurry at 50 ºC. The starch was cooked in 5% dry matter at 92 ºC and cooled to 72 ºC for 30 minutes. Prepared calcite and starch slurries (w/w) with adding 0.03% CPAM by weight of dry fiber were transferred into a reactor and mixed for ten minutes (Figure 1).

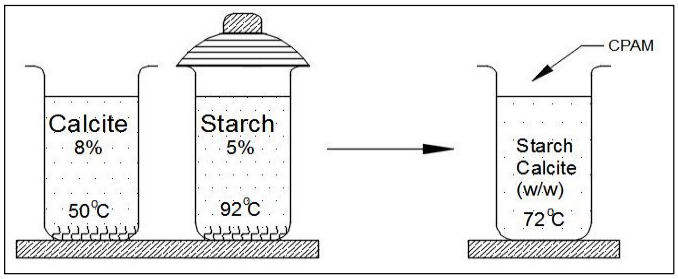

Figure 1. *Schematic view of calcite modification in this study.*

Starch-calcite encapsulation occurs in filler modification with alum effect of cPAM. In addition to the encapsulation of a single filler particle as shown in Figure 2, it is thought that it is possible to encapsulate several particles simultaneously to bind each other (Nelson and Deng, 2008; Shen et al., 2009; Yan et al., 2005; Zhao et al., 2008).

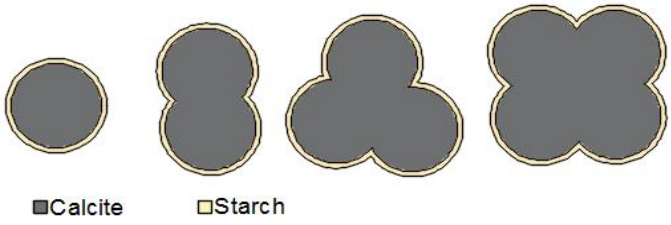

Figure 2. *Encapsulation structures of filler and starch*

1.3. Paper production and tests

Recycled OCC pulps were beaten to 40±2 Schopper-Riegler (ºSR) freeness level by using a Hollander beater. Beaten pulps were blended with modified (MC) and unmodified (UC) calcites and fluting papers with 90 grammages ($g.m^{-2}$) were produced with Rapid Kothen paper machine according to ISO 5269-2 standard. Starch (5%) was used only with UC filler in the paper production. Since calcite was modified with starch, no starch was added to the process with MC. Base papers (filler-free) were manufactured from the OCC pulps without the use of fillers in order to determine the effects of UC and MC on some mechanical properties.

The papers were incinerated in a crematorium at 575 ºC and resulting ash was weighed. The filler retention rates were calculated by the Equation 1 given below.

$$Retention\ Rate\ (\%) = \frac{Ash\ weight}{Paper\ weight\ (Oven-dried)} X\ 100 \quad (1)$$

After being conditioned for 24 hours in a conditioning room at 23±1 ºC and 50±2% relative humidity according to the TAPPI T402 standard, the fluting papers were subjected to tests according to relative standards given in Table 2.

Table 2. *The tests and standards applied to the fluting papers*

Tests	Standards
Breaking length (km)	TS EN ISO 13121
Burst strength (kg.cm^{-2})	TS EN ISO 2758
SCT (short span compression) (kN/m)	TS EN ISO 9895
CMT (corrugating medium test) (N)	TS EN ISO 9895
Scott bond (j.m^{-2})	TAPPI T569
Air permeability (s)	TAPPI T460
Filler rate (%)	TS EN ISO 1683

Ten fluting papers produced from each experiment were subjected to the tests specified in Table 2. To evaluate the effects of UC and MC on the fluting paper properties, the mean values of the properties were used. SEM images of produced papers were obtained using a ZEIZZ (Germany) microscope at an accelerating voltage of 0–30 kV.

2. Results and discussion

2.1. Findings on filler retention

Table 3 shows the measured filler doses and retention values in the manufacturing of fluting paper using UC and MC. The filler content of the base (filler-free) paper was determined as 10.4%. The filler rate is realized as 13.4% with using of 10% UC, while the increase in filler retention was 28.5%. Accordingly, the remaining part of the calcite was deposited onto the paper during sheet formation and the starch was effective for the filler retention. With the addition 10% MC during paper production, the filler retention increased about 58.7%.

Table 3. *Filler dosages and retention values in the fluting paper production using UC and MC*

Paper type	Filler Dosages (%)	Filler Retention (%)	Retention Increase (%)
Base paper	-	10.4	-
Paper filled UC	10*	13.4	28.5
Paper filled MC	5	14.2	36.4
	10	16.5	58.7
	15	21.4	105
	20	19.6	88.3

**Generally 10% filler is used in fluting paper production.*

When UC and MC were compared, it is clear that the use of MC significantly increases filler retention compared to UC (Figure 3). However, as the MC usage rate rises above 15%, its effect on the retention decreased from 105% to 88.3%. The advantages of using carbohydrate polymers in filler modifications can include low cost, ease of availability and environmental ease of modifiers, improved paper strength, enhanced filler retention or higher filling loading levels and successful marketing of the corresponding technology based on existing scientific papers (Fahmy and Mobarak, 2008; Fan et al., 2017; Fatehi et al., 2013; Shen et al., 2010).

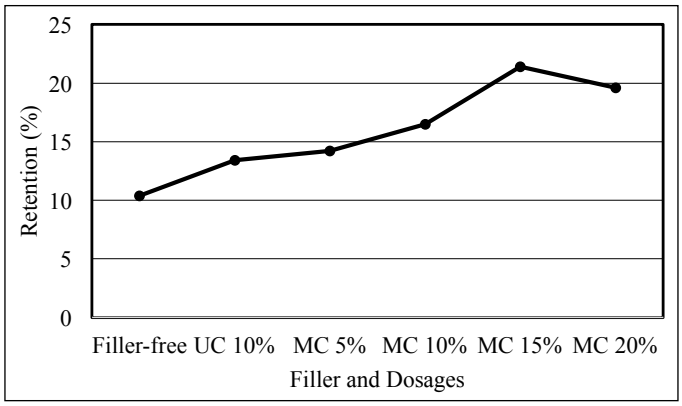

Figure 3. *Filler retention in the fluting paper production*

The amount of filler used in the system can be reduced if the filler particles are deposited into paper structure. Approximately 60% of the calcite filler used in paper production could be retained, with the remainder lost in circulation and cleaning water. By using less calcite in paper production, the recirculating water under the wire (white water) is less polluted. As a result, calcite damage in the treatment plant will be minimized by reducing the treatment load.

2.2. Mechanical properties of the fluting papers

The mechanical test results of the fluting papers containing no-filler, UC and MC were shown in Table 4. It is generally accepted that it has a negative effect on the strength-mechanical properties of papers with the increase of the filler content in the literature. Strength values of the papers used starch increased significantly compared to the filler-free paper due to the internal bonding property of starch.

Table 4. *Some mechanical properties of the fluting papers*

Papers	Filler Dosage (%)	SCT (kN.m^{-1})	Burst Strength (kg.cm^{-2})	CMT (N)	Scott Bond (j.m^{-2})	Breaking length (km)	Density (gr.cm^{-3})	Air permeability (s)
Filler-free	-	1.05	0.99	53.2	80.1	2.13	0.32	2.1
Starch	10	1.26	1.05	72.2	97.8	2.31	0.29	2.8
UC	10	1.20	1.00	65.0	89.5	2.04	0.29	2.6
MC	5	1.29	1.09	66.3	88.4	2.13	0.29	2.9
	10	1.33	1.19	68.9	85.6	2.12	0.31	3.3
	15	1.28	1.21	70.6	91.0	2.34	0.30	4.1
	20	1.44	1.31	72.0	97.8	2.45	0.29	5.4

In accordance with the general studies, the filler addition showed a significant decrease in values such as CMT and breaking length (Bajpai, 2018). Nevertheless, it is thought to be higher than the filler-free paper values, which is due to the internal bonding effect of starch. As the modified filler add-on increased, the generally expected strength values did not decrease, but an increase in non-significant values was observed (Figure 4). As the reason for the increases, it is seen that the effect of starch internal adhesion was realized, and with the increase in MC dosage, calcite grains encapsulated with cPAM support increased the retention by mak-

ing wet-end bonding to the fibers and also preserved the strength (Chen et al., 2020; Mousavipazhouh et al., 2018) carboxymethyl cellulose (CMC.

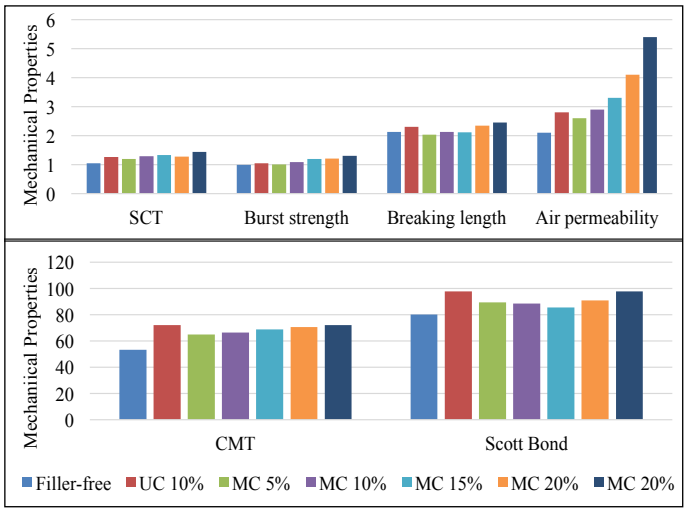

Figure 4. *The effects of the fillers on some fluting paper mechanical properties*

While the air permeability of the filler-free samples was measured as 2.1 s, the values increased as the MC dosage increases. Based on this, it can be said that the pores of the fluting paper were closed and the filler retention increased (Wu et al., 2016). SCT and CMT values of the fluting papers were increased by using 10% MC compared to 10% UC and filler-free papers. The respective values increased by 10.8% and 6% as a result of the use of MC. Filler addition often has effect of reducing stiffness (Hubbe and Gill, 2016). The CMT values are also high parallel to good paper stiffness values (Kiaei et al., 2016). The MC used in this study provided better stiffness than UC, and therefore the CMT values of MC-filled fluting papers were higher. Due to the buckling stability provided by short length tests compared to traditional test method, the material feature "compressive strength" can be measured with high accuracy using SCT. Starch use directly affects SCT, and an increase in the amount of starch used also positively affects SCT values (Andersson et al., 2013)therefore, is postulated to provide an added tool to support the necessary absorption control of the starch in respect to the packing density/permeability of the sheet as well as surface charge. To illustrate this behaviour, unfilled and filled laboratory-formed sheets without internal size are initially used, in which the starch is either cationically or anionically charged. The ground calcium carbonate (GCC. Scott Bond test is widely used method for determining paper and board delamination resistance. Scott Bond is a kind of indicator of inter fiber bond strength (Fellers et al., 2012). As mentioned before, the use of filler in paper production negatively affects the number of fiber-fiber bonds, and the MC used in this study minimized this negativity. As with other mechanical properties, breaking length and bursting strength of MC-filled fluting papers were better than UC-filled papers.

2.3. SEM images of the fluting papers

Figure 5 depicts scanning electron microscopy (SEM) images of the UC- and MC-filled fluting papers. It was discovered that the surface morphology of modified filler differed from that of unmodified filler, implying that surface encapsulation occurred during the modification process.

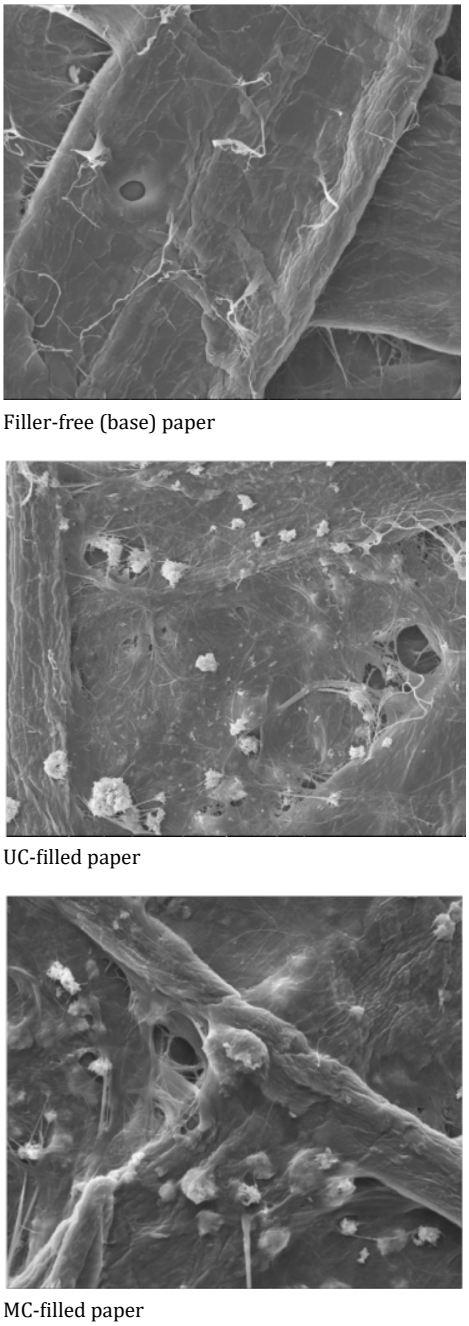

Filler-free (base) paper

UC-filled paper

MC-filled paper

Figure 5. *SEM images of the fluting papers (2000x)*

The morphology of the paper sheet was changed when fillers were included, and the filler particles stored in the fiber-based matrices onto the fiber surfaces. In compared to UC particles, the MC particles were noticeably more strongly and effectively attached to and bonded to the fiber surfaces.

Conclusion

The present study was designed to determine the effects of using MC as filler on filler retention and some mechanical properties of the fluting papers. The findings clearly indicate that the filler retention rate increased from 13.4% to 21.4% use of MC in fluting paper production. In this circumstance, the excess filler dosage given to the process could be decreased. Besides, the amount of calcite transferred to the white water could be decreased, and the load required for the treatment of the process water could be

reduced. The results of this investigation show that the strength losses caused by filler addition of fluting papers production could also be minimized with use of MC. The breaking length (2.34 km) and burst index (1.21 kg.cm-2) of the MC-filled fluting papers were higher than those of filler-free fluting papers. The insights gained from this study may be of assistance to new researches about the calcite modification and its effects.

3. Acknowledgment

This study was carried out at the R&D Center of Kahramanmaraş Paper Industry Inc. (Turkey) and the authors would like to thank to the R&D staff for their kind supports in the laboratory.

References

Andersson, L., Ridgway, C.J., Gane, P.A.C. 2013. Defining the mechanism of sizepress starch penetration in filled unsized fibrous products - A traditional technology revisited. Nordic Pulp & Paper Research Journal. 28(4), 547–558. https://doi.org/10.3183/npprj-2013-28-04-p547-559

Bajpai, P. 2018. Biermann's Handbook of Pulp and Paper. Academic Press, London. 273-281.

Beazley, K. 1991. Mineral fillers in paper. The Paper Conservator. 15(1), 17–27.

Cadotte, M., Tellier, M.E., Blanco, A., Fuente, E., Van De Ven, T. GM., Paris, J. 2007. Floculation, retention and drainage in papermaking: A comparative study of polymeric additives. Canadian Journal of Chemical Engineering. 85(2), 240–248.

Cao, S., Song, D., Deng, Y., Ragauskas, A. 2011. Preparation of starch-fatty acid modified clay and its application in packaging papers. Industrial and Engineering Chemistry Research. 50(9), 5628–5633. https://doi.org/10.1021/ie102588p

Chen, N., Wang, L., Wen, J., Yao, X., Zhao, W. 2020. Filler modified by a sequential encapsulation and preflocculation method and its effect on paper properties. Nordic Pulp and Paper Research Journal. 35(1), 89–95. https://doi.org/10.1515/npprj-2019-0047

Cicekler, M., Tutus, A. 2021. Effects of cellulase enzyme in deinking of Solvent-Based inks from mixed office wastes. Biocatalysis and Biotransformation. 39(2), 152–160. https://doi.org/10.1080/10242422.2020

Fahmy, T.Y.A., Mobarak, F. 2008. Nanocomposites from natural cellulose fibers filled with kaolin in presence of sucrose. Carbohydrate Polymers. 72(4), 751–755.

Fan, J., Li, T., Ren, Y., Qian, X., Wang, Q., Shen, J., Ni, Y. 2017. Interaction between two oppositely charged starches in an aqueous medium containing suspended mineral particles as a basis for the generation of cellulose-compatible composites. Industrial Crops and Products. 97, 417–424. https://doi.org/10.1016/j.indcrop.2016.12.048

Fatehi, P., Hamdan, F.C., Ni, Y. 2013. Adsorption of lignocelluloses of pre-hydrolysis liquor on calcium carbonate to induce functional filler. Carbohydrate Polymers. 94(1), 531–538. https://doi.org/ 10.1016/j.carbpol.2013.01.081

Fellers, C., Östlund, S., Mäkelä, P. 2012. Evaluation of the Scott bond test method. Nordic Pulp&Paper Research Journal. 27(2), 231–236. https://doi.org/10.3183/npprj-2012-27-02-p231-236

Geng, C., Ma, T., Liu, J. 2021. Eco-environmental benefits analysis of Eco-Partnerships program of production technology of calcium carbonate from lime mud produced by alkaline papermaking. Environmental Progress and Sustainable Energy. https://doi.org/10.1002/ep.13697

Gigac, J., Kuna, V., Schwartz, J. 1995. Effects of fibers and fillers on the optical and mechanical characteristics of paper. Tappi Journal. 78(2), 162–167.

Hubbe, M.A., Gill, R.A. 2016. Fillers for papermaking: A review of their properties, usage practices, and their mechanistic role. BioResources. 11(1), 2886–2963. https://doi.org/10.15376/biores.11.1.2886-2963

Karademir, A., Varlibas, H., Cicekler, M. 2013. A study on the chemical retention of CaCO3 on paper production. SDU Faculty of Forestry Journal. 14(1), 48–52.

Kiaei, M., Samariha, A., Farsi, M. 2016. Effects of montmorillonite clay on mechanical and morphological properties of papers made with cationic starch and neutral sulfite semichemical or old corrugated container pulps. BioResources. 11(2), 4990–5002. https://doi.org/ 10.15376/biores.11.2.4990-5002

Kim, H., Kim, C.H., Seo, J.M., Lee, J.Y., Kim, S.H., Park, H.J., Kim, G.C. 2011. Use of modified lignocellulosic fillers to improve paper properties. Appita Journal. 64(4): 338–343).

Kuusisto, J., Maloney, T.C. 2016. Preparation and characterization of corn starch–calcium carbonate hybrid pigments. Industrial Crops and Products. 83, 294–300. https://doi.org/10.1016/j.indcrop.2016.01.026

Laftah, W.A., Wan Abdul Rahman, W.A. 2016. Pulping Process and the Potential of Using Non-Wood Pineapple Leaves Fiber for Pulp and Paper Production: A Review. Journal of Natural Fibers. 13(1): 85-202. https://doi.org/10.1080/15440478.2014.984060

Lee, M.W., Jung, S.Y., Seo, Y.B. 2021. Energy saving in papermaking by application of hybrid calcium carbonate. BioResources. 16(3), 5011–5023. https://doi.org/10.15376/biores.16.3.5011-5023

Lourenço, A.F., Godinho, D., Gamelas, J.A.F., Sarmento, P., Ferreira, P.J.T. 2019. Carboxymethylated cellulose nanofibrils in papermaking: influence on filler retention and paper properties. Cellulose. 26(5), 3489–3502. https://doi.org/10.1007/s10570-019-02303-5

Mousavipazhouh, H., Azadfallah, M., Jouybari, I.R. 2018. Encapsulation of precipitated calcium carbonate fillers using carboxymethyl cellulose / polyaluminium chloride: Preparation and its influence on mechanical and optical properties of paper. Maderas: Ciencia y Tecnologia. 20(4), 703–714. https://doi.org/10.4067/S0718-221X2018005041601

Nelson, K., Deng, Y. 2008. Enhanced bondability between inorganic particles and a polysaccharide substrate by encapsulation with regenerated cellulose. Journal of Applied Polymer Science. 107(5), 2830–2836. https://doi.org/10.1002/app.27398

Nikkhah Dafchahi, M., Resalati, H., Zabihzadeh, S.M., Nazarnezhad, N., Asadpour, G., Pirayesh, H. 2021. Novel calcium carbonate filler for cellulose industry. Nordic Pulp&Paper Research Journal. https://doi.org/10.1515/npprj-2021-0018

Shen, J., Song, Z., Qian, X., Liu, W. 2009. Modification of papermaking grade fillers: A brief review. BioResources. 4(3), 1190–1209.

Shen, J., Song, Z., Qian, X., Yang, F. 2010. Carboxymethyl cellulose/alum modified precipitated calcium carbonate fillers: Preparation and their use in papermaking. Carbohydrate Polymers. 81(3), 545–553. https://doi.org/10.1016/J.CARBPOL.2010.03.012

Strand, A., Sundberg, A., Retulainen, E., Salminen, K., Oksanen, A., Kouko, J., Ketola, A., Khakalo, A., Rojas, O. 2017. The effect of chemical additives on the strength, stiffness and elongation potential of paper. Nordic Pulp&Paper Research Journal. 32(3), 324–335. https://doi.org/10.3183/npprj-2017-32-03-p324-335

Tutus, A., Cicekler, M., Killi, U., Kaplan, M. 2018. Comparison of GCC and PCC as Coating Material in Paper Production. 1st International Technological Sciences and Design Symposium, 1822–1829, Giresun, Turkey.

Tutus, A., Killi, U., Cicekler, M. 2020. Evaluation of eggshell wastes in office paper production. Biomass Conversion and Biorefinery. https://doi.org/10.1007/s13399-020-00768-0

Wu, Y., Zhao, C., Jiang, Y., Han, W. 2016. Study on modification of calcium carbonate for paper filler. Proceedings of the 2016 4th International Conference on Machinery, Materials and Computing Technology, 395-398. https://dx.doi.org/10.2991/icmmct-16.2016.80

Xie, W., Chen, F., Wang, C., Liu, Z. 2019. Modification of PCC with agar and its application in papermaking. IOP Conference Series: Materials Science and Engineering. https://doi.org/10.1088/1757-899X/490/2/022054

Yan, Z., Liu, Q., Deng, Y., Ragauskas, A. 2005. Improvement of paper strength with starch modified clay. Journal of Applied Polymer Science. 97(1), 44–50.

Yang, H., Qiu, L., Qian, X., Shen, J. 2013. Filler modification for papermaking with cationic starch and carboxymethyl cellulose: A comparative study. BioResources. 8(4), 5449–5460.

Yoon, S. Y., Deng, Y. 2006. Starch-fatty complex modified filler for papermaking. Tappi Journal. 5(9), 3–9.

Zhang, M., Song, S., Wang, J., Sun, J., Li, J.Z., Ni, Y., Wei, X. 2013. Using a novel fly ash based calcium silicate as a potential paper filler. BioResources. 8(2), 2768–2779.

Zhao, Y., Kim, D., White, D., Deng, Y., Patterson, T., Jones, P., Turner, E., Ragauskas, A.J. 2008. Developing a new paradigm for linerboard fillers. Tappi Journal. 7(3), 3–7.

Madencilik - Mining, 2022, 61(1), 19-24

BİLİMSEL MADENCİLİK DERGİSİ
SCIENTIFIC MINING JOURNAL
TMMOB Maden Mühendisleri Odası Yayını / The Publication of the Chamber of Mining Engineers of Turkey

www.mining.org.tr

Original Research / Orijinal Araştırma

Investigation of factors affecting hearing loss of open pit coal mine employees with categorical data analyses

Açık ocak kömür madeni çalışanlarının işitme kaybını etkileyen faktörlerin kategorik veri analizleri ile araştırılması

Mustafa Onder[a,*], Burcu Demir Iroz[b,**], Seyhan Onder[a,***]

[a] *Eskisehir Osmangazi University, Mining Engineering Department, 26040 Eskisehir, TURKEY*
[b] *Turkish Coal Enterprises, Ankara, TURKEY*

Geliş-Received: 2 Ağustos - August 2021 • Kabul-Accepted: 20 Eylül-Sepember 2021

A B S T R A C T

One of the most important occupational diseases encountered in mining is the noise induced hearing loss (NIHL). In this study, analyses were carried out to examine the NIHL in the open pit lignite mine in Turkey. The NIHL was evaluated in accordance with the miners' age, experience, occupation, exposure value (L_{ex}), and maximum noise level (L_{peak}). Noise levels exposed the employees were measured with noise dosimeters and a hearing test was applied to the employees by a special hearing center. To determine the parameters that could be effective in NIHL, all of the obtained data were evaluated by the logistic regression analysis (LRA) and hierarchical log-linear analysis (HLA) methods. It was determined that the NIHL probability of field staff is approximately 6 times higher than operators and drivers. According to the 21-29 age group, it was found that the probability of NIHL in the 57-65 and in the 48-56 age group was 11.4 and 4.41 times higher, respectively. Experience and maximum noise levels were found to be the most important parameters in hearing loss. Besides these, it was determined that the interactions of age×experience, occupation×maximum noise levels, and occupation×average noise exposure levels increased the likelihood of NIHL. A logistic regression model has been developed for the NIHL estimation of employees and hearing loss was found to be a problem mostly for those working in the field. It was determined that hearing loss increased with age and experience, and varied according to occupational groups. In order to prevent NIHL, it is a priority to consider the noise levels to which occupational groups are exposed and to apply technical or personal precautions for all employees of the relevant occupational group.

Keywords: Hierarchical log-linear analysis, Logistic regression, Mining, Noise induced hearing loss, Occupational disease.

Introduction

Excessive noise, in addition to its negative social and physiological effects, is an occupational health hazard, particularly NIHL. The World Health Organization reports that 16% of adult hearing loss occurs as a result of exposure to occupational noise (Nelson et al., 2005). Since the 18th century, the NIHL has been considered an occupational disease for copper employees who suffered hearing loss from hammering metal (Hong el al., 2013) .

In the studies of Kovalchik et al., they emphasized that hearing loss was classified in the category of "all other illnesses" by the Bureau of Labor Statistics before 2004, it was categorized as a separate illness among work-related diseases in 2004. They express that occurred from hearing loss 11% of work-related diseases in 2004 and 2005 (Kovalchik et al., 2008). Picard et al., found that hearing loss may occur at noise levels exceeding 89 dBA and also that high noise levels increase occupational accidents (Picard et al., 2008).

One of the industries with the highest NIHL risk is mining (Concha-Barrientos et al., 2004; Vipperman et al., 2007). Noise in mining is one of the most important factors damaging employee health. The possibility of hearing loss increases as a result of exposure due to noise. In coal mining, noise exposure is higher than the specified limit levels and high noise levels are generated by the operation of powerful machines (Kovalchik et al., 2008). Almost all equipment used in open pit mine is a source of noise itself. Mean noise level of some machines used in open cast mining given in Table 1 (Sharma et al., 1998).

* Corresponding author / Sorumlu yazar: monder@ogu.edu.tr • https://orcid.org/0000-0002-9267-1543
** e.burcudemir@hotmail.com • https://orcid.org/0000-0003-0969-2739
*** sonder@ogu.edu.tr • https://orcid.org/0000-0003-0396-9995

https://doi.org/10.30797/madencilik.977752

Table 1. *Mean noise levels of machines (dB)*

Source	Idling	Fully accelerated
Shovel	80	97
Dumper	75	92
Bulldozer	84	100
Pay loder	82	100
Drill	85	90
Scraper	85	101
Air compresssor	-	96

Continuous exposure of employees to high noise levels may cause hearing loss due to noise (Sharma et al., 1998; Sensogut and Cinar, 2007). For NIHL, exposure of employees to noise levels of 82 dB (A) poses a risk, while levels above 90 dB (A) pose a high risk (Phillips et al., 2007). The NIHL is currently not curable and irreversible, but it can certainly be avoided, so it is important to implement adequate preventive programs (Goelzer, 2001).

Kursunoglu and Gogebakan (2021) used multinomial logistic regression to predict spontaneous combustion tendencies of coal mines. Iwasaki et al (2021) studied the changes in element concentrations of approximately 100 untreated discharges from old mines in Japan by a hierarchical-linear model. Since there are few studies aimed at preventing occupational hearing loss in mining (Bauer et al., 2006), in this study, a statistical investigation by the LRA and HLA methods was conducted and the parameters that could be effective in the formation of NIHL were tried to be determined.

1. Materials and methods

LRA is used to determine the probability of an event occurring, while HLA is used to evaluate the interaction between parameters that affect the occurrence of the event. In this study, since the variables are suitable for categorical data analysis and these methods are mostly used in the medical sciences to study disease occurrences, a logistic regression model was created first and the relationships between risk factors and NIHL formation were quantitatively evaluated. Then, the HLA was used to examine the interaction between parameters that affect the formation of NIHL (Onder et al., 2021; Onder, 2013). The common results obtained by using LRA and HLA methods together were tried to be interpreted. Detailed explanations about LRA and HLA are available in the categorical data analysis book prepared by *Agresti* (2002).

1.1. Measurement methodology

The study was achieved in the open pit lignite mine belonging to Turkish Coal Enterprises in Turkey. The location map of the open pit lignite mine is given in Figure 1.

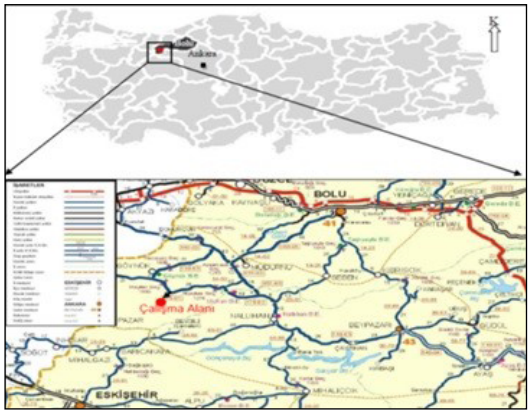

Figure 1. *Location map of the open pit lignite mine*

The open pit mine carries out its production with 100 employees. For excavating and loading are used excavators, and for transportation are used trucks. Within the scope of the occupational health and safety law in Turkey, in accordance with the regulation on protection of employees from noise related risks, the maximum action value for noise in the workplace is 85 dB (A) and the exposure limit value is 87 dB (A). Employers in Turkey, due to legal requirements, are obliged to have it made noise measurements in the workplaces. In addition, hearing loss is examined within the scope of health checks of employees (Official Gazette, 2013). After the enterprise management and employees approved the measurements, the personal noise exposure levels and hearing loss of all employees in the open pit lignite mine were determined. The data required for the study were compiled with special permission.

Noise measurements were recorded with noise dosimeter in order to measure the noise level of 100 employees working in different positions in open pit lignite mine. For dosimetric measurements, the CIRRUS CR-110 A personal dosimeter was used. Noise dosimeters have been developed to determine the noise that employees are exposed to during normal working days. This is a small, light, and compact piece of equipment that should be worn by the employees. It measures the total A-weighted sound energy received and expresses this as a ratio of the maximum A-weighted energy that can be received per day. This device is very useful when there are significant changes in exposure during the working day. A view showing the catalog and application of the measuring instrument used is given in Figure 2. Noise measurements were made with respect to TS 2607 ISO 1999 (2005).

Figure 2. *CIRRUS CR-110 A personal dosimeter*

The noise dosimeter can be worn without disrupting work. It is attached to the clothes of employees the microphone close to the ear. The noise values recorded by the instrument are transferred to the computer program and the data are evaluated, analysis and reports are generated. The dosimetric measurement results for an employee are shown in Figure 3.

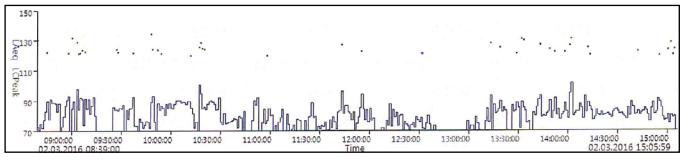

Figure 3. *Dosimetric measurement results for an employee*

1.2. Examination of NIHL

After this measurements it was made pure tone odyometri test for all employees. Dosimetric noise measurements and hearing loss tests were performed for 100 employees in the enterprise and occupation categories were determined with a single group code for those working in similar fields.

In this study, audiogram results of the employees were interpreted together with the workplace doctor. Also, the NIHL was evaluated to the occupation, miners' age, experience, L_{ex}, and L_{peak}. In the study, NIHL was accepted as the dependent variable because it caused by the noise in the working environment. It was categorized as no disease (No) and disease (Yes). Factors affecting the occurrence of NIHL were categorized into five groups in the study, such as occupation, age, experience, exposure value, and maximum noise, which are independent variables. Main categories determined as independent variables were divided into their subcategories. The coding plan and employees' distributions for the NIHL were given in Table 2.

(48%), age distributions are close to homogeneity, and the number of employees with less experience (66%) is high. Employees are often exposed to noise of 78.26-85.10 dB(A) (58%). Employees are often exposed to the maximum value of 138.6-143 dB(C) (84%). As a result of the calculations made to examine the NIHL rates in occupation sub-categories, because 8 out of 12 employees of the field staff had hearing loss, the NIHL rate was 66%. When the rates of the occupation sub-category among all employees with NIHL were calculated, it was determined that the number of drivers with hearing loss was 21 and the ratio was 47.73% in a total of 44 cases. All NIHL rates given in Table 2 were calculated similarly.

Table 2. *Coding plan and distributions for NIHL*

Variable	Categories	Code	Subcategories	%	NIHL	NIHL ratios in subcategories	Ratios by total NIHL
Y	NIHL	0	No	56			
		1	Yes	44			
$X_{Occupation}$	Occupation	1	Technical staff	15	6	40.00	13.64
		2	Operator	25	9	36.00	20.45
		3	Driver	48	21	43.75	47.73
		4	Field staff	12	8	66.67	18.18
X_{Age}	Age	1	21-29	24	6	25.00	13.64
		2	30-38	17	6	35.29	13.64
		3	39-47	18	8	44.44	18.18
		4	48-56	21	10	47.62	22.73
		5	57-65	16	10	62.50	22.73
		6	66-74	4	4	100.00	9.09
$X_{Experience}$	Experience	1	1-8 yrs	66	27	40.91	61.36
		2	9-16 yrs	13	7	53.85	15.91
		3	17-24 yrs	3	2	66.67	4.55
		4	25-32 yrs	12	4	33.33	9.09
		5	33-40 yrs	6	4	66.67	9.09
X_{Lex}	Exposure Value	1	71.4-78.25 dB(A)	42	17	40.48	38.64
		2	78.26-85.10 dB(A)	58	27	46.55	61.36
X_{Lpeak}	Maximum Value	1	134.1-138.5 dB(C)	16	6	37.50	13.64
		2	138.6-143 dB(C)	84	38	45.24	86.36

The categories of the occupation variables are technical staff, operator, driver, and field staff. Employees in the technical staff group are engineers, topographers, and technicians. Its general responsibilities are production, planning, supervision, and topographic measurements. Operators use large mining equipment such as excavators, while drivers use trucks. The employees in the field staff group are shunter, weigher, lubricator. The responsibilities of these staff working in the open pit area are to guide the maneuvers of the mining machinery, determine the weight of the shipped ore and refuel the mining machinery. The age variable was divided into six subcategories, the experience variable into five groups, and the exposure to noise (L_{ex}) and maximum noise variables (L_{peak}) into two groups. As shown in Table 2, 44% of all employees have NIHL. It was determined that the majority of the employees are driver

2. Results

In the study, the variables $X_{Occupation}$, X_{Age}, $X_{Experience}$, X_{Lex} and X_{Lpeak} are independent variables and the variable Y is the dependent variable (Table 2). After this determination, the interactions of parameters in NIHL formation were evaluated with advanced statistical techniques, and the important results obtained are given below.

LRA was carried out using SPSS package program to analyze data. The results of LRA including all variables are given in Table 3 and it can be interpreted as follows.

Table 3. *Results of the logistic regression model for NIHL*

Effect	Variable	β	p	Exp(β)	Probability (1/Exp(β))	95% C.I.for EXP(B) Lower	Upper
Occupation	Field staff		.092				
	Technical staff	-1.275	.101	.279	3.58	.061	1.281
	Operator	-1.842	.042*	.159	6.29	.027	.939
	Driver	-1.690	.040*	.185	5.41	.037	.925
Age	21-29		.291				
	30-38	.614	.430	1.847	1.847	.403	8.479
	39-47	1.018	.184	2.769	2.769	.616	12.434
	48-56	1.484	.062**	4.411	4.411	.931	20.907
	57-65	2.434	.018*	11.409	11.409	1.519	85.700
	66-74	23.390	.999	14388002142	-	.000	.
Experience	1-8 yrs		.511				
	9-16 yrs	.412	.560	1.510	1.510	.378	6.035
	17-24 yrs	.558	.683	1.746	1.746	.120	25.362
	25-32 yrs	-1.292	.142	.275	3.64	.049	1.538
	33-40 yrs	-.602	.638	.548	1.82	.045	6.714
Exposure Value	78.26-85.10 dB(A)	-.414	.600	.661	1.51	.140	3.112
Maximum Value	138.6-143 dB(C)	.492	.540	1.636	1.636	.338	7.914

* Significant at 95% probability level
**Significant at 90% probability level

According to the field staff, being an operator and the the truck driver increases the possibility of not having NIHL 6.29 times, 5.41 times, respectively. Compared to being the 21-29 age group, working in the 57-65 age group and 48-56 age group increases the probability of NIHL by 11.41 times and 4.41 times respectively. Being experienced for 25-32 years increases the likelihood of not having NIHL by 3.64 times compared to being experienced for 1-8 years. Being the most experienced employee increases the likelihood of not having NIHL by 1.82 times compared to being the least experienced employee. According to the exposure value of 71.4-78.25 dB (A), the exposure value of 78.26-85.10 dB (A) increases the probability of employees not NIHL by 1.5 times. Being the maximum value 138.6-143 dB (C) increases the probability of having NIHL by 1.64 times compared to being the maximum noise level of 134.1-138.5 dB (C).

According to the β coefficients (Table 3), the logistic regression model for NIHL can be written as in Equation 1.

$$\hat{Y} = -0.414X_{(78.26-85.1\ dB(A))} - 1.275X_{(Technical\ staff)} - 1.842X_{(Operator)} + 1.690X_{(Driver)} + 0.614X_{(30-38)} + 1.018X_{(39-47)} + 1.484X_{(48-56)} + 2.434X_{(57-65)} + 23.390X_{(66-74)} + 0.412X_{(9-16)} + 0.558X_{(17-24)} - 1.292X_{(25-32)} - 0.602X_{(33-40)} + 0.492X_{(138.6-143\ dB(C))} \quad (1)$$

While 56 of the 100 workers in the enterprise do not have the NIHL, 44 of them have the NIHL. The rate of correct classification employees without hearing loss in the developed logistic regression model is 82.1%, while the rate of predicting those with hearing loss is 56.8%. The correct classification rate of the model created for NIHL was determined as 71% and can be interpreted as a successful model. It is appropriate to use the generated logistic regression model to estimate NIHL in this mine (Onder and Mutlu, 2017).

For employees with NIHL, a HLA model has been established with the SPSS 17 version to specify which parameters cause the disease. The hierarchical log-linear model was established from five-way contingency table of occupation (O), age (A), experience (E), average noise exposure (L_{ex}) and maximum noise level (L_{peak}). A five-way h×i×j×k×l cross-classification of response variables O, A, E, L_{ex} and L_{peak} has several potential types of independence (Agresti, 2002). The saturated model includes terms corresponding to all possible main effects and interactions. In this study, the main effects for NIHL considered as O, A, E, L_{ex}, and L_{peak}. In other words, with the help of hierarchical log-linear models, the importance level of the main factors considered in the formation of the disease and the different interactions of these factors can be determined. The main effects and higher-order interaction terms of the hierarchical log-linear model were given in Table 4. The importance of interaction terms was determined by the likelihood-ratio (χ^2) test (Maiti et al., 2001).

The fourth and third order interaction terms were not evaluated in the study because they were not statistically significant. For more detailed data analysis, the statistically significant (p<.05) parameters in Table 4 were examined. Main effects and interaction parameters Age×Experience, Occupation×L_{ex} and Occupation× L_{peak} were found to be statistically significant. When c2 values are examined, it is determined that the most important main effect is experience. This is followed by L_{peak}, L_{ex}, occupation and age parameters according to the highest c2 value, respectively.

Table 4. *Results of the HLA for NIHL*

Degree of Interaction	Interaction	df	χ^2	p
2	Age×Experience	30	67.146	.000
	Occupation×L_{peak}	8	46.667	.000
	Occupation×L_{ex}	8	37.390	.000
	Occupation×Age	24	16.302	.877
	Occupation×Experience	20	13.776	.842
	Experience×L_{peak}	10	12.596	.247
	Age×L_{peak}	12	10.559	.567
	Age×L_{ex}	12	3.088	.995
	Experience×L_{ex}	10	1.846	.997
	L_{ex}×L_{peak}	4	.968	.915
Main effects	Experience	5	144.772	.000
	L_{peak}	2	131.788	.000
	L_{ex}	2	83.664	.000
	Occupation	4	74.312	.000
	Age	6	48.760	.000

In SPSS, one of the estimate parameters is the lambda coefficient. These parameters can be labeled as β coefficients and Exp (β) is the odds ratio (OR). The odds ratio is the measure of the effect size. The odds ratio of 1 indicates that there is no effect, a variable greater than 1 indicates that the variable in question increases the probabilities, and a variable less than 1 indicates that the variable decreases the rates. If the probability ratio is greater than 1, it can be said that a factor considered constitutes a significant risk for occupational diseases (Agresti, 2002). Second-order interaction results are given in Table 5.

Table 5. *Second-order interaction results for the log-linear model*

Effect	Variable	β	Exp(β)
Occupation×L_{ex}	Driver×78.26-85.10	.119	1.126
	Operator×71.4-78.25	.064	1.066
	Driver×71.4-78.25	-.079	0.924
Age×Experience	21-29 age×1-8 years	.192	1.212
	57-65 age×33-40 years	.070	1.073
	30-38 age×1-8 years	.069	1.071
Occupation×L_{peak}	Driver×138.6-143	.103	1.108
	Technical staff×134.1-138.5	.067	1.069
	Operator×138.6-143	.040	1.041

When the 2nd order interactions in Table 5 were evaluated Occupation×L_{ex} interaction shows that drivers and operators have a high possibility of NIHL in 71.4-78.25 and 78.26-85.10 dB(A) noise levels. Similarly, when Age×Experience association is evaluated, it can say that 21-29 age group with 1-8 years of experience has a high possibility of NIHL. Additionally, 57- 65 age group with 33-40 years of experience is mostly exposed to NIHL. Moreover, it can be said that, drivers and operators exposed to noise in 138.6-143 dB(C) have high risk. It is obvious that the higher the noise level exposed, the higher the possibility of hearing loss for drivers and operators. It is seen that the youngest employee group with less experience considered in this study has a high probability of hearing loss.

3. Discussion

Occupational diseases are among the most important risks to which employees must be protected and can be prevented by taking the necessary precautions in the working environment and for the employees at an early stage. LRA and HLA methods used in categorical data analysis can be used to evaluate the factors that affect the occurrence of occupational diseases. While LRA evaluates all employees with and without illness within a population, HLA can only be used to evaluate employees with occupational diseases. While the purpose of using LRA is to develop a prediction model, the purpose of HLA is to examine the factors in the occurrence of occupational disease and the interactions of these factors. Standard ISO 1999 (2013) can be used to estimate the risk of noise-induced hearing loss. With this standard, noise-related hearing losses can be estimated for each employee, taking into account age, noise, and experience periods.

When the presence of NIHL was examined with the logistic regression model, according to the field staff, operator is 6.29 times more likely to not have NIHL, and driver is 5.41 times more likely to not have NIHL. In other words, it can be said that the NIHL probability of field staff is approximately 6 times higher than the probability of operators and drivers. The reduction in NIHL of operators and drivers is due to the adaptation of the work equipment to technological developments. As the noise exposures of the field staff working beside the high capacity mining equipment are generally high, the probability of hearing loss increases. It was found that the probability of NIHL was 11.4 times higher in the 57-65 age group and 4.41 times higher in the 48-56 age group according to in the 21-29 age group. NIHL has been found to increase with increasing age.

When the data of the employees with the presence of hearing loss were examined by HLA; the factors affecting the likelihood of having NIHL were found to be experience, maximum noise level, average noise exposure level, occupation, and age respectively. It was found that Age×Experience interaction had the highest effect on the probability of NIHL, followed by Occupation×Lpeak and Occupation×L_{ex} interactions. Employees in the 21-29 age group with 1-8 years of experience are likely to experience hearing loss. It was determined that drivers were exposed to average exposure levels of 78.26 - 85.10 dB (A) and were more likely to NIHL. It can be said that drivers are exposed to maximum noise of 138.6-143 dB (C), which increases hearing loss. It can be said that if drivers and operators are exposed to noise without personal protection under normal working conditions, their possibility of hearing loss will increase. The reason for this can be explained by the fact that drivers and operators are more exposed to the noise generated by mining machines when idling or fully accelerated, compared to other occupational groups. The majority of young workers and those with less experience are field staff. Therefore, the possibility of hearing loss in this occupational group should not be overlooked in the interaction of Age×Experience.

Conclusion

Noise-induced hearing loss is one of the most common occupational diseases encountered in mining and various parameters are effective in its formation. Within the scope of the study, these parameters were determined as miners' age, experience, occupation, L_{ex}, and L_{peak}. It was found that the probability of NIHL for field

personnel is approximately 6 times higher than that of operators and drivers. It has been found that NIHL increases up to 11 times with age. With the developed logistic regression model, NIHL can be successfully predicted in this enterprise and similar studies can be performed in other enterprise. Age × experience, occupation × maximum noise levels and occupation × average noise exposure levels are the interactions that has the highest impact on the probability of NIHL. In order to prevent NIHL in enterprises, it is necessary to follow the technological developments in equipment selection, organize the working environment, provide training and take personal precautions. In addition, the use of personal protective equipment must be supervised. To prevent occupational diseases and to eliminate the risks that may be encountered, personal exposure levels must be below the legal limits and the measurements are carried out periodically.

Acknowledgements

The authors would like to thank the authorities of the Turkish Coal Enterprises for their valuable understanding in the data provision and evaluation during the work undertaken.

References

Agresti, A. 2002. Categorical Data Analysis. New Jersey: John Wiley and Sons. Inc.

Bauer, E.R., Babich, D.R., Vipperman, J.R. 2006. Equipment noise and worker exposure in the coal mining industry (No. 9492). Department of Health and Human Services, Public Health Service, Centers for Disease Control and Prevention, National Institute for Occupational Safety and Health, Pittsburgh Research Laboratory.

Concha-Barrientos, M., Campbell-Lendrum, D., Steenland, K. 2004. Occupational noise: assessing the burden of disease from work-related hearing impairment at national and local levels. WHO Environmental Burden of Disease Series, No:9, Geneva

Goelzer, B.I.F. 2001. Hazard prevention and control programmes. Goelzer, B., Hansen, C.H., Sehrndt, G.A. (Ed.). Occupational Exposure to Noise: Evaluation, Prevention and Control, WHO, Geneva, 233-244.

Hong, O., Kerr, M.J., Poling, G.L., Dhar, S. 2013. Understanding and preventing noise-induced hearing loss. Disease-a-Month 59(4):110-118. doi:10.1016/j.disamonth.2013.01.002

ISO 1999. 2013. Acoustics—estimation of noise-induced hearing loss, in international standard. ISO, Switzerland

Iwasaki, Y., Fukaya, K., Fuchida, S., Matsumoto, S., Araoka, D., Tokoro, C., Yasutaka, T. 2021. Projecting future changes in element concentrations of approximately 100 untreated discharges from legacy mines in Japan by a hierarchical log-linear model. Science of the Total Environment, 786, doi:10.1016/j.scitotenv.2021.147500

Kovalchik, P.G., Matetic, R.J., Smith, A.K., Bealko, S.B. 2008. Application of prevention through design for hearing loss in the mining industry. Journal of Safety Research, 39(2), 251-254. doi:10.1016/j.jsr.2008.02.029

Kursunoglu, N., Gogebakan M. 2021. Prediction of spontaneous coal combustion tendency using multinomial logistic regression, International Journal of Occupational Safety and Ergonomics, doi: 10.1080/10803548.2021.1944535

Maiti, J., Bhattacherjee, A., Bangdiwala, S.I. 2001. Loglinear model for analysis of cross-tabulated coal mine injury data. Injury control and safety promotion, 8(4), 229-236. doi:10.1076/icsp.8.4.229.3335

Nelson, D.I., Nelson, R.Y., Concha-Barrientos, M., Fingerhut, M. 2005. The global burden of occupational noise-induced hearing loss. American Journal of Industrial Medicine, 48(6), 446-458. doi:10.1002/ajim.20223

Official Gazette. 2013. Regulation on protection of employees from noise related risks. No. 28721. https://www.resmigazete.gov.tr/eskiler/2013/07/20130728-11.htm. [Accessed 02 August 2013].

Onder, M., Demir Iroz, B., Onder, S. 2021. Using categorical data analyses in determination of dust-related occupational diseases in mining, International Journal of Occupational Safety and Ergonomics. 27(1),112-120. doi:10.1080/10803548.2018.1531535

Onder, S. 2013. Evaluation of occupational injuries with lost days among opencast coal mine workers through logistic regression models. Safety Science. 59, 86-92. doi:10.1016/j.ssci.2013.05.002

Onder, S., Mutlu, M. 2017. Analyses of non-fatal accidents in an opencast mine by logistic regression model - a case study. International Journal of Injury Control and Safety Promotion. 24(3), 328-337. doi:10.1080/17457300.2016.1178299

Phillips, J.I., Heyns, P.S., Nelson, G. 2007. Rock drills used in South African mines: a comparative study of noise and vibration levels. The Annals of occupational hygiene, 51(3), 305-310. doi:10.1093/annhyg/mel082

Picard, M., Girard, S.A., Simard, M., Larocque, R., Leroux, T., Turcotte, F. 2008. Association of work-related accidents with noise exposure in the workplace and noise-induced hearing loss based on the experience of some 240,000 person-years of observation. Accident Analysis & Prevention, 40(5), 1644-1652. doi:10.1016/j.aap.2008.05.013

Sensogut, C., Cinar, I. 2007. An empirical model for the noise propagation in open cast mines–A case study. Applied Acoustics, 68(9), 1026-1035. doi:10.1016/j.apacoust.2006.04.016

Sharma, O., Mohanan, V., Singh, M. 1998. Noise emission levels in coal industry. Applied Acoustics, 54(1), 1-7. doi:10.1016/S0003-682X(97)00073-X

TS 2607 ISO 1999. 2005. Acoustics - Determination of occupational noise exposure and estimation of noise-induced hearing impairment. ISO, Ankara (in Turkish).

Vipperman, J. S., Bauer, E.R., Babich, D.R. 2007. Survey of noise in coal preparation plants. The Journal of the Acoustical Society of America,

Madencilik - Mining, 2022, 61(1), 25-30

BİLİMSEL MADENCİLİK DERGİSİ
SCIENTIFIC MINING JOURNAL

TMMOB Maden Mühendisleri Odası Yayını / The Publication of the Chamber of Mining Engineers of Turkey

www.mining.org.tr

Original Research / Orijinal Araştırma

Predicting screening/classification products via the pseudorandom number selection routine

Eleme ve sınıflandırma ürünlerinin sözde rastgele sayı üretme rutiniyle tahmini

Mahmut Camalan[a,*]

[a] *Ankara, TÜRKIYE*

Geliş-Received: 3 Haziran - June 2021 • Kabul-Accepted: 23 Eylül - September 2021

A B S T R A C T

Screening/classification is performed for the separation of particles by their sizes. There are empirical, phenomenological, and numerical models for predicting the size distributions of screening/classification products. This paper introduces a new algorithm for the same purpose, which partially mimics phenomenological and numerical models. The algorithm iteratively selects the monosize fractions with pre-defined probabilities, then carries particle masses from the selected fractions either to the oversize or undersize product. The applicability of the algorithm was validated against the product size distributions from some industrial-scale screening/classification equipment - namely rake classifier, sieve bend (0.212 mm), vibrating screen (20 mm), and hydrocyclone - which are provided in the literature. The results show that the algorithm is predictive if each particle has a selection probability proportional to the mass of its monosize fraction and some power of its diameter. Results also suggest that vibrating screens can provide the sharpest size separation.

Keywords: Screening, Classification, Pseudorandom number generation, Particle selection, Algorithm

Introduction

Screening/classification operations include the separation of minerals or other particulate materials based on their sizes. Comprehensive reviews on the fundamentals of both operations are provided in the relevant literature (Gupta and Yan, 2016; Mular, 2009; Wills and Finch, 2016): The separation in screening is achieved by carrying the particles to screen apertures, which are either retained over or pass through the apertures. Meanwhile, the particles are classified under a moving fluid such that they are separated by their velocities in the fluid. The choice for screening/classification generally depends on the size distribution of the feed material: The latter is preferred over the former if the feed particles are finer, which may cause blinding at screen apertures. However, some successful attempts have been made to replace hydrocyclones with high-frequency vibration screens (Dündar, 2020; Frausto et al., 2021).

Three main approaches, namely empirical (Austin, et al., 1984; Coelho and Medronho, 1992; King, 2012; Mular, 2009; Nageswararao et al., 2004; Napier-Munn and Lynch, 1992; Wills and Finch, 2016), phenomenological (Elskamp and Kruggel-Emden, 2015; Heiskanen, 1996; King, 2012; Muñoz et al., 2017; Nageswararao et al., 2004; Napier-Munn and Lynch, 1992; Wills and Finch, 2016), and numerical (Elskamp and Kruggel-Emden, 2015; Heiskanen, 1996; Khoshdast et al., 2017; Mangadoddy et al., 2020; Narasimha et al., 2007; Wills and Finch, 2016) models, are adopted for predicting the coarse and fine product size distributions of screening/ classification process. Empirical models are the mathematical functions - e.g., partition curves (Gupta and Yan, 2016; Svarovsky and Svarovsky, 1992) - to predict the process outputs although they cannot describe the separation process. Phenomenological models - e.g., first-order screening kinetics (Elskamp and Kruggel-Emden, 2015) and particle velocity equations in hydrocyclone (Heiskanen, 1996) - are the semi-empirical functions that are based on the fundamental aspects of separation. Numerical models use the iterative computation routines - e.g., (i) Discrete Element Model (Davoodi et al., 2019; Dong and Yu, 2012; Elskamp and Kruggel-Emden, 2015; Kruggel-Emden and Elskamp, 2014; Zhao et al., 2016) for vibrating screens/ sieve bends, (ii) Computational Fluid Dynamics (Khoshdast et al.,

* Corresponding author / Sorumlu yazar: camalanmahmut@gmail.com • https://orcid.org/ 0000-0001-7071-7910

https://doi.org/10.30797/madencilik.947610

2017; Mangadoddy et al., 2020; Narasimha et al., 2007) and their coupling (Mangadoddy et al., 2020; Tang et al., 2018) for hydrocyclones/hydraulic classifiers - to predict the motion of particles in the separation vessels.

This paper presents a computational algorithm to predict the size distributions of oversize (coarse) and undersize (fine) products of different screening/classification operations. The algorithm implements a pseudorandom number generator into a particle selection routine, which iteratively distributes particles to the coarse or fine product. The proposed algorithm mimics (i) the phenomenological models by taking account of the size-mass balance, and (ii) the numerical models by iterative carriage of particles to the coarse or fine product. However, the algorithm cannot predict the percentage of water recovery from feed to undersize (or oversize) at wet classification. The applicability of the algorithm was validated against the coarse and fine product size distributions of some industrial-scale separations (Austin et al., 1984; Olson and Turner, 2002) that were performed with the rake classifier, sieve bend (0.212 mm), vibrating screen (20 mm), and hydrocyclone.

1. Experimental methodology

Figure 1 demonstrates the flowsheet for the simulation of screening/classification. The algorithm started by selecting a size fraction from the initial feed mass, using the pseudorandom selection routine through the pre-defined selection probabilities. The mass of the mean particle of the selected size fraction was removed from the feed and further moved to the same size fraction of the undersize product. Then, the masses and the size distributions of the remaining feed and undersize product were calculated. The mean particle masses were (i) successively selected from the feed size fractions and (ii) moved to corresponding undersize fractions until the simulated 80 % passing size (d_{80}) of the remaining feed exceeded the experimental d_{80} of oversize. The remaining feed mass was then assigned to the oversize product. Finally, the simulated masses and size distributions of the oversize and undersize products were calculated. The simulated data were compared with the corresponding data of experimental products. During the successive particle selection stage, the masses of particles were calculated assuming that they were spherical. The mean particle size of each size fraction, except the finest unbounded size fraction (pan), was taken as the geometric mean of its lower and upper screen sizes. Meanwhile, the mean particle size of the pan was taken as the average between the aperture size of the finest screen and zero.

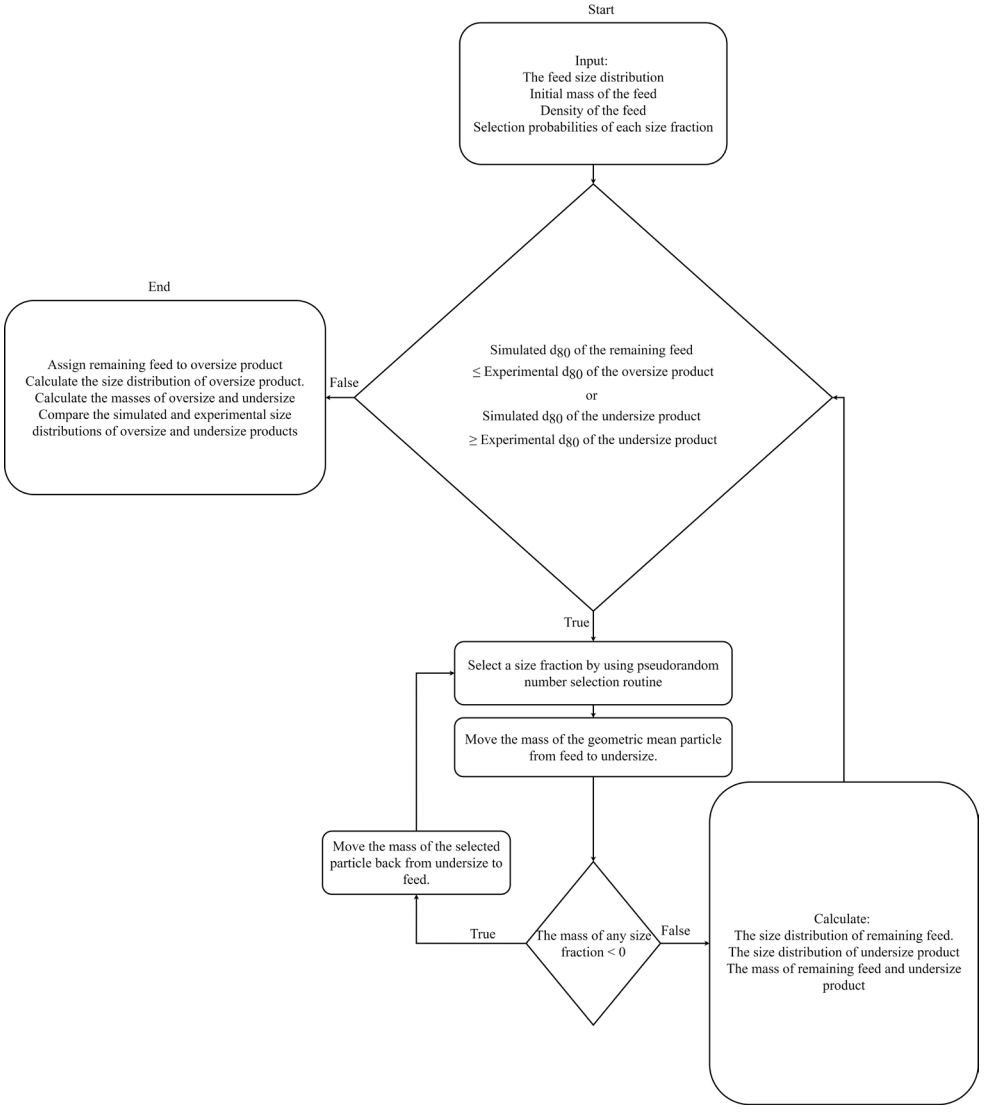

Figure 1. *The flowsheet for the simulation of screening/classification by selecting and carrying feed particles to undersize product*

Each particle selection event was simulated by using the MATLAB's built-in DATASAMPLE function. The routine used the MATLAB's built-in DATASAMPLE function to generate the integer index of a size fraction for particle selection (Figure 1). The function used the Mersenne Twister algorithm (Matsumoto and Nishimura, 1998) coupled with a binary search tree algorithm (Wong and Easton, 1980) for the weighted sampling of the data. The size fractions were selected with a probability (p_i) being proportional to their mass (m_i) and a power (n) of its geometric mean diameter (x_i):

$$p_i = \frac{m_i x_i^n}{\sum_{i=1}^{z}(m_i x_i^n)} \quad \textit{(Camalan, 2021)} \qquad (1)$$

where i=1 is the top size fraction, and z is the sink size fraction of the feed.

The algorithm was tested against the coarse and fine product size distributions of some industrial-scale separations achieved at (i) a rake classifier, (ii) a sieve bend (0.212 mm), (iii) a vibrating screen (20 mm), and (iv) a hydrocyclone. The experimental feed and product (oversize, undersize) size distributions at (i)-(ii)-(iii) were taken from Austin et al. (1984). Meanwhile, the respective experimental size distributions at (iv) were taken from Olson and Turner (2002). However, it was not explicitly stated whether the experimental size distribution errors were reduced by performing mass balancing around (i)-(iv). For the purpose of simulation, the feeds for (i) and (iii) were assumed as quartz (density = 2.75 g/cm^3) while the feeds for (ii) and (iv) were coal (1.3 g/cm^3) and iron ore (3 g/cm^3), respectively. The top size fractions that had been unbounded in the experimental feed size distributions were discarded from the simulation and evaluation. The total mass of oversize product after an experimental screening/classification process was estimated by averaging mass balances on the experimental size distribution curves:

$$Oversize\ or\ Coarse\ Mass\ (\%\ Feed\ Mass) = \frac{\sum_j 100 * \frac{U_j - F_j}{U_j - O_j}}{q}, U_j \neq O_j \qquad (2)$$

where q is the total number of screens around which the mass balances are taken. F_j, U_j, and O_j are the cumulative masses % of feed, undersize, and oversize, respectively, which are passing through the screen j.

2. Results and discussion

Table 1 shows the simulated and experimental masses of oversize (coarse) and undersize (fine) products of the different screening/classification equipment. The results show that simulated masses are comparable to experimental masses, indicating the algorithm's success in predicting the separation products. Meanwhile, Figure 2 demonstrates the experimental and simulated size distributions of oversize and undersize products of the rake classifier (Figure 2a), the sieve bend (Figure 2b), the vibrating screen (Figure 2c), and the hydrocyclone (Figure 2d). The experimental feed size distributions are also shown with symbols in the figure. Figure 2a-d shows that the simulated size distributions of oversize and undersize products shift downwards and upwards from their corresponding feed size distributions, respectively. In other words, the simulated oversize is qualitatively coarser than its feed, yet the simulated fine product is finer. This suffices to prove that the algorithm can make logical predictions on the separation products. Figure 2 also shows that all simulated size distributions of undersize products agree quite well with the respective experimental size distributions. However, the simulated size distributions of coarse products may deviate from the respective experimental curves at the fine size scale. Such deviations are visible between the simulated and experimental curves of the coarse products of rake classifier (Figure 2a), sieve bend (Figure 2b), and vibrating screen (Figure 2c). A possible reason for these deviations may be the misclassification of fines to the coarse product in the screening/classification operations, which may not be reflected in the particle selection routine (Section 2). Some operational factors that may cause the fines' misclassification can be defined as (i) insufficient drainage and passage of fine particles to the screen aperture (Dong et al., 2013), and (ii) bypassing of fines with water flow in classifiers (Kelly, 1991).

Table 1. *The simulated and experimental masses of the oversize products of the screening/classification equipment*

Equipment	Oversize Mass (% of the Feed)	
	Simulated	Experimental
Rake Classifier	55.49	62.16
Sieve Bend	50.55	55.45
Vibrating Screen	32.90	32.89
Hydrocyclone	66.06	59.97

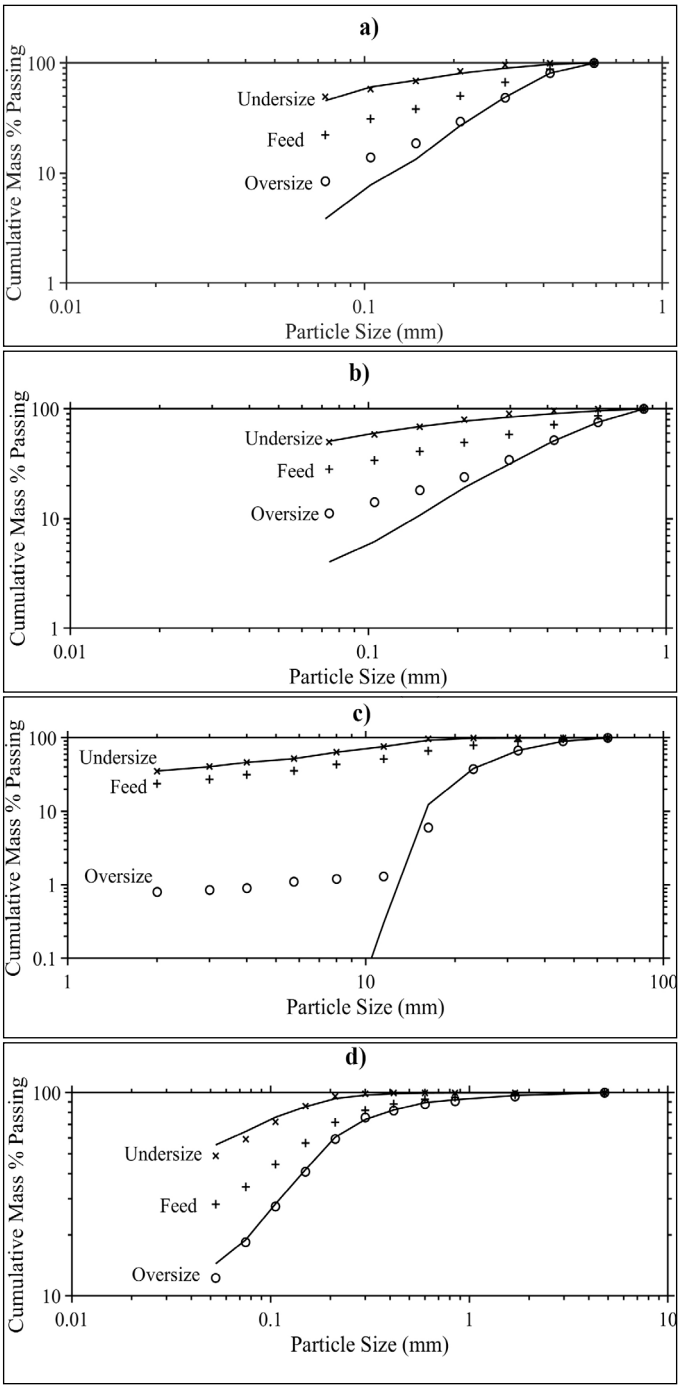

Figure 2*. The experimental (symbols) and simulated (lines) size distributions of oversize and undersize products of (a) rake classifier, (b) sieve bend, (c) vibrating screen, and (d) hydrocyclone. The experimental feed size distributions are also included in the figure. The experimental size distributions in (a)-(c) and (d) were taken from Austin et al. (1984), and Olson and Turner (2002), respectively.*

Table 2 shows the 'n' values used to generate the probabilities (Equation 1) for the selection of particles to undersize products at different screening/classification equipment. The table shows that the 'n' values required to simulate the products at rake classifier, sieve bend and hydrocyclone are similar to each other. However, the respective 'n' value for the vibrating screen are visibly the lowest. Using lower 'n' values must provide more chance for relatively finer particles to get selected into the undersize product, as indicated by Equation 1. Therefore, this result strongly suggests that the vibrating screens can outperform sharp separation of fine particles from the coarse ones. Some additional evidences are also available in the literature showing that the vibrating screens yield sharper tromp curves as compared to hydrocyclones (Dündar, 2020; Wills and Finch, 2016).

Table 2. *The 'n' values used to generate the probabilities (Equation 1) for particle selection to undersize products of different screening/classification equipment*

Equipment	"n" value (Equation 1)
Rake Classifier	-4.5
Sieve Bend	-4.25
Vibrating Screen	-6.5
Hydrocyclone	-4.2

The default form of the algorithm is to select and carry particles from feed to undersize product till the simulated d_{80} of the remaining feed is larger than the experimental d_{80} of oversize product (Figure 1). Also, the algorithm can be revised in a way that the feed particles were selected and carried to the oversize product (Figure 3). In this case, the algorithm is executed till the simulated d_{80} of the remaining feed is lower than the experimental d_{80} of the undersize product. The applicability of this revised algorithm was also tested against the experimental product size distributions of the rake classifier, the sieve bend, the vibrating screen, and the hydrocyclone (Section 2). Figure 4 shows that the simulated and experimental product size distributions are in good agreement when the selection probability of feed particles to oversize product is calculated by the p_i formulation (Equation 1). Table 3 also shows the simulated masses of oversize (coarse), which are comparable to the experimental masses (Table 1).

Table 3. *The simulated masses of the oversize products of the screening/classification equipment*

Equipment	Simulated Oversize Mass (% of the Feed)
Rake Classifier	62.70
Sieve Bend	57.49
Vibrating Screen	33.18
Hydrocyclone	67.63

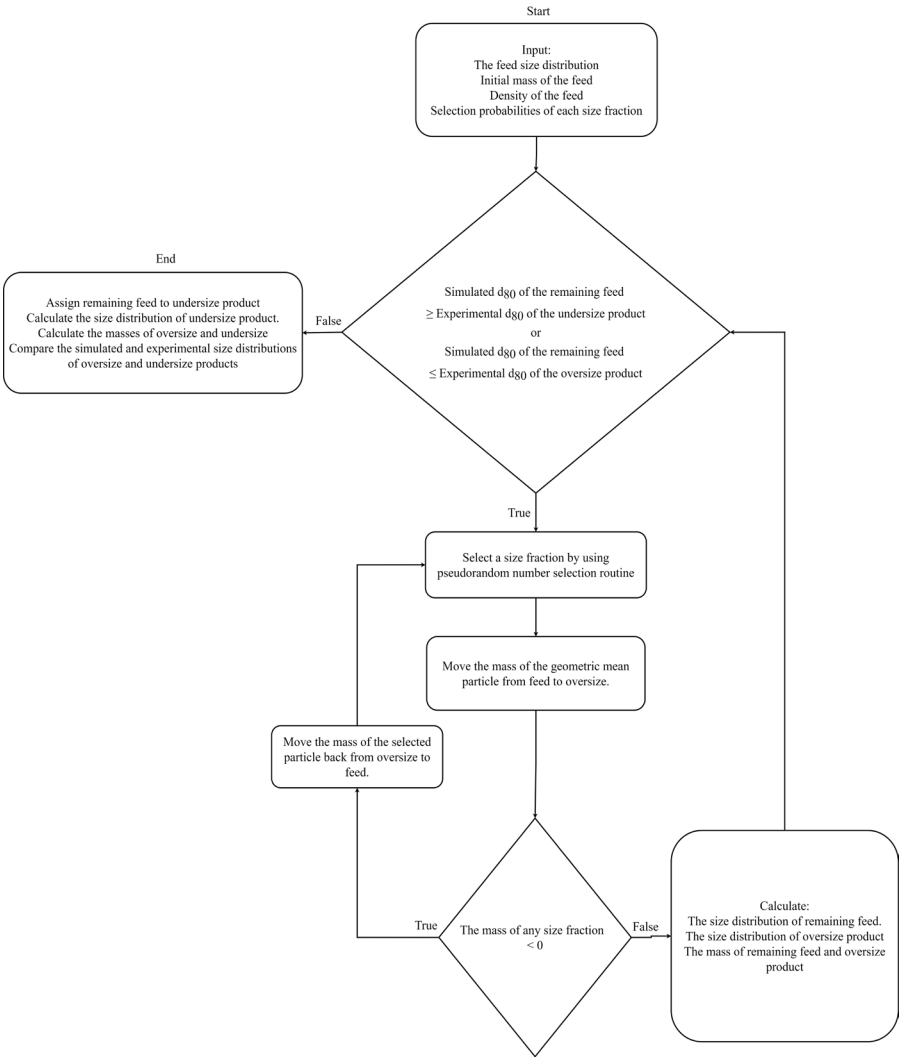

Figure 3. *The flowsheet for the simulation of screening/classification by selecting and carrying feed particles to oversize product*

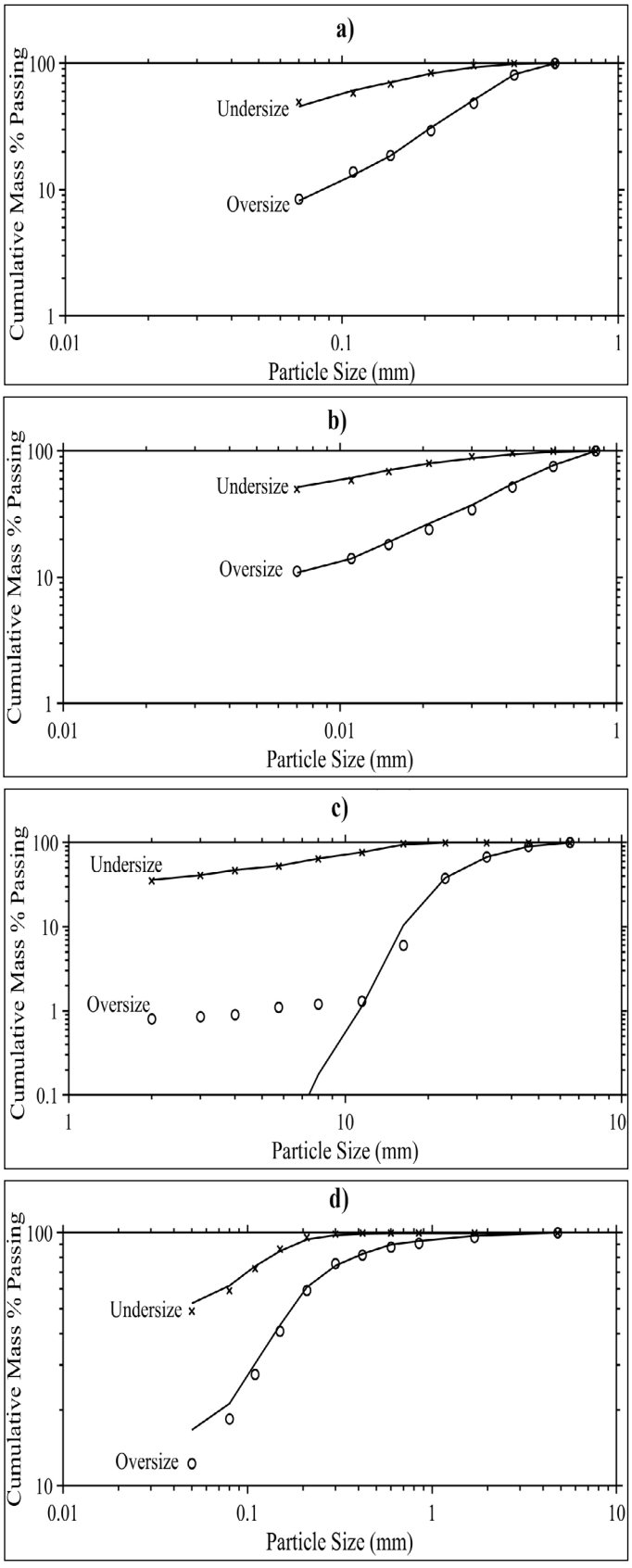

Figure 4. *The experimental (symbols) and simulated (lines) size distributions of coarse and fine products of (a) the rake classifier, (b) the sieve bend, (c) the vibrating screen, and (d) the hydrocyclone. The simulated size distributions were produced by selecting and carrying feed particles to oversize products. The experimental size distributions in (a)-(c) and (d) were taken from Austin et al. (1984), and Olson and Turner (2002), respectively.*

Table 4 shows the 'n' values used to generate the selection probabilities (p_i) of particles for the oversize products. These values are quite higher than the respective 'n' values used to select particles for the undersize products (Table 2). Therefore, that coarse and fine particles in the feed have more chance to be carried to the oversize and undersize products, respectively. More importantly, if there is a large difference between the p_is, congruently the 'n' values, for oversize and undersize selection, a sharp size separation can be achieved. Referring to the 'n' exponents in Table 2 and Table 4, the greatest differences in the p_is are possible at vibrating screen, suggesting that it yields the sharpest size separation. When a particle is to be separated by a vibrating screen either to oversize or undersize fraction, its separation only depends on the particle dimensions and the aperture size of the screen. Meanwhile, the separation of a particle to oversize or undersize fraction is based on its motion (trajectory) in a classifier. However, this trajectory is not only affected by the particle size but also particle density (Wills and Finch, 2016). Therefore, it is very likely that vibrating screen should provide better size separation than the classifiers, as supported by sharper partition curves in the former (Dündar, 2020).

Table 4. *The '' values used to generate the (Equation 1) for the particle selection to oversize products of different screening/classification equipment*

Equipment	"n" value (Equation 1)
Rake Classifier	-1.8
Sieve Bend	-2
Vibrating Screen	+2
Hydrocyclone	-2.1

Conclusions

An algorithm is presented to predict the size distributions of oversize and undersize products of screening/classification operations. The algorithm mimics (i) the phenomenological models by taking account of the size-mass balance, and (ii) the numerical models by iterative carriage of particles to coarse or fine products. The algorithm iteratively (i) selects a monosize fraction, (ii) takes a particle from the size fraction, and (iii) carries the particle either to oversize or undersize product. The algorithm can predict the size distributions of screening/classification products if each particle has a selection probability proportional to the mass of its monosize fraction and some power of its diameter. Results also suggest that vibrating screens can provide the sharpest size separation.

References

Austin, L. G., Klimpel, R. R., Luckie, P. T. 1984. Process Engineering of Size Reduction: Ball Milling. New York: AIME.

Camalan, M. 2021. A Computational Algorithm to Understand the Evolution of Size Distribution with Successive Breakage Events at Grinding. Environmental Sciences Proceedings, 6 (1), 7. https://doi.org/10.3390/iecms 2021-09381.

Coelho, M. A. Z., Medronho, R. A. 1992. An Evaluation of the Plitt and Lynch & Rao Models for the Hydrocyclones. In L. Svarovsky and T. M. Thew (Eds.), Hydrocyclones Analysis and Applications, Southampton: Kluwer Academic Publishers, 63-72.

Davoodi, A., Asbjörnsson, G., Hulthén, E., Evertsson, M. 2019. Application of the Discrete Element Method to Study the Effects of Stream Characteristics on Screening Performance. Minerals, 9 (12), 788. https://doi.org/10.3390/min9120788.

Dong, K. J., Wang, B., Yu, A. B. 2013. Modeling of particle flow and sieving behavior on a vibrating screen: From discrete particle simulation to process performance prediction. Industrial and Engineering Chemistry Research, 52 (33), 11333–11343. https://doi.org/10.1021/ie3034637

Dong, K. J., and Yu, A. B. 2012. Numerical simulation of the particle flow and sieving behaviour on sieve bend/low head screen combination. Minerals Engineering, 31, 2–9. https://doi.org/10.1016/j.mineng.2011.10.020

Dündar, H. 2020. Investigating the benefits of replacing hydrocyclones with high-frequency fine screens in closed grinding circuit by simulation. Minerals Engineering, 148 (January), 106212. https://doi.org/10.1016/j.mineng.2020.106212

Elskamp, F., Kruggel-Emden, H. 2015. Review and benchmarking of process models for batch screening based on discrete element simulations. Advanced Powder Technology, 26 (3), 679–697. https://doi.org/10.1016/j.apt.2014.11.001

Frausto, J. J., Ballantyne, G. R., Runge, K., Powell, M. S., Wightman, E. M., Evans, C. L., Gonzalez, P., Gomez, S. 2021. The effect of screen versus cyclone classification on the mineral liberation properties of a polymetallic ore. Minerals Engineering, 169 (April), 106930. https://doi.org/10.1016/j.mineng.2021.106930

Gupta, A., Yan, D. 2016. Mineral Processing Design and Operations. Amsterdam: Elsevier.

Heiskanen, K. G. H. 1996. Developments in wet classifiers. International Journal of Mineral Processing, 44–45 (SPEC. ISS.), 29–42. https://doi.org/10.1016/0301-7516(95)00015-1

Kelly, E. G. 1991. The significance of by-pass in mineral separators. Minerals Engineering, 4 (1), 1–7. https://doi.org/10.1016/0892-6875(91)90113-A

Khoshdast, H., Shojaei, V., Khoshdast, H. 2017. Combined application of computational fluid dynamics (CFD) and design of experiments (DOE) to hydrodynamic simulation of a coal classifier. International Journal of Mining and Geo-Engineering, 51 (1), 9–22. https://doi.org/10.22059/ijmge.2016.218483.594634

King, R. P. 2012. Modeling and Simulation of Mineral Processing Systems (C. L. Schneider and E. A. King, eds.). Littleton: SME.

Kruggel-Emden, H., Elskamp, F. 2014. Modeling of screening processes with the discrete element method involving non-spherical particles. Chemical Engineering and Technology, 37 (5), 847–856. https://doi.org/10.1002/ceat.201300649

Mangadoddy, N., Vakamalla, T. R., Kumar, M., Mainza, A. 2020. Computational modelling of particle-fluid dynamics in comminution and classification: a review. Mineral Processing and Extractive Metallurgy: Transactions of the Institute of Mining and Metallurgy, 129 (2), 145–156. https://doi.org/10.1080/25726641.2019.1708657

Matsumoto, M., Nishimura, T. 1998. Mersenne Twister: A 623-Dimensionally Equidistributed Uniform Pseudo-Random Number Generator. ACM Transactions on Modeling and Computer Simulation, 8 (1), 3–30. https://doi.org/10.1145/272991.272995

Mular, A. L. 2009. Size Separation. In M. C. Fuerstenau and K. Han (Eds.), Principles of Mineral Processing, Littleton: SME, 119–172.

Muñoz, D. A., Diaz, J. L., Taborda, S., Alvarez, H. 2017. Hydrocyclone Phenomenological-Based Model and Feasible Operation Region. International Journal of Mining, Materials, and Metallurgical Engineering, 3, 1–9.

Nageswararao, K., Wiseman, D. M., Napier-Munn, T. J. 2004. Two empirical hydrocyclone models revisited. Minerals Engineering, 17 (5), 671–687. https://doi.org/10.1016/j.mineng.2004.01.017

Napier-Munn, T. J., Lynch, A. J. 1992. The modelling and computer simulation of mineral treatment processes - current status and future trends. Minerals Engineering, 5 (2), 143–167. https://doi.org/10.1016/0892-6875(92)90039-C

Narasimha, M., Brennan, M., Holtham, P. N. 2007. A Review of CFD Modelling for Performance Predictions of Hydrocyclone. Engineering Applications of Computational Fluid Mechanics, 1 (2), 109–125. https://doi.org/10.1080/19942060.2007.11015186

Olson, T. J., Turner, P. A. 2002. Hydrocyclone selection for plant design. In A. L. Mular, N. D. Halbe, and D. J. Barratt (Eds.), Mineral Processing Plant Design, Practice, and Control Proceedings, Littleton: SME, Volumes 1-2, 880–893.

Svarovsky, L., Svarovsky, J. 1992. A New Method of Testing Hydrocyclone Grade Efficiencies. In L. Svarovsky and T. M. Thew (Eds.), Hydrocyclones Analysis and Applications, Southampton: Kluwer Academic Publishers, 68-70.

Tang, Z., Yu, L., Wang, F., Li, N., Chang, L., Cui, N. 2018. Effect of particle size and shape on separation in a hydrocyclone. Water (Switzerland), 11 (1), 1–19. https://doi.org/10.3390/w11010016

Wills, B. A., Finch, J. A. 2016. Wills' Mineral Processing Technology. Amsterdam: Elsevier.

Wong, C. K., Easton, M. C. 1980. An Efficient Method for Weighted Sampling without Replacement. SIAM Journal on Computing, 9 (1), 111–113. https://doi.org/10.1137/0209009

Zhao, L., Zhao, Y., Bao, C., Hou, Q., Yu, A. 2016. Laboratory-scale validation of a DEM model of screening processes with circular vibration. Powder Technology, 303, 269–277. https://doi.org/10.1016/j.powtec.2016.09.034

Madencilik - Mining, 2022, 61(1), 31-40

BİLİMSEL MADENCİLİK DERGİSİ
SCIENTIFIC MINING JOURNAL
TMMOB Maden Mühendisleri Odası Yayını / The Publication of the Chamber of Mining Engineers of Turkey

www.mining.org.tr

Original Research / Orijinal Araştırma

Kalsitik ve dolomitik kireçtaşlarının çimentolu macun dolgunun çevresel davranışına etkisi

Effect of calcitic and dolomitic limestones on environmental behavior of cemented paste backfill

Tekin Yılmaz[a,*] , Bayram Erçıkdı[b,**]

[a] *Abdullah Gül Üniversitesi, Nanoteknoloji Mühendisliği Bölümü, Kayseri, TÜRKİYE*
[b] *Karadeniz Teknik Üniversitesi, Maden Mühendisliği Bölümü, Trabzon, TÜRKİYE*

Geliş-Received: 8 Temmuz - July 2021 • Accepted: 27 Eylül - September 2021

ÖZ

Çimentolu macun dolgunun (ÇMD) dayanım ve duraylılığını iyileştirmek için ÇMD'de bağlayıcı veya atık yerine alkali özelliğe sahip birçok malzeme ikame veya ilave olarak kullanılmaktadır. Fakat bu alkali malzemelerin ÇMD'nin yeraltı suyu kirliliği üzerindeki etkisinin kapsamlı bir şekilde araştırılması gerekmektedir. Bu çalışmada, ÇMD karışımında sülfürlü maden atığı (S-MA) yerine ikame (ağırlıkça %10) olarak kalsitik ve dolomitik kireçtaşı (KK ve DK) kullanılmasının ÇMD'nin uzun dönem çevresel davranışına etkileri araştırılmıştır. Bu amaçla, ÇMD numuneleri 360 güne kadar dinamik tank liçi testlerine tabi tutulmuş ve elde edilen sızıntı suları üzerinde pH, sülfat (SO_4^{2-}) ve ağır metal analizleri gerçekleştirilmiştir. Ayrıca, mineraloji ve mikroyapı özelliklerinin ÇMD'nin çevresel davranışına etkisi X-ışınları difraktometre ve porozite testleri ile incelenmiştir. Bulgular, KK ve DK kullanımı ile sızıntı suyu pH'ının alkali seviyelerde seyrettiğini ve SO_4^{2-} salınımının önemli ölçüde azaltıldığını göstermiştir. Dahası, KK ve DK ikameli ÇMD numunelerindeki daha yoğun mikroyapı ÇMD'den ağır metallerin (Cu, Mo ve Pb hariç) salınımının engellenmesine veya büyük ölçüde azaltılmasına katkı sağlamıştır. Sonuçlar, ÇMD'nin mekanik özelliklerinin yanısıra yeraltı suyu kirliliği üzerindeki etkisinin de dikkatle değerlendirilmesinin gerektiğini ortaya koymaktadır.

Keywords: Kalsitik-dolomitik kireçtaşı, Çevresel davranış, Dinamik tank liçi, Ağır metal

ABSTRACT

To enhance the strength and stability of cemented paste backfill (CPB), many alkaline materials are utilised as replacement or additive to binder or tailings in CPB. However, the effect of these materials on groundwater pollution of CPB needs to be comprehensively investigated. In this study, effects of the utilization of calcitic and dolomitic limestone (CL and DL) as replacement (10 wt.%) to sulphide mine tailings (S-MT) in CPB mixture on the long-term environmental behaviour of CPB were investigated. For this purpose, CPB samples (CPBs) were subjected to dynamic tank leaching tests over 360-days and the analyses of pH, sulphate (SO_4^{2-}) and heavy metals (HMs) on the leachates were carried out. The effects of mineralogy and microstructure on the environmental behavior of CPBs were also examined by X-ray diffractometry and porosity tests. The findings showed that with the utilization of CL and DL, the pH of leachates remained at alkaline levels and the release of SO_4^{2-} was significantly reduced. Furthermore, the denser microstructure in CPBs of CL and DL contributed to be prevented or be remarkably reduced the HMs-releases (except Cu, Mo and Pb). The results reveal that the mechanical properties of CPB as well as its impact on the groundwater pollution should be carefully evaluated.

Keywords: Calcitic-dolomitic limestone, Environmental behaviour, Dynamic tank leaching, Heavy metal

Giriş

Metal madencilik sektöründe, değerli metallerin (Cu, Pb ve Zn vb.) kazanımında kullanılan flotasyon gibi cevher zenginleştirme işlemleri sırasında büyük miktarda ince öğütülmüş (<100µm) sülfürlü maden atığı (S-MA) açığa çıkmaktadır (Yılmaz vd., 2020). Avrupa Birliği, çimentolu macun dolgu (ÇMD) teknolojisinin açığa çıkan bu atıkların yeraltında güvenli bir şekilde depolanmasına imkân sunan en uygun atık yönetim tekniklerinden birisi olduğunu belirtmiştir (European Commission, 2018). ÇMD, susuzlandırılmış tesis atığı,

* Corresponding author / Sorumlu yazar: tekin.yilmaz@agu.edu.tr • https://orcid.org/0000-0003-3288-5192
** bercikdi@ktu.edu.tr • https://orcid.org/0000-0003-4900-5382

https://doi.org/10.30797/madencilik.967090

çimento (ağırlıkça %2-9) ve karışım suyundan oluşan kompozit bir mühendislik ürünüdür. ÇMD'nin ekonomik, teknik, operasyonel ve çevresel faydalarından dolayı, cevher üretimi sonucu oluşan yeraltı madeni açıklıklarının ÇMD ile doldurulması uygulaması son yıllarda tüm dünyada artmıştır (Yılmaz ve Ercikdi 2021). Sadece Avrupa'da 17 ÇMD tesisinin aktif ve 16'sının inşaat ve/veya kurulum aşamasında olduğunu belirten Yumlu (2020) bugün dünya genelinde en az 400 yeraltı ÇMD tesisi olduğunu ve 100'e yakınının ise proje, inşaat ve/veya kurulum aşamasında olduğunu bildirmiştir. ÇMD, maden atıklarının yaklaşık %50-55'inin yeraltı maden açıklıklarında depolanmasına imkân verir ve bu sayede, özellikle sülfür içeriği yüksek olan sorunlu maden atıklarının verimli bir şekilde bertaraf edilmesi, komşu kayaç formasyonlarının desteklenmesi, cevher kayıplarının ve seyrelmenin önlenmesi ile cevher kazanımının iyileştirilmesi, yüzey çökmelerinin önlenmesi, yerüstü depolama ve iyileştirme/onarma maliyetlerinin azaltılması veya ortadan kaldırılması sağlanır (Jiang vd., 2020; Koohestani vd., 2020; Yan ve Yilmaz, 2020; Cao vd., 2021). Ayrıca, ÇMD karışımlarında daha düşük oranda bağlayıcı kullanılması ve bu teknoloji ile büyük boyutlu cevher topuklarının üretilmesinin sağlanması işletme maliyetlerini azaltarak ciddi oranda ekonomik fayda sunar (Pokharel ve Fall, 2013; Ercikdi vd., 2017). Madeni alınmış üretim boşluklarının ÇMD ile doldurulması, yeraltı açıklıklarının duraylılığını koruyarak zemin, yan duvar ve tavan için tahkimat görevi görmesinin yanı sıra işçiler ve maden ekipmanları için güvenli çalışma platformlarının oluşturulması gibi çok sayıda teknik amaca hizmet eder. Dahası, ÇMD teknolojisinin kullanımı ile işçilik gereksinimlerinin azalması, maden üretim döngüsünün hızlanması ve madencilik faaliyetlerinin iyileştirilmesi sağlanır (Yilmaz ve Yilmaz, 2018). Ekonomik, teknik ve operasyonel avantajlarının yanı sıra, ÇMD, S-MA'nın çimentolu (alkali) ortamda güvenle depolanmasını sağlayarak yeraltı suyuna ağır metallerin (As, Zn, Cu, Pb, Cd, vb.) salınımını kolaylaştıran asit maden drenajını (AMD) azaltır. Ayrıca, ÇMD içerisine eklenen bağlayıcı ve asit nötralize edici malzemeler (mermer atığı: MA, yüksek fırın cürufu: YFC, C-sınıfı uçucu kül: C-UK, inşaat-yıkıntı atığı: İYA vb.) ÇMD'nin porozite ve geçirgenliğini (10^{-4}-10^{-7} m/s) düşürerek ÇMD'nin içindeki ve etrafındaki hava ve su akışını kısıtlar (Coussy vd., 2011; Ercikdi vd., 2017; Yilmaz ve Fall, 2017; Cihangir ve Akyol, 2018; Yang vd., 2020, Yılmaz vd., 2018; Yılmaz vd., 2020; Yılmaz vd., 2021).

Maden çıkarma işlemleri esnasında yüzeyden ve/veya yeraltından gelen ve kirletici bileşenler içerebilen sular yeraltı madeni tabanına gönderilir ve oradan dışarı deşarj edilir. Bu yüzden, madeni alınmış yeraltı açıklıklarında depolanan ÇMD, uzun yıllar (30 yıl vb.) boyunca yeraltı su seviyesinin (YSS) üzerinde kalabilir. Bu durumda, özellikle uzun dönemde, S-MA içeren ve YSS'nin üzerinde olan ÇMD kütlesinde atmosferik koşullara bağlı oksidasyon meydana gelebilir ve oksidasyon sonucu yeraltı suyunu kirletme potansiyeline sahip yüksek miktarda asit ve ağır metal salınımı oluşabilir. Dahası, tesise geri gönderilen proses suyunun tikinerlerde koyulaştırılmasıyla bu ağır metallerin çoğunun geri kazanılmasına rağmen çok sayıda ağır metal türü içeren bir miktar proses suyu ÇMD kütlesi tarafından yeraltına gönderilebilir. Fakat madendeki çalışmalar sona erdikten ve maden kapatma işlemi başladıktan sonra, YSS yükselebilir ve ÇMD kütlesi YSS'nin altında kalabilir. Bu durumda ise, cevher üretimi ve dolgu uygulaması sürecinde ÇMD kütlesinde üretilen ve depolanan oksidasyon ürünleri (asit, sülfat ve ağır metaller) salınabilir ve yeraltı suyunu kirletebilir. Öte yandan, ÇMD kütlesi su altında kaldığında, ÇMD içindeki yeterli su doygunluğu AMD oluşumunun önlenmesi veya azaltılması ile sonuçlanan sülfür oksidasyonunu önleyebilir veya azaltabilir. Böylelikle, oksijen, oksidasyon hızı açısından suda havaya göre daha az çözünür olduğundan dolayı S-MA içeren ÇMD'den kirletici bileşenlerin (sülfat, çözünür ağır metaller, vb.) salınımı önemli ölçüde sınırlandırılabilir (MEND, 2006; Schafer, 2016; Hamberg vd., 2017; Hamberg vd., 2018; Bull ve Fall 2020; Yang vd., 2020; Yılmaz vd., 2021).

Ekonomik, teknik, operasyonel ve çevresel açıdan birçok avantaja sahip olan ÇMD, yeraltı madenlerinde uzun yıllardan beri kullanılmasına rağmen, ÇMD'den yeraltı suyuna zararlı kirleticilerin sızma riskinden dolayı son yıllarda ÇMD'nin çevresel davranışının titizlikle değerlendirilmesi büyük önem kazanmıştır (Liu vd., 2020). Bu yüzden, monolitik (yekpare) ÇMD numunelerinin laboratuvar şartlarında dinamik tank liçi (DTL) testine tabi tutularak YSS altında kalmış ÇMD kütlesinin çevresel davranışının tahmin edilebilmesi için bazı çalışmalar gerçekleştirilmiştir (Coussy vd., 2011; Jiao vd., 2011; Hamberg vd., 2015; Schafer, 2016; Hamberg vd., 2017; Seipel vd., 2017; Hamberg vd., 2018). Arsenopirit atıkları içeren ÇMD'den arsenik (As) salınımını inceleyen Coussy vd. (2011), 64 güne kadar DTL testine tabi tuttukları ÇMD numunelerinin bulunduğu suların oldukça alkali (pH≥10,4) olduğunu ve yüksek pH'ın arsenik (As) salınımını hızlandırdığını rapor etmişlerdir. Jiao vd. (2011), ÇMD'nin yeraltı sularına etkisini belirlemek için en doğru yöntemin, bütün haldeki ÇMD numunelerinin doğal olarak saf su içerisinde uzun süre bekletilerek jeokimyasal analizlerinin yapılması olduğunu belirtmiştir. Araştırmacılar, hazırladıkları kübik ÇMD numunelerini 8-75 gün arasında saf su içerisinde bekleterek ağır metal (As, Pb, Cd ve Zn) salınımı miktarlarındaki değişimi incelemişlerdir. Sonuçlardan, ÇMD'nin yeraltı madenlerinde kullanımının yeraltı suları açısından problem oluşturmadığı bildirilmiştir (Jiao vd., 2011). Başka bir çalışmada, Hamberg vd. (2015) siyanürlü maden atığı ve bu atık ile üretilen ÇMD numunelerinin (Portland çimentosu: PÇ ve PÇ-Uçucu kül: PÇ-UK) çevresel davranışını (pH ve ağır metal salınımı (As, Ca, Fe, S, vb.)) araştırmak için 64 güne kadar DTL testleri yapmıştır. Atık ile karşılaştırıldığında, ÇMD numunelerinde sülfür (S) salınımının azaldığı ve numunelerin (PÇ ve PÇ-UK) alkali pH seviyelerinde (7,9-10,4>3,9-6,0) seyrettiği gözlenirken, atık ve PÇ-UK'ya kıyasla PÇ ile üretilen numunelerden daha yüksek As salındığı belirlenmiştir. Schafer (2016) yüksek As içerikli altın atıkları (S^{2-}= %0,22, pH= 7,71) kullanarak %3-12 arasında değişen bağlayıcı oranlarında ÇMD numuneleri hazırlamış ve DTL testini kullanarak ÇMD'nin jeokimyasal davranışını incelemiştir. Araştırmacı, bağlayıcı oranının %3'ten %12'ye arttırılmasının toplam As salınımını önemli derecede (0,076<0,423 mg/l) azalttığını belirlemiştir. Ayrıca, geleneksel test yöntemleri (statik ve kinetik testler) ile karşılaştırıldığında, monolitik ÇMD numuneleri ile gerçekleştirilen DTL testinin ÇMD'nin uzun dönem çevresel davranışını değerlendirmek için daha temsili kimyasal salınım sonuçları sağladığı rapor edilmiştir (Schafer, 2016). Diğer çalışmalarda (Hamberg vd., 2017; Hamberg vd., 2018), yazarlar düşük dayanımlı (0,2 MPa) ÇMD numunelerini 31 (normal su altında bırakma) ve 446 (geç su altında bırakma) günlük kür süresi sonunda DTL testine tabi tutmuşlardır. Sonuçlar, düşük dayanıma sahip ÇMD'nin AMD oluşumunu engelleme veya azaltma konusunda yetersiz kalabildiğini ve böylece çevresel problemlerin (kirletici bileşenlerin salınımında artış vb.) ortaya çıkabileceğini göstermiştir. Ayrıca, oksidasyonun engellenmesi veya azaltılması için ÇMD kütlesinin hızlı bir şekilde su altında kalmasının gerektiği vurgulanmıştır. ÇMD'nin yeraltı sularına etkisinin belirlenmesine yönelik gerçekleştirilen deneysel çalışmalarda (Coussy vd., 2011; Jiao vd., 2011; Hamberg vd., 2015; Schafer, 2016; Hamberg vd., 2017; Hamberg vd., 2018) kullanılan atık malzemelerin sülfür içeriği oldukça düşüktür (%0,22-2,0) ve jeokimyasal ölçümler 75 güne kadar yapılmıştır. Fakat Türkiye'de, Çayeli Bakır (Rize) ve Etibakır Küre (Kastamonu) işletmelerinde ÇMD malzemesi olarak kullanılan maden atıklarının sülfür içerikleri atık tipine bağlı olarak sırasıyla %34,68-37,40 ve %15,82-29,12 arasında değişmektedir (Yılmaz vd., 2021). Önceki çalışmalar ile kıyaslandığında, Yılmaz vd. (2021) DTL testini kullanarak S-MA (%15,82 S^{2-}) yerine %10 oranında endüstriyel atık malzeme (YFC ve C-UK) ikamesinin ÇMD'nin uzun dönem (360 güne kadar) çevresel davranışına etkisini incelemişlerdir. Araştırmacılar alkali endüstriyel atık malzeme ikamesinin ÇMD'den salınan sülfat ve ağır metal (Mo ve Zn hariç) miktarlarını önemli oranda azalttığını ve ÇMD pH'sını 360 güne kadar alkali seviyelere (10,3'e kadar) doğru yükselttiğini rapor etmişlerdir. ÇMD'nin çevresel davranışının araştırıldığı önceki çalışmalarda karışım içerisinde kullanılan PÇ veya S-MA'ya YFC ve

C-UK gibi endüstriyel atık malzemeler ikame veya ilave edilmiştir. Fakat puzolanik özelliği bulunmayan ve yüksek CaO veya $CaCO_3$ içeriğine sahip doğal alkali malzemelerin (mermer atığı, kireçtaşı vb.) ÇMD'nin uzun dönem çevresel özelliklerine etkisinin incelendiği herhangi bir çalışma bulunmamaktadır.

Bu araştırmada, sülfürlü maden atığı (S-MA= %15,82 S^{2-}) yerine %10 oranında ikame edilen kalsitik kireçtaşı (KK) ve dolomitik kireçtaşının (DK) ÇMD'nin çevresel davranışı üzerine etkisi değerlendirilmiştir. Bu amaçla, %8,5 PÇ oranında hazırlanan kontrol numuneleri (%100 S-MA içeren) ve iki farklı kireçtaşı (KK ve DK) ikameli ÇMD numuneleri 180 günlük kür süresi sonunda 30-360 gün boyunca dinamik tank liçi (DTL) testine tabi tutulmuştur. Her liç süresi sonunda pH, sülfat (SO_4^{2-}) ve ağır metal (Cu, As, Pb, Cd, Co, Ni, Cr, Mo) analizleri gerçekleştirilmiştir. Elde edilen ağır metal salınımları yeraltı suyu sınır değerleri (YS-SD) ile karşılaştırılmıştır (WHO, 2011). Ayrıca, mineraloji (XRD) ve mikroyapı (MIP) testleri yapılarak malzemelerin (S-MA, KK ve DK) ÇMD'nin çevresel davranışı üzerindeki etkisi detaylı olarak incelenmiştir.

1. Deneysel çalışmalar

1.1. Sülfürlü maden atığı ve bağlayıcı

ÇMD karışımında kullanılan sülfürlü maden atığı (S-MA) ve bağlayıcı (PÇ: CEMI 42,5R) sırasıyla Etibakır İşletmesi (Kastamonu–Küre) ve Aşkale Çimento Fabrikası'ndan (Trabzon) temin edilmiştir. S-MA ve PÇ'nin tane boyut dağılımı (TBD), özgül ağırlık (ÖA) ve özgül yüzey alanı (ÖYA) testleri için Malvern Mastersizer, piknometre ve yüzey alanı ölçer cihazı kullanılmıştır. S-MA'nın şlam (<20 µm) malzeme miktarı, ÖA ve ÖYA sırasıyla %48,41, 3,37 g/cm^3 ve 4440 cm^2/g olarak ölçülmüştür (Şekil 1 ve Çizelge 1). Ayrıca, yapılan ÖA ve ÖYA testlerinden, ÇMD karışımında kullanılan PÇ'nin 3,12 g/cm^3 ÖA ve 4330 cm^2/g ÖYA'ya sahip olduğu tespit edilmiştir (Çizelge 1).

Malzemelerin kimyasal özelliklerinin belirlenmesi için XRF ve gravimetrik yöntem kullanılmıştır. Sonuçlar, S-MA'nın büyük bir bölümünün demir (III) oksit (Fe_2O_3) ve silisyum dioksit (SiO_2) minerallerinden oluştuğunu gösterirken, PÇ'de kalsiyum oksit (CaO) ve silisyum dioksit (SiO_2) baskın minerallerdir (Çizelge 1). S-MA ve PÇ'nin mineralojik karakterizasyonları X- ışınları difraktometre (XRD) cihazı ile gerçekleştirilmiştir. Mineralojik karakterizasyona göre, S-MA'da baskın mineralin pirit (FeS_2= %29,66) olduğu ve dolayısıyla %15,82 oranında sülfür (S^{-2}) içeriğine sahip olduğu belirlenmiştir (Çizelge 1).

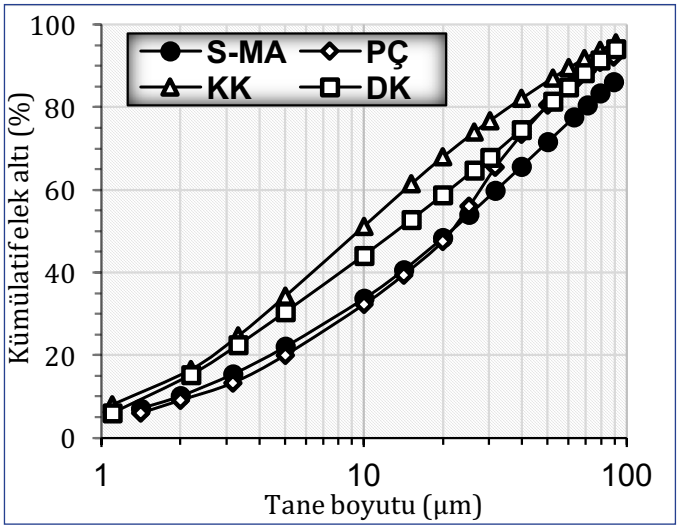

Şekil 1. *S-MA, PÇ, KK ve DK'nın tane boyutu dağılımları (Yılmaz vd., 2020)*

Çizelge 1. *Malzemelerin fiziksel, kimyasal ve mineralojik özellikleri (Yılmaz vd., 2020)*

Malzemeler	Kimyasal Özellikler						
	SiO_2	Al_2O_3	Fe_2O_3	MgO	CaO	S^{-2}	FeS_2
S-MA	31,89	8,97	33,09	4,08	3,48	15,82	29,66
KK	0,86	0,23	0,06	0,22	55,26	-	-
DK	0,12	0,09	0,06	20,18	32,28	-	-
PÇ	21,02	5,27	3,06	2,19	62,91	-	-

Malzemeler	Fiziksel Özellikler		Mineralojik *Özellikler*
	Özgül ağırlık (g/cm^3)	Özgül yüzey alanı (cm^2/g)	
S-MA	3,37	4440	Pirit, Albit, Kuvars, Kalsit, Klorit
KK	2,63	5665	Kalsit
DK	2,79	5020	Kalsit, Dolomit
PÇ	3,12	4335	-

1.2. Kalsitik ve dolomitik kireçtaşı

ÇMD karışımı içerisinde S-MA yerine %10 oranında ikame edilecek olan kireçtaşları (KK ve DK) sırasıyla Araklı-Taşönü hammadde ocağından (Aşkale Çimento A.Ş.) ve Antalya-Karaöz bölgesinden temin edilmiştir. Laboratuvara getirilen KK ve DK (Şekil 2a,b), çeneli kırıcı ile kırılarak -2 mm boyutlu malzemeler elde edilmiştir (Şekil 2c,d). Ardından, öğütme işlemi öncesinde malzemeler etüvde (50°C/36 saat) kurutularak KK ve DK'nın doğal nemi uzaklaştırılmıştır. Sonra KK ve DK bilyalı değirmen kullanılarak -100 µm boyutuna öğütülmüştür (Şekil 2e,f) (Yılmaz vd., 2020).

Şekil 2. *KK (a,c,e) ve DK'nın (b,d,f) boyut küçültme süreci*

KK ve DK'nın fiziksel karakterizasyonu (TBD, ÖA ve ÖYA) için S-MA ve bağlayıcı malzemelerin analizlerinde belirtilen cihazlar kullanılmıştır. KK ve DK'nın şlam (<20 µm) malzeme miktarı, ÖA ve ÖYA değerleri Şekil 1 ve Çizelge 1'de gösterilmiştir. XRF analizleri, KK'nın çoğunlukla kalsiyum oksit (CaO) içerdiğini, DK'nın ise kalsiyum oksit (CaO) ve magnezyum oksit (MgO) bileşimlerinden oluştuğunu göstermiştir. XRD ile belirlenen mineralojik kompozisyonlarından ise KK'nın kalsit mineralinden, DK'nın ise kalsit ve dolomit minerallerinden oluştuğu tespit edilmiştir (Çizelge 1).

1.3. Asit-baz hesaplama (A-BH) testi

Bu statik test yöntemi ile S-MA ve kireçtaşlarının (KK ve DK) asit potansiyelleri (AP) ve nötralizasyon potansiyelleri (NP) hesaplanarak S-MA'nın asit üretme potansiyeline karşılık KK ve DK'nın

nötralizasyon potansiyelleri belirlenmiştir. Bu kapsamda, standart Sobek test metodu (Sobek vd., 1978) doğrultusunda S-MA'nın AP değeri, Eşitlik 1 yardımı ile hesaplanmıştır (Çizelge 2). Ardından, S-MA, KK ve DK'nın NP değerlerinin hesaplanmasında kullanılan fışırdama sınıfları belirlenmiştir. Daha sonra, asit-baz titrasyon testi yapılarak malzemelerin NP ve net nötralizasyon potansiyeli (NNP) değerleri Eşitlik 2 ve 3 vasıtasıyla hesaplanmıştır (Çizelge 2). A-BH testi ile ilgili bilgiler Yılmaz vd. (2021)'nin çalışmasında daha detaylı olarak açıklanmıştır.

$$AP = 31{,}25 \times S^{2-} \quad (1)$$

$$NP = ((A_n \times A_h)-(B_n \times B_h))/a \quad (2)$$

$$NNP = NP - AP \quad (3)$$

Burada, A_n ve A_h; sırasıyla kullanılan asitin normalitesi (N) ve hacmi (ml), B_n ve B_h; sırasıyla kullanılan bazın normalitesi (N) ve hacmi (ml) ve a; numune ağırlığıdır (g).

1.4. ÇMD numunelerinin hazırlanması

Testlerde kullanılan tüm ÇMD numuneleri %8,5 PÇ oranında ve 19,05 cm akışkanlıkta hazırlanmıştır. Çünkü, yapılan ön testlerde ÇMD'nin dayanım ve duraylılığını koruyabilmesi ve maden üretim döngüsünün güvenli bir şekilde yürütülebilmesi için maden operatörleri tarafından 28 günde istenen kritik basınç dayanımı değeri (≥1,0 MPa) (Yumlu, 2001) bu bağlayıcı oranında ve akışkanlıkta sağlanmıştır. Kontrol numuneleri tamamen (%100) S-MA ile üretilirken, diğer ÇMD numunelerinin (10KK ve 10DK) üretiminde S-MA yerine %10 oranında KK ve DK ikame edilmiştir. Düşük oranda KK ve DK ikamesinin sebebi; giriş bölümünde açıklandığı üzere, ÇMD teknolojisi ile maden atıklarının yaklaşık %50-55'inin yeraltı maden açıklıklarında depolanabilmesinden dolayı ÇMD operatörlerinin yeraltında depolanacak maden atığı miktarının mümkün olduğunca azaltılmasını istememeleridir. İki farklı kireçtaşı kullanılmasının sebebi ise, farklı fiziksel, kimyasal ve mineralojik özelliklere (Çizelge 1) sahip malzemelerin ÇMD'nin çevresel özelliklerine etkisinin araştırılmak istenmesidir. ÇMD karışım tasarımında kullanılan parametreler Çizelge 3'te detaylı olarak verilmiştir.

Hazırlanan ÇMD karışımları, 20,8 lt hacimli karıştırıcıda (105 devir/dk dönme hızı ve 7 dk) karıştırılmıştır. Homojenleştirilen ÇMD karışımları, 5x10cm (çap x boy) boyutlu silindirik kalıplara doldurulmuş ve 24 saat boyunca drenaj masasında bekletilerek ÇMD karışımları içerisindeki fazla suyun dışarı atılması sağlanmıştır (Şekil 3a). Daha sonra, kür dolabında (%85 nem ve 20°C sıcaklık) açık bir biçimde 180 güne kadar kür işlemi uygulanmıştır (Şekil 3b).

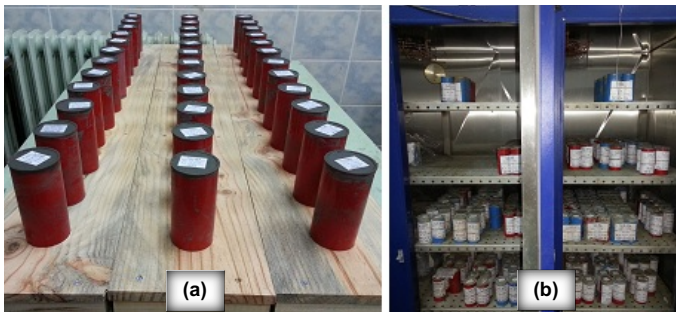

Şekil 3. *Drenaj masası (a) ve kür dolabındaki (b) ÇMD numunelerinin görünümü (Yılmaz ve Ercikdi, 2021)*

Çizelge 2. *Malzemelerin A-BH testi sonuçları (Yılmaz vd., 2020)*

Özellikler	S-MA	KK	DK	Özellikler	S-MA	KK	DK
S^{2-} içeriği(%)	15,82	-	-	Asit hacmi (ml)	20	40	80
CaO içeriği (%)	3,48	55,26	32,28	AP*	494,4	0	0
Fışırdama sınıfı	Yok	Sert	Orta	NP*	8,6	987,6	741,3
Asit normalitesi (N)	0,1	0,5	0,5	NNP*	-485,8	987,6	741,3

*: kg $CaCO_3$/ton atık

Çizelge 3. *ÇMD numunelerine ait karışım parametreleri*

Parametreler	Kontrol	KK	DK	Parametreler	Kontrol	KK	DK
İkame oranı (%)	0	10		Su/çimento oranı	4,20	4,20	4,13
Bağlayıcı oranı (%)	8,5			Slamp (cm)	19,05		
Katı oranı (%)	73,70	73,69	74,03	180 günlük dayanım (MPa)	1,56	1,62	1,67

Çizelge 4. *ÇMD'lerin metal analizi sonuçları ve WHO (2011)'ya göre yeraltı suyu sınır değerleri*

Karışım tipi	Ana elementler (%)				Eser Elementler (ppm)							
	Fe	Ca	Al	Mg	Cu	Co	As	Ni	Pb	Cr	Mo	Cd
Kontrol	16,88	4,99	2,84	1,79	1153	582	144	54	88	126	9,6	3,1
10KK	15,19	7,02	2,48	1,60	1023	522	130	46	80	109	8,6	2,8
10DK	14,76	5,89	2,44	2,41	1010	516	124	46	74	104	8,7	2,6
Yeraltı suyu sınır değerleri				(mg/L)	2,0	-	0,01	0,07	0,01	0,05	0,07	0,03
				(mg/m^2)	201	-	1,0	7,0	1,0	5,0	7,0	3,0

1.5. Dinamik tank liçi (DTL) testi

180 günlük kür işlemi sonunda ÇMD numuneleri (Kontrol, 10KK ve 10DK) kalıplardan çıkarılarak yüzeyleri (alt ve üst) düzeltilmiş ve uzunluğu (h) kumpas ile ölçülmüştür. Numunelerin kap (tank) içerisinde tamamen ıslanabilmesi amacıyla her bir numunenin geometrik yüzey alanı (GYA) ve buna bağlı olarak saf su hacmi (Vs) Eşitlik 4 ve 5 ile hesaplanmıştır (ASTM C1308-08, 2017; US-EPA 1315, 2013; Yılmaz vd., 2021).

$$GYA\ (cm^2) = 2\pi r \times (r+h) \quad (4)$$

$$Vs\ (cm^3) = GYA \times 9 \pm 1 \quad (5)$$

Üç farklı karışım tipinde (Çizelge 3) 3'er tane olmak üzere toplam 9 adet ÇMD numunesi her analiz tankı içerisine 1 adet olacak şekilde bırakılmış ve tank, numunelerin üzeri tamamen kaplanacak şekilde saf su ile doldurulmuştur. Numuneler, ağzı kapalı bir şekilde 30, 60, 90, 180, 270 ve 360 günlük liç süreleri boyunca tank içerisinde bekletilmiş (Şekil 4a) ve her liç süresi sonunda yeni analiz tankına alınarak üzerine taze saf su eklenmiştir (Yılmaz vd., 2021).

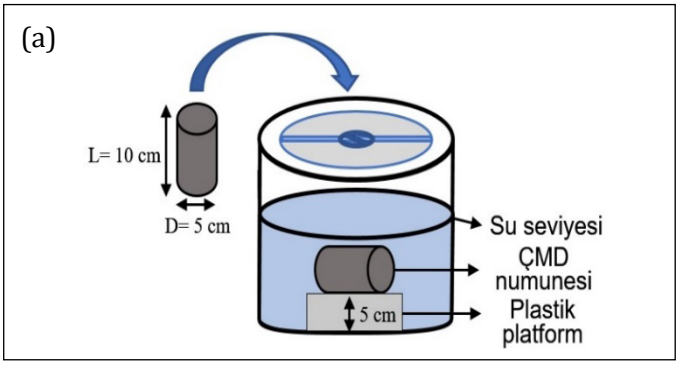

Şekil 4. *DTL testinin şematik görünümü (a) (Yılmaz ve Ercikdi, 2021), pH (b) ve SO_4^{2-} (c) analizleri*

Her liç süresi tamamlandığında alınan su numunelerinin 0,45 µm'lik vakum filtre ile filtrasyon işlemi gerçekleştirilmiştir. Sonrasında, alınan su numunelerinin pH ve SO_4^{2-} analizleri yapılırken (Şekil 4b,c), ICP-MS cihazı kullanılarak ağır metal (Cu, As, Pb, Cd, Co, Ni, Cr ve Mo) analizleri gerçekleştirilmiştir. Ayrıca 180 gün sonunda DTL testine tabi tutulan numuneler ile aynı karışım özelliklerinde hazırlanan ÇMD numuneleri DTL testi öncesinde öğütülerek ICP-MS cihazı ile metal analizine tabi tutulmuştur (Çizelge 4).

1.6. MIP ve XRD testleri

ÇMD'nin çevresel davranışına etkisini incelemek için DTL testinde kullanılan numuneler ile aynı karışım özelliklerinde hazırlanan 3 adet ÇMD numunesi (Kontrol, 10KK ve 10DK) 180 günlük kür süresi sonunda öncelikle etüvde (50^{0}C ve 60 saat) kurutulmuştur. Ardından, cıvalı Porozimetre (Micromeritics Autopore IV 9410) cihazı kullanılarak mikroyapı (MIP) testine tabi tutulmuştur (ASTM D 4404-18. 2018). Test prosedürü hakkında daha fazla bilgiye Yılmaz vd. (2018)'nin çalışmasından ulaşılabilir. Ayrıca, mineralojik özelliklerdeki değişimlerin ÇMD'nin çevresel davranışı üzerindeki etkisinin belirlenmesi için DTL testi öncesi ve sonrasında toplam 6 adet ÇMD numunesinin Bruker D8 Discover model cihaz vasıtasıyla XRD analizleri yapılmıştır (Şekil 6).

2. Bulgular ve tartışma

2.1. Asit (pH) özellikleri

30-360 günlük liç süresi boyunca DTL testine tabi tutulan ÇMD numunelerinden (Kontrol, 10KK ve 10DK) elde edilen sızıntı sularındaki pH değişimleri Şekil 5'de gösterilmiştir. Genel olarak tüm ÇMD numunelerinden elde edilen sızıntı sularının nötral seviyenin üzerinde (6,57-8,21) pH değerlerine sahip olduğu belirlenmiştir. Kireçtaşı ikameli numunelerde (10KK ve 10DK) ilk liç süresi (30 gün) sonunda daha düşük pH değerleri ölçülmesine rağmen, sonraki liç sürelerinde (60-360 gün) kontrol numunelerine kıyasla %11,55'e kadar daha yüksek pH değerleri gözlemlenmiştir. Ayrıca, kontrol ÇMD numunelerinin pH'ı 180 günlük liç süresinden sonra düşme eğilimi göstermiştir. Fakat kireçtaşı ikame edilen ÇMD numunelerinden elde edilen sızıntı sularının pH değerlerinde sürekli olarak artış tespit edilmiştir (Şekil 5). Kontrol ÇMD numuneleri ile karşılaştırıldığında, 10KK ve 10DK numunelerinde elde edilen daha yüksek pH'ın muhtemel sebebi, alkali malzemelerin oldukça yüksek nötralizasyon potansiyeline (Çizelge 2) ve daha yüksek ÖYA'ya (Çizelge 1) sahip olmalarıdır. Potgieter-Vermaak vd. (2006) ÖYA'daki artışın malzemenin nötralizasyon potansiyelini arttırdığını rapor etmiştir. Bu olumlu katkılara ek olarak, alkali malzemelerde bulunan kalsit ve dolomitin çözünmesi 10KK ve 10DK numunelerinin bazikliğini arttırmıştır (Şekil 6b,c) (Yılmaz vd., 2020). Jones ve Cetin (2017) geri dönüştürülmüş agrega içerisindeki çimentomsu bileşenlerin (kireç: CaO, kalsit: $CaCO_3$, vb.) çözünmesinin AMD'nin pH'ını yükselttiğini bildirmişlerdir. Önceki çalışma ile uyumlu olarak, kireçtaşlarının kimyasal analiz sonuçları, KK ve DK'nın önemli miktarda CaO içerdiğini göstermektedir (Çizelge 1). Geçmiş çalışmalarda gerçekleştirilen 64 günlük DTL testlerinde oldukça düşük asit oluşumu (pH≥ 10,4) gözlemlenmiştir (Coussy vd., 2011; Taha vd., 2019) ve bu çalışmayla karşılaştırıldığında, düşük asit oluşumu beton ve ÇMD'de kullanılan atık kayaç ve atık malzemelerin oldukça düşük oranda sülfür (%0,5-0,8%<%15,8) içermesine bağlanabilir.

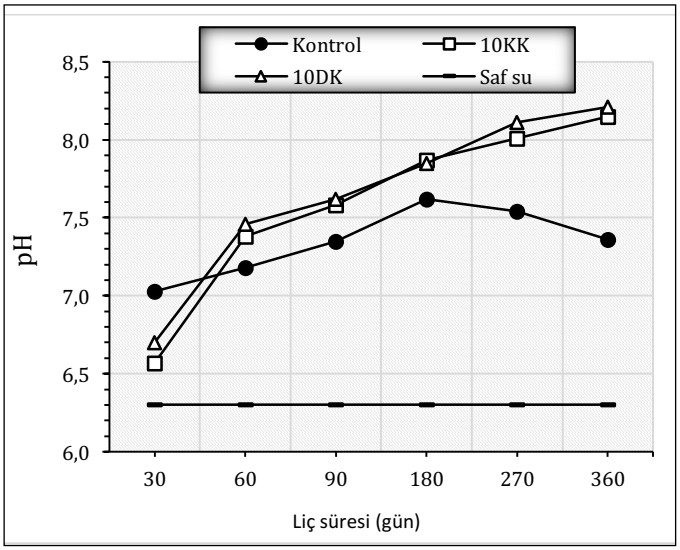

Şekil 5. ÇMD'nin sızıntı sularındaki pH değişimleri

ÇMD karışımlarına ikame edilen KK ve DK'nın ÇMD numunelerinden elde edilen sızıntı sularının pH değerlerine etkileri incelendiğinde ise, malzemelerin pH değişimine katkıları oldukça benzer seviyededir (Şekil 5). Bunun muhtemel sebepleri, malzemelerin asit nötralize etme gücünü gösteren NNP değerlerinin birbirine oldukça yakın olması (Çizelge 2) ve porozite gelişimine katkı sağlayan benzer ÖYA değerleriyle (Çizelge 1) sonuçlanan birbirine oldukça yakın miktarda daha ince boyutlu tane (Şekil 1) içermesidir.

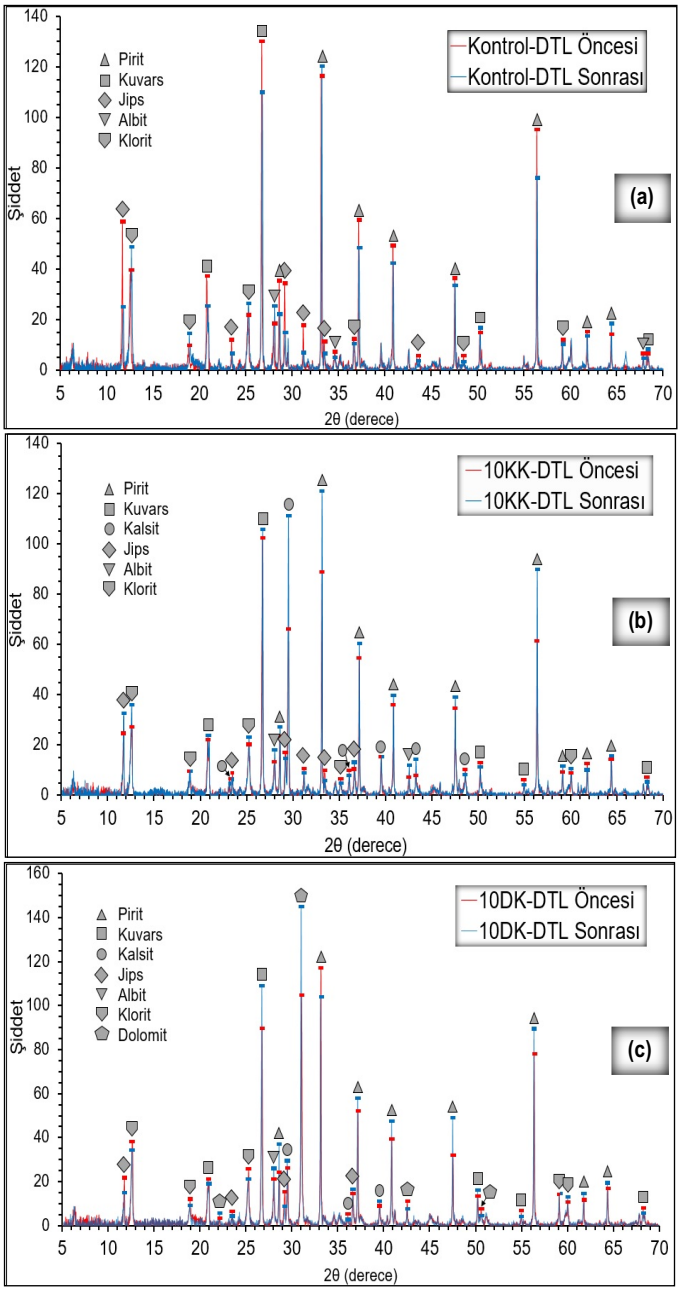

Şekil 6. Kontrol (a), 10KK (b) ve 10DK (c) numunelerinin XRD profilleri

2.2. Oksidasyon (SO_4^{2-}) özellikleri

Şekil 7, DTL testine tabi tutulan ÇMD numunelerinden (Kontrol, 10KK ve 10DK) 30-360 günlük liç süresi boyunca pirit mineralinin oksidasyonu sonucu üretilen ve birincil oksidasyon ürünü olan sülfat (SO_4^{2-}) salınımı sonuçlarını göstermektedir. Tüm liç süreleri boyunca ÇMD numunelerinden salınan sülfat konsantrasyonu miktarları 57,90-96,33 g/m^2 arasında ölçülmüştür. ÇMD numunelerinden salınan sülfat iyonlarının DTL testi sırasında elde edilen sızıntı sularının pH değerleri ile bağlantılı olduğu belirlenmiştir. Yani, sızıntı suyunun pH değeri ne kadar yüksekse ÇMD numunelerinden salınan SO_4^{2-} iyonları miktarı o kadar düşüktür (Yılmaz vd., 2021). Bu bağlamda, Kontrol numuneleri ile karşılaştırıldığında, 10KK ve 10DK numuneleri liç süresinden bağımsız olarak %23,7'ye kadar daha düşük SO_4^{2-} salınımı üretmişlerdir. DTL testlerinden önce ve sonra ÇMD numuneleri üzerinde gerçekleştirilen XRD analizlerinin sonuçları, Kontrol ÇMD numunelerinde nispeten daha fazla pirit oksidasyonunun meydana geldiğini göstermektedir. Ayrıca, KK ve DK ikameli numunelerden daha düşük sülfat iyonu salınması, sırasıyla kalsitin çözünmesi ve pirit oksidasyonu sonucu oluşan serbest Ca^{2+} ve SO_4^{2-} iyonlarının jips minerallerini oluşturmasıyla ilişkilendirilebilir (Şekil 6). Bu çalışma ile uyumlu olarak Hakkou vd. (2008) jips minerallerinin çözünmesinin sülfat iyonu salınımını arttırdığını belirtmiştir. Kireçtaşlarının ÇMD'den sızıntı suyuna 30-360 günlük liç süreleri boyunca salınan sülfat miktarına etkisi değerlendirildiğinde ise, sızıntı sularının pH değerleri (Şekil 5) ile uyumlu olarak 10KK ve 10DK numunelerinin sülfat iyonu salınımlarının birbirine çok yakın seyrettiği görülmektedir (Şekil 7).

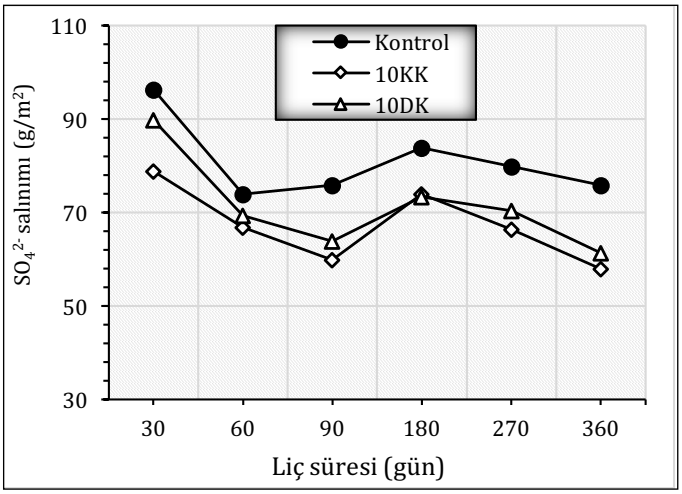

Şekil 7. *ÇMD numunelerin sülfat (SO_4^{2-}) salınımı sonuçları*

2.3. Ağır metal salınımı sonuçları

30-360 günlük liç süreleri boyunca DTL testlerine tabi tutulan ÇMD numunelerinden (Kontrol, 10KK ve 10DK) sızıntı sularına salınan ağır metallerin (As, Cu, Co, Cd, Ni, Cr, Mo ve Pb) toplam konsantrasyonları Şekil 8'de gösterilmiştir. ÇMD'lerden salınan toplam Cu-iyonu miktarları incelendiğinde (Şekil 8a), kireçtaşları içeren ÇMD numunelerinden (10KK ve 10DK) Kontrol numunelerine kıyasla oldukça yüksek miktarda Cu-iyonunun (38,4-62,9 mg/m^2>4,5 mg/m^2) salındığı görülmektedir. 10KK ve 10DK numunelerinden daha yüksek miktarda Cu salınımının muhtemel sebebi; KK ve DK'nın oldukça yüksek nötralizasyon potansiyeline sahip olmasından dolayı (Çizelge 2), bu numunelerin nispeten daha yüksek pH seviyesine (8,15-8,21>7,62) sahip olmalarıdır (Hamberg vd., 2018; Yılmaz ve Ercikdi 2021). Bu çalışmadaki bulgularla uyumlu olarak, Dayioglu vd. (2018), Cu çözünürlüğünün en düşük olduğu pH değerinin 6,5–7,0 olduğunu, ancak daha yüksek pH seviyelerinde (yani alkali) Cu çözünürlüğünün önemli ölçüde arttığını bildirmiştir. Karışım içerisindeki sülfür miktarının oldukça düşük olduğu beton (Gwenzi ve Mupatsi 2016) ve ÇMD numunelerinde (Hamberg vd., 2018) gerçekleştirilen önceki çalışmalarda, 64 günlük DTL testleri boyunca benzer Cu-iyonu salınımları (50,0 mg/m^2 ve 17,4 mg/kg'a kadar) ölçülmüştür. Ayrıca, tüm ÇMD'lerdeki Cu-iyonu salınımları (4,5-62,89<201 mg/m^2), yeraltı suyu sınır değerlerinin (YS-SD) altında kalmıştır (Çizelge 4).

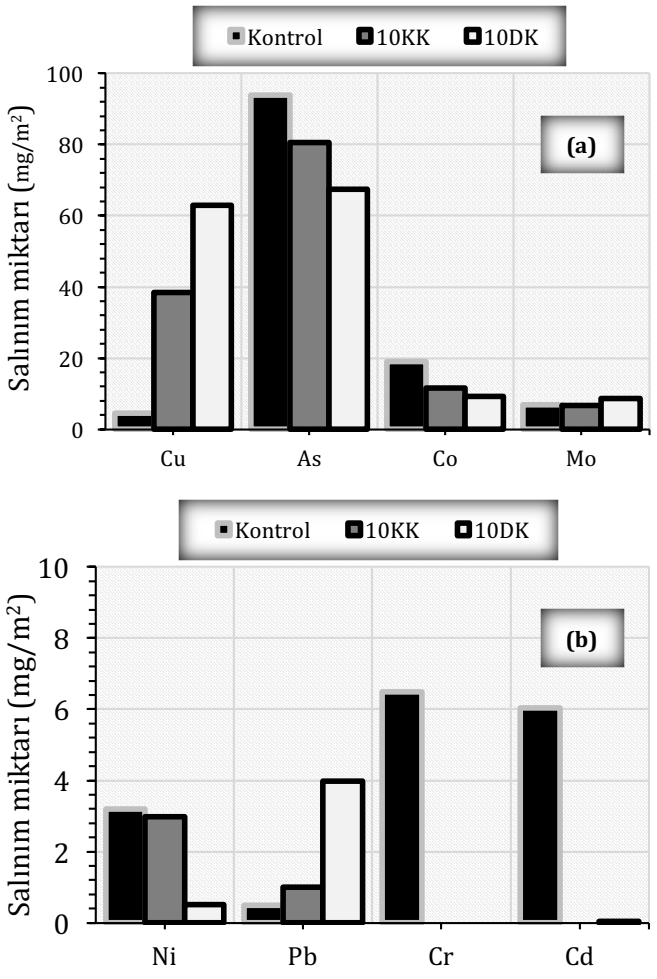

Şekil 8. ÇMD numunelerinden salınan ağır metal konsantrasyonu sonuçları

Şekil 8a'ya bakıldığında, tüm ÇMD numunelerinin sülfür oksidasyonu nedeniyle oldukça yüksek As-iyonu salınımı (67,4-93,8 mg/m^2) ürettiği aşikârdır. Bu çalışmadaki bulgularla uyumlu olarak, geçmiş çalışmalarda maden atıklarından yeraltı suyu ortamına As-iyonu transferinin kimyasal süreçlerle (alkali desorpsiyon, sülfürlü minerallerin oksidasyonu ve ferrik oksihidroksitlerin indirgeyici çözünmesi, vb.) güçlü bir şekilde bağlantılı olabileceği rapor edilmiştir (Salzsauler vd., 2005; Sracek vd., 2014). Ayrıca Sracek vd. (2014), nötr veya alkali pH seviyelerinin, sülfürlü minerallerin oksidasyonundan dolayı katı partiküllerin yüzeyinden desorbe edilen As-iyonlarının transferini engelleyemediğini belirtmiştir. Bununla birlikte, ÇMD karışımlarında S-MA yerine sırasıyla ağırlıkça %10 oranında KK ve DK ikamesinin, muhtemelen devam eden daha fazla alkali pH'ın faydalı etkisinden dolayı (Şekil 5) As-iyonu süzülmesini önemli ölçüde (%28,2'ye kadar) azalttığı görülmüştür. Dahası, 10KK ve 10DK'da gerçekleşen daha düşük As-iyonu salınımı, ÇMD gözenek yapısının iyileştirilmesi ve böylece sülfür oksidasyonunun azaltılmasıyla sonuçlanan yüksek bağlayıcı dozajı (ağırlıkça %8,5) ve S-MA'ya kıyasla daha küçük tane boyutlu KK ve DK (Şekil 1) kullanımı ile ilişkilendirilebilir. Bu bağlamda, iri boyutlu S-MA taneleri arasındaki boşlukların daha ince boyutlu kireçtaşı taneleri ile doldurulması sayesinde 10KK ve 10DK numunelerinin toplam porozitelerinin (p_{toplam}) Kontrol numunesine kıyasla %3,8'e kadar azaldığı belirlenmiştir (Şekil 9). Daha ince boyutlu KK ve DK tanelerinin iri boyutlu atık taneleri arasını doldurmasıyla sonuçlanan porozitedeki kısmi iyileşme KK ve DK ikameli ÇMD numunelerinin dayanımını hafif seviyede arttırmıştır (Şekil 1 ve Çizelge 3). Porozite ve dayanım özelliklerindeki iyileşmeye ek olarak, ÇMD'nin içsel dayanımını olumsuz etkileyen jips çözünmesinin Kontrol numunelerinde daha fazla oluşması daha yüksek As-iyonu salınımının bir diğer muhtemel sebebi olabilir (Şekil 6 ve Şekil 8a) (Yılmaz ve Ercikdi 2021). As-iyonunda gözlemlenen bu salınım seviyeleri YS-SD'nin (1,0 mg/m^2) oldukça üzerinde görünmektedir (Şekil 8a ve Çizelge 4) (WHO, 2011). Bundan dolayı, yüksek zehirlilik özelliği göz önüne alındığında, ÇMD'lerden özellikle As-iyonu salınımı oldukça endişe vericidir.

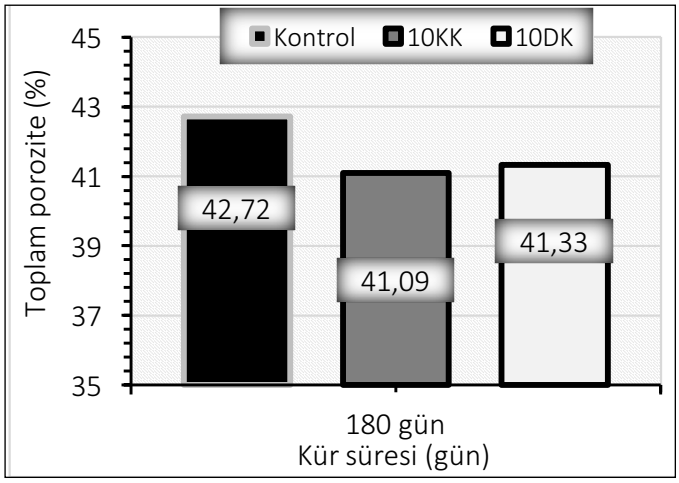

Şekil 9. ÇMD numunelerinin toplam porozite (p_{toplam}) sonuçları

ÇMD numunelerinden sızıntı sularına geçen Co-iyonu konsantrasyonları değerlendirildiğinde, Co-iyonu salınımı değerlerinin 9,3-19 mg/m^2 arasında değiştiği ve S-MA yerine %10 oranında KK ve DK ikamesinin numunelerden salınan Co-iyonu konsantrasyonlarını yaklaşık %51'e kadar azalttığı tespit edilmiştir (Şekil 9a). Co-iyonu salınımlarındaki dikkate değer kısıtlama, KK ve DK'nın oldukça yüksek miktarda CaO içermesi sebebiyle Co-iyonlarının hidrasyon ürünleri (C–S–H, vb.) içindeki CaO bağlarındaki Ca-iyonları ile yer değiştirmesi ve Co-iyonlarının C–S–H kafes yapılarına zarar vermeden hidrasyon ürünlerinin yüzeylerine tutunması (yapışması) ile açıklanabilir (Yang vd., 2020). YFC ve C-UK içeren ÇMD (1,20 mg/m^2 kadar) ve geri dönüşüm agregası içeren betonda (≈2 mg/m^2) gerçekleştirilen geçmiş çalışmalarda bu çalışmaya kıyasla oldukça düşük miktarlarda Co-iyonu salınımları ölçülmüştür (Taha vd., 2019; Yılmaz vd., 2021). Bu sonuçların nedenleri, YFC ve C-UK'nın daha düşük CaO içermesine rağmen ilave bağlayıcılık ve puzolanik özelliklerinin bulunmasından dolayı (Fall vd., 2009; Erçıkdı ve Yılmaz, 2019; Yılmaz vd., 2020), ÇMD'nin mikroyapısının iyileştirilmesine daha fazla katkı sağlaması ve betonda oldukça yüksek miktarda (340 kg/m^3) bağlayıcı kullanılmasıdır. Ayrıca, WHO (2011) tarafından yeraltı sularında kobalt (Co) için bir sınır değeri belirlenmemiştir. Diğer taraftan, tüm ÇMD karışımlarından (Kontrol, 10KK ve 10DK) benzer seviyede (6,6-8,6 mg/m^2) Mo-iyonu salınımları meydana gelmiştir. Ayrıca, sızıntı suyuna benzer miktarlarda Mo-iyonu salınmasına rağmen, sadece 10DK'nın Mo-iyonu salınım miktarı YS-SD'nin hemen üzerinde (8,6>7,0 mg/m^2) gerçekleşmiştir (Şekil 8a ve Çizelge 4).

Şekil 8b, ÇMD karışımı içerisinde S-MA yerine özellikle %10 DK ikamesinin Ni-iyonu hareketliliğini (0,5 mg/m^2) neredeyse önlediğini göstermektedir. 10KK numunesi ise, Kontrole kıyasla Ni-iyonu hareketliliği konusunda nispeten daha başarılı olmuştur. Bu da Chen vd. (2009) tarafından önerildiği üzere KK ve DK gibi alkali malzemelerin eklenmesinin ÇMD'den Ni-iyonu salınımının engellenmesi veya azaltılması yönündeki faydalı etkisini göstermektedir. Bu çalışma ile karşılaştırıldığında, Hamberg vd. (2018) ağırlıkça %1,0 çimento dozajında hazırlanan ve 446 günlük kür süresine tabi tutulan ÇMD'lerden nispeten yüksek bir Ni-iyonu sa-

lınımı (8,5 mg/m^2) bildirmiştir. Araştırmacılar, bağlayıcı dozajını %3'e çıkarıp kür süresini 31 güne düşürdüklerinde Ni-iyonu salınımında önemli bir azalma (3,3 mg/m^2'ye kadar) gözlemlemişlerdir. Böylece, ÇMD kütlesinin tamamen su altında kalma süresinin uzamasının Ni-iyonu salınımında önemli miktarda artışa yol açtığı belirlenmiştir (Hamberg vd., 2018). Dahası, bu çalışmada elde edilen Ni-iyonu salınımları WHO (2011) tarafından belirlenen YS-SD'nin epey altında kalmıştır (Şekil 8b ve Çizelge 4).

ÇMD numunelerinden 30-360 günlük DTL testi boyunca sızıntı suyuna geçen toplam Pb-iyonu konsantrasyonları değerlendirildiğinde, en düşük (0,5 mg/m^2) salınım Kontrol numunelerinden elde edilirken en yüksek (4,0 mg/m^2) salınım DK ikameli ÇMD numunelerinde ölçülmüştür. Kireçtaşı içeren numunelerden daha yüksek Pb-iyonu salınması, sızıntı suyunun pH değerinin alkali seviyelere doğru yükselmesiyle Pb-iyonu çözünürlüğünün artmasıyla açıklanabilir (Yılmaz vd., 2021). Ek olarak, sadece 10DK'dan Pb-iyonu salınımının, yeraltı suyu için belirlenen sınır değeri (<1,0 mg/m^2) aştığını belirtmek yerinde olacaktır (Şekil 8b ve Çizelge 4). Bu çalışmanın aksine, monolitik beton numunelerinin çevresel davranışını araştırmak için farklı karışım özelliklerinde beton numuneleri üreten araştırmacılar (Taha vd., 2019; Gwenzi ve Mupatsi, 2016) DTL testlerindeki tüm betonlardan yüksek miktarda toplam Pb-iyonu salınımları (sırasıyla ≈9,0 mg/m^2 ve 10,0–25,0 mg/kg) rapor etmişlerdir.

ÇMD karışımı içerisinde tespit edilen diğer bir ağır metal olan Cr-iyonu salınımı Şekil 8b'den incelendiğinde, Kontrol numunelerinden sızıntı suyuna 6,5 mg/m^2 Cr-iyonu geçerken 10KK ve 10DK numunelerinde herhangi bir salınım tespit edilmemiştir. Bu faydalı katkılar, Cr-elementinin C–S–H ile fiziko-kimyasal bağının geliştirilmesine bağlanabilir (Taha vd., 2019). Böylece, daha yüksek dayanıma (Çizelge 3) ve daha düşük toplam poroziteye (Şekil 9) sahip ÇMD numunelerinde daha yoğun olarak bulunan hidratasyon ürünleri (C-S-H, vb.) ile metal taşıyan fazlar kapsüllenmiş olabilir (Şekil 8b) (Zheng vd., 2016; Hamberg vd., 2018; Yılmaz vd., 2020; Yılmaz vd., 2021). Ayrıca, ÇMD numuneleri Cd-iyonu salınımı konusunda benzer davranış sergilemişlerdir. Kontrol ÇMD numunelerinden sızıntı suyuna 6,0 mg/m^2 Cd-iyonu salınırken, KK ve DK içeren ÇMD numunelerinde salınım ya oldukça düşük (0,05 mg/m^2) olarak gerçekleşmiş ya da salınım olmamıştır (Şekil 8b). KK ve DK ikameli ÇMD numunelerinden Cd-iyonu hareketliliğinin neredeyse tamamen engellenmesinin nedenleri, nispeten daha alkali pH seviyelerinde (Şekil 5) Cd-çözünürlüğünün düşük olması ve daha düşük poroziteyle sonuçlanan daha yoğun ÇMD mikroyapısının olmasıdır (Şekil 9) (Yılmaz ve Ercikdi 2021). Dahası, Yang vd. (2020) Ca ve Cd iyonlarının elektrik potansiyeli özellikleri benzerlik gösterdiğinden dolayı, ÇMD'lerden Cd-iyonu salınımının, Ca ve Cd arasındaki iyon değişiminden sonra Cd-iyonlarının hidratasyon ürünleri içerisine absorbe olmasıyla (emilmesiyle) azaltılmış/engellenmiş olabileceğini belirtmiştir. Cr ve Cd iyonlarının salınımı miktarları WHO (2011) tarafından belirlenen YS-SD'ye göre incelendiğinde, sadece Kontrol numunelerinden salınan Cr ve Cd iyonlarının sınır değerleri aştığı belirlenmiştir (Şekil 8b ve Çizelge 4).

Sonuçlar

Bu çalışmada, laboratuvar ölçekli DTL testleri uygulanarak S-MA yerine ikame olarak ağırlıkça %10 oranında KK ve DK kullanılmasının ÇMD'nin uzun dönem çevresel davranışı üzerine etkileri araştırılmıştır. Bu amaç kapsamında, 180 günlük kür süresinin ardından ÇMD numuneleri 30-360 günlük liç periyotları boyunca DTL testlerine tabi tutulmuş ve elde edilen sızıntı sularının pH, sülfat (SO_4^{2-}) ve ağır metal (Cu, As, Pb, Cd, Co, Ni, Cr ve Mo) analizleri yapılmıştır. Ayrıca, ÇMD numunelerinin XRD ve MIP testleri yapılarak mineraloji ve mikroyapının ÇMD'lerin çevresel davranışı üzerindeki etkileri incelenmiştir.

Sonuçlar değerlendirildiğinde, Kontrol numunelerinin sızıntı sularında gözlemlenen pH artışı, 180 günlük liç süresinin ardından düşüş trendine girmiştir. İlk liç süresinde (30 gün) kontrole kıyasla daha düşük pH değerlerine sahip olan 10KK ve 10DK numuneleri ilerleyen liç süreleri boyunca pH artışı trendini sürdürmüş ve alkali seviyelerde kalmayı başarmıştır. Kontrol ile karşılaştırıldığında, KK ve DK'nın S-MA'ya ikame olarak kullanılmasının, ÇMD'den sızıntı suyuna geçen sülfat (SO_4^{2-}) iyonu konsantrasyonunu liç süresinden bağımsız olarak %23,7'ye kadar azalttığı tespit edilmiştir. Ayrıca, KK ve DK ikameli ÇMD numunelerinde ortaya çıkan daha düşük poroziteli mikroyapı ile uyumlu olarak kireçtaşı içeren ÇMD'den ağır metallerin (Cu, Mo ve Pb hariç) salınımının engellendiği veya büyük ölçüde azaltıldığı gözlemlenmiştir. Kontrolden As, Cr ve Cd salınımının WHO tarafından belirlenen YS-SD'yi aştığı belirlenirken, DK içeren ÇMD'den Cr ve Cd salınımının YS-SD'yi aştığı tespit edilmiştir. Öte yandan, 10KK'dan yalnızca As-iyonu salınımı, YS-SD'nin üzerinde gerçekleşmiştir.

Bu sonuçlardan, ÇMD karışımlarında alkali malzemelerin (KK, DK, vb.) kullanılmasının, ÇMD'nin kalitesini (mekanik, mikroyapı, vb.) ve çevresel etkilerini önemli ölçüde iyileştirebileceği çıkarılabilir. Fakat, bu bulgular, gelecekteki çalışmaların özellikle As gibi yeraltı suyu kirliliği bakımından oldukça zararlı kirleticilerin salınımının engellenmesi/kontrol altına alınması amacıyla daha yüksek kaliteli ÇMD tasarımlarının geliştirilmesine odaklanması önem arz etmektedir.

Teşekkür

Yazarlar, mali destek ve analiz desteği için sırasıyla KTÜ Bilimsel Araştırma Projeleri Birimi'ne (Proje No: FDK 2016-5500) ve Dr. Soner TOP nezdinde AGÜ Merkez Araştırma Laboratuvarı'na teşekkürlerini sunarlar.

Kaynaklar

ASTM C1308-08, 2017. Standard test method for accelerated leach test for diffusive releases from solidified waste and a computer program to model diffusive, fractional leaching from cylindrical waste forms. Annual Book of ASTM Standards, ASTM International, West Conshohocken, PA.

ASTM D 4404-18, 2018. Standard test method for determination of pore volume and pore volume distribution of soil and rock by mercury intrusion porosimetry. Annual Book of ASTM Standards, ASTM International, West Conshohocken, PA.

Bull, A.J., Fall, M. 2020. Thermally induced changes in metalloid leachability of cemented paste backfill that contains blast furnace slag. Minerals Engineering. 156, 106520. https://doi.org/10.1016/j.mineng.2020.106520

Cao, S., Xue, G., Yilmaz, E., Yin, Z., Yan, F. 2021. Utilizing concrete pillars as an environmental mining practice in underground mines. Journal of Cleaner Production. 278, 123433. https://doi.org/10.1016/j.jclepro.2020.123433

Chen, Q., Zhang, L., Ke, Y., Hills, C., Kang, Y. 2009. Influence of carbonation on the acid neutralization capacity of cements and cement-solidified/stabilized electroplating sludge. Chemosphere. 74(6), 758-764. https://doi.org/10.1016/j.chemosphere.2008.10.044

Cihangir, F., Akyol, Y. 2018. Mechanical, hydrological and microstructural assessment of the durability of cemented paste backfill containing alkali-activated slag. International Journal of Mining, Reclamation and Environment. 32(2), 123-143. https://doi.org/10.1080/17480930.2016.1242183

Coussy, S., Benzaazoua, M., Blanc, D., Moszkowicz, P., Bussière, B. 2011. Arsenic stability in arsenopyrite-rich cemented paste backfills: a leaching test-based assessment. Journal of Hazardous Materials. 185(2-3), 1467-1476. https://doi.org/10.1016/j.jhazmat.2010.10.070

Dayioglu, A.Y., Aydilek, A.H., Cimen, O., Cimen, M. 2018. Trace metal leaching from steel slag used in structural fills. Journal of Geotechnical and Geoenvironmental Engineering. 144(12), 04018089. https://doi.org/10.1061/(ASCE)GT.1943-5606.0001980

Ercikdi, B., Cihangir, F., Kesimal, A., Deveci, H. 2017 Practical importance of tailings for cemented paste backfill. Yilmaz, E. and Fall, M. (Eds). Paste Tailings Management, Springer International Publishing. Cham, 7-32. https://doi.org/10.1007/978-3-319-39682-8

Erçıkdı, B., Yılmaz, T. 2019. Çimentolu macun dolgunun dayanım ve mikroyapı özellikleri; C-sınıfı uçucu külün etkisi. Dokuz Eylül Üniversitesi Mühendislik Fakültesi Fen ve Mühendislik Dergisi. 21 (61), 15-23. DOI:10.21205/deufmd.2019216102

European Commission, 2018. Best available techniques (BAT) reference document for the management of waste from extractive industries, pp. 195.

Fall, M., Adrien, D., Célestin, J.C., Pokharel, M., Touré, M. 2009. Saturated hydraulic conductivity of cemented paste backfill. Minerals Engineering. 22 (15), 1307-1317. https://doi.org/10.1016/j.mineng.2009.08.002

Gwenzi, W., Mupatsi, N.M. 2016. Evaluation of heavy metal leaching from coal ash-versus conventional concrete monoliths and debris. Waste Management. 49, 114-123. https://doi.org/10.1016/j.wasman.2015.12.029

Hakkou, R., Benzaazoua, M., Bussiere, B. 2008. Acid mine drainage at the abandoned Kettara mine (Morocco): 2. Mine waste geochemical behavior. Mine Water and the Environment. 27 (3), 160-170. https://doi.org/10.1007/s10230-008-0035-7

Hamberg, R., Maurice, C., Alakangas, L. 2015. The use of low binder proportions in cemented paste backfill–effects on As-leaching. Minerals Engineering. 78, 74-82. https://doi.org/10.1016/j.mineng.2015.04.017

Hamberg, R., Maurice, C., Alakangas, L. 2017. Lowering the water saturation level in cemented paste backfill mixtures–effect on the release of arsenic. Minerals Engineering. 112, 84-91. https://doi.org/10.1016/j.mineng.2017.05.005

Hamberg, R., Maurice, C., Alakangas, L. 2018. The formation of unsaturated zones within cemented paste backfill mixtures—effects on the release of copper, nickel, and zinc. Environmental Science and Pollution Research. 25 (21), 20809-20822. https://doi.org/10.1007/s11356-018-2222-9

Jiang, H., Fall, M., Yilmaz, E., Yang, L., Ren, L. 2020. Effect of mineral admixtures on flow properties of fresh cemented paste backfill: Assessment of time dependency and thixotropy. Powder Technology. 372, 258-266. https://doi.org/10.1016/j.powtec.2020.06.009

Jiao, H. Z., Wu, A.X., Wang, H.J., Yang, S.K., Li, R., Xiao, Y.T. 2011. The influence of cemented paste backfill on groundwater quality. Procedia Earth and Planetary Science. 2, 183-188. https://doi.org/10.1016/j.proeps.2011.09.030

Jones, S.N., Cetin, B. 2017. Evaluation of waste materials for acid mine drainage remediation. Fuel. 188, 294-309. https://doi.org/10.1016/j.fuel.2016.10.018

Koohestani, B., Darban, A.K., Mokhtari, P., Darezereshki, E., Yilmaz, E., Yilmaz, E. 2020. Influence of hydrofluoric acid leaching and roasting on mineralogical phase transformation of pyrite in sulfidic mine tailings. Minerals. 10(6), 513. https://doi.org/10.3390/min10060513

Liu, H., Zhang, J., Li, B., Zhou, N., Xiao, X., Li, M., Zhu, C. 2020. Environmental behavior of construction and demolition waste as recycled aggregates for backfilling in mines: leaching toxicity and surface subsidence studies. Journal of Hazardous Materials. 389, 121870. https://doi.org/10.1016/j.jhazmat.2019.121870

MEND, 2006. MEND Report 10.2 – Paste backfill geochemistry – Environmental effects of leaching and weathering, Mine Environment Neutral Drainage (MEND) Program, April 2006, Canada.

Pokharel, M., Fall, M. 2013. Combined influence of sulphate and temperature on the saturated hydraulic conductivity of hardened cemented paste backfill. Cement and Concrete Composites. 38, 21-28. https://doi.org/10.1016/j.cemconcomp.2013.03.015

Potgieter-Vermaak, S.S., Potgieter, J.H., Monama, P., Van Grieken, R. 2006. Comparison of limestone, dolomite and fly ash as pre-treatment agents for acid mine drainage. Minerals Engineering. 19(5), 454-462. https://doi.org/10.1016/j.mineng.2005.07.009

Salzsauler, K.A., Sidenko, N.V., Sherriff, B.L. 2005. Arsenic mobility in alteration products of sulfide-rich, arsenopyrite-bearing mine wastes, Snow Lake, Manitoba, Canada. Applied Geochemistry. 20 (12), 2303-2314. https://doi.org/10.1016/j.apgeochem.2005.06.007

Schafer, W. 2016. Geochemical evaluation of cemented paste tailings in a flooded underground mine. Annual Meeting of the International-Mine-Water-Association (IMWA), July, Germany, 11-15.

Seipel, K.S., Sheumaker, D.L., Kirk, L.B. 2017. Kinetic tests of non-amended and cemented paste tailings geochemistry in subaqueous and subaerial settings. 13th International Mine Water Association Congress, June, Lappeenranta, 830-835.

Sobek, A.A., Schuller, W.A., Freeman, J.R., Smith, R.M. 1978. Field and laboratory methods applicable to overburdens and minesoils, EPA-600/2-78-054, Cincinnati, Ohio: U.S. Environmental Protection Agency, p. 203.

Sracek, O., Mihaljevič, M., Kříbek, B., Majer, V., Filip, J., Vaněk, A., Penížek, V., Ettler, V., Mapani, B. 2014. Geochemistry of mine tailings and behavior of arsenic at Kombat, northeastern Namibia. Environmental Monitoring and Assessment. 186 (8), 4891-4903. https://doi.org/10.1007/s10661-014-3746-1

Taha, Y., Benarchid, Y., Benzaazoua, M. 2019. Environmental behavior of waste rocks based concrete: Leaching performance assessment. Resources Policy. 101419. https://doi.org/10.1016/j.resourpol.2019.101419

US-EPA 1315-1, 2013. Mass transfer rates of constituents in monolithic or compacted granular materials using a semi-dynamic tank leaching procedure. Test methods for evaluating solid waste, physical/chemical methods. Office of Wastewater Management, Washington DC.

WHO (World Health Organization), 2011. Guidelines for drinking water quality. WHO Chron 4,104.

Yan, B., Yilmaz, E. 2020. Analytical solution for stress distribution in cementitious backfills considering stope inclinations. Recep Tayyip Erdogan University Journal of Science and Engineering,1 (2), 26-33.

Yang, Y., Zhao, T., Jiao, H., Wang, Y., Li, H. 2020. Potential effect of porosity evolution of cemented paste backfill on selective solidification of heavy metal ions. International Journal of Environmental Research and Public Health. 17 (3), 814. https://doi.org/10.3390/ijerph17030814

Yılmaz, T., Ercikdi, B., Deveci, H. 2018. Utilisation of construction and demolition waste as cemented paste backfill material for underground mine openings. Journal of Environmental Management. 222, 250-259. https://doi.org/10.1016/j.jenvman.2018.05.075

Yılmaz, T., Ercikdi, B., Cihangir, F. 2020. Evaluation of the neutralization performances of the industrial waste products (IWPs) in sulphide-rich environment of cemented paste backfill. Journal of Environmental Management. 258, 110037. https://doi.org/10.1016/j.jenvman.2019.110037

Yılmaz, T., Ercikdi, B., Deveci, H. 2021. Evaluation of geochemical behaviour of flooded cemented paste backfill of sulphide-rich tailings by dynamic-tank leaching test. International Journal of Mining, Reclamation and Environment. 35(5), 336-355. https://doi.org/10.1080/17480930.2020.1829778

Yılmaz, T., Ercikdi, B. 2021. Effect of construction and demolition waste on the long-term geo-environmental behaviour of cemented paste backfill. International Journal of Environmental Science and Technology. 1-14. https://doi.org/10.1007/s13762-021-03359-2

Yilmaz, E., Fall, M. 2017 Introduction to paste tailings management. Yilmaz, E. Fall, M. (Eds). Paste Tailings Management. Springer International Publishing. Cham, 1-5. https://doi.org/10.1007/978-3-319-39682-8

Yilmaz, E., Yilmaz, E. 2018. Sustainability and tailings management in the mining industry: paste technology. Mugla Journal of Science and Technology, 4 (1), 16-26. https://doi.org/10.22531/muglajsci.383095

Yumlu, M. 2001. Backfill Practices at Cayeli Mine. Proceedings of the International Mining Conference, 19-22 June, Ankara, Turkey, 333–339.

Yumlu, M. 2020. The general framework and international applications regarding the paste backfill method. Workshop on the evaluation of paste backfill support system in terms of technical, environmental and legislation, Turkey Miner Association, 26 August, Ankara, Turkey (In Turkish).

Zheng, J., Zhu, Y., Zhao, Z. 2016. Utilization of limestone powder and water-reducing admixture in cemented paste backfill of coarse copper mine tailings. Construction and Building Materials. 124, 31-36. https://doi.org/10.1016/j.conbuildmat.2016.07.055

Madencilik - Mining, 2022, 61(1), 41-48

BİLİMSEL MADENCİLİK DERGİSİ
SCIENTIFIC MINING JOURNAL
TMMOB Maden Mühendisleri Odası Yayını / The Publication of the Chamber of Mining Engineers of Turkey

www.mining.org.tr

Original Research / Orijinal Araştırma

Quantifying the effect of the grinding aids in a batch stirred mill by a modelling approach

Modelleme yaklaşımıyla kesikli karıştırmalı bir değirmende öğütme yardımcılarının etkisinin ölçülmesi

Kemal Bilir[a,*]

[a] *Eskişehir Osmangazi Üniversitesi, Maden Mühendisliği Bölümü, Eskişehir, Türkiye*

Geliş-Received: 8 Ekim-October 2021 • Kabul-Accepted: 10 Kasım-November 2021

A B S T R A C T

Grinding aids are commonly used in dry grinding to disperse the material in the system effectively and to improve grinding performance. Most of the time, different grinding aids with varying dosages are tested in laboratory conditions by trial and error. A simple methodology is required to compare the results of different grinding aids and dosages in batch milling. In this study, the utilization of the modelling approach in comparing the effect of grinding aid types and dosages were aimed. In order to achieve this, an experimental program has been conducted using a laboratory-scale batch stirred ball mill. The empirical model developed using the Farazdaghi-Harris model offers a new approach to determine the effect of grinding aids on grinding performance.

Keywords: Stirred ball mill, Fine grinding, Grinding aids, Modelling, Farazdaghi-Harris model

Introduction

Efficient fine grinding becomes increasingly essential due to the increasing industrial demand for finely ground products. This demand has led to the development of the new fine grinding mills, i.e., stirred ball mills (Valery and Jankoviç, 2002). Stirred ball mills provide higher energy efficiency compared to conventional ball mills in fine and ultrafine grinding operations due to their operational characteristics and particle breakage mechanisms. The energy efficiency of the stirred mills is mainly ensured with the use of smaller grinding media that is mixed at high stirrer speeds and operated at high filling ratios. It can also produce fine-grained products with narrow particle size distributions after the grinding process by stirred mills (Gao and Forssberg, 1995, Zheng et al., 1996, Kwade and Schwedes, 1997, Kwade, 1999). In recent years, stirred ball mills are widely used for fine and ultrafine grinding processing in the ceramics, chemical, food, cement, paint, pharmaceutical, plastics and cosmetic industries (Jankovic et al., 2004, Altun et al., 2013, Ouattara and Frances, 2014, Toprak et al., 2014, Gokcen et al., 2015). Demand for stirred ball mills is increasing because of their ease of use, simple construction, high size reduction ratio, low energy consumption compared to other fine grinding machines and its suitability for modelling studies (Gao and Forssberg, 1995, Zheng et al., 1996).

Various mathematical models have been developed, aiming to identify events occurring in the mill to assist in the design and optimization of the ball mill operations. The developed models also aim to describe the events occurring in the stirred ball mills. These mathematical models can be used to estimate product size, mill performance, and process simulation as well (Ferrara et al., 1987, Gao and Forssberg, 1995).

Empirical modelling is one of the most widely used analytical methods to produce practical solutions in engineering and industrial studies and is extremely rich in terms of problem-solving

* Corresponding author / Sorumlu yazar: kbilir@ogu.edu.tr • https://orcid.org/0000-0002-6747-6666

https://doi.org/10.30797/madencilik.1006284

potential. The empirical approach combines measurable process variables, energy use and product size so that it can be used to estimate a single size such as p_{80}, 50 etc. or size distribution of a mill discharge (Mannheim, 2007). Empirical models are generally developed using experimental data for a specific mill application.

The empirical model developed in this study presents a new approach for modelling the vertical stirred ball mill by employing the Farazdaghi-Harris model to determine the effect of grinding aids on grinding performance.

Grinding aids (GAs) are generally organic compounds added to the mill during the grinding, and their principal purposes are to reduce the energy consumed in grinding and increase the efficiency of the mill. During the grinding process, fine particles produced may agglomerate. The particles that agglomerated reduce the fluidity of the material to be ground. Furthermore, the cushioning effect caused by the coating of the grinding medium and the liner with fine particles reduces the dry grinding efficiency (Wang and Forssberg, 1995). Grinding aids commonly used in dry milling significantly increase milling efficiency by preventing particle agglomeration, effectively dispersing particles, and improving material fluidity (Paramasivam and Vedaraman, 1992, Fuerstenau, 1995, Altun et al., 2015, Prziwara et al., 2018, Toprak et al., 2018). In addition, they also increase grain liberation by promoting breakage along grain boundaries. They are added to the mill during the grinding in proportions calculated depending on the material weight to reduce particle agglomeration. Grinding aids promote crack propagation when they enter the existing crack in the particle, causing the particle to break more easily (Choi et al., 2009). GAs are generally organic compounds that contain glycols and amines. They are categorized into three groups based on their structure: aliphatic amines-base, glycols-base and phenol-base. The high polarity of their chemical functioning groups reduces the surface energy forces, which cause agglomeration of the newly produced particles (Jeknavorian et al., 1998, Hashem et al., 2019)

Most of the time, different grinding aids with varying dosages are tested in laboratory conditions by trial and error. A simple methodology is required to compare the results of different grinding aids and dosages in batch milling. In this study, the utilization of the modelling approach in comparing the effect of grinding aid types and dosages was aimed. For this purpose, an experimental program was carried out using a stirred ball mill.

1. Material and methods

1.1. Material

Potassium feldspar, which was used as the test material in grinding experiments, was supplied by Kütahya Porcelain Company. After density analyses, the mean density of the test material was calculated as 2.65 g/cm^3. The particle size distributions of the feed and ground products were characterized using Malvern Mastersizer 2000 Particle Size Analyzer. The average values of three measurements were used for evaluating the experimental results.

1.2. Method

The HD-01 model laboratory scale vertical stirred ball mill, used in both dry and wet milling modes, was developed by Union Process (USA) (Figure 1). This model ball mill is designed for using at stirring speeds ranging from 100 to 600 rpm. The HD-01 model ball mills use alumina balls in diameters ranging from 3 to 6 mm as grinding media. The typical feed size is less than 100 microns. The HD-01 series mills have water-cooled jackets for cooling (or heating) the grinding tank. The grinding system has a data acquisition software developed by the manufacturer company. The software monitors the parameters used in the experiments and records the observed experimental data in an Excel worksheet for future references.

Figure 1. *The Model HD-01 stirred ball mill used in the experiments*

The grinding system consists of a grinding chamber and a centrally positioned rotating stirrer. A constant gap of 6.35 mm was left between the bottom end of the centrally positioned stirrer and the bottom of the tank. The material to be ground is placed in the tank with the grinding media and then is stirred by the shaft rotating at high speed. When the stirrer starts to rotate, the experimental parameters begin to be recorded with online data acquisition software. The high-speed stirring process causes the grinding media to exert both shearing and impact forces on the material. The ultimate result of the grinding process is an extremely fine-grained product with narrow particle size distributions, measured in micron or micron fractions. It is also possible to add chemicals or additives to the mill at any time during milling or to take samples from the mill.

Table 1 shows the technical specifications of the stirred ball mill used in the grinding experiments.

Table 1. *Technical data of the stirring ball mill*

Mill Diameter, mm	80
Mill length, mm	120
The volume of the mill, cm^3	592
The total weight of the ball, g	997.4
The diameters of alumina balls used as grinding media, mm	3 and 5
The fraction of mill volume filled by the ball bed at rest (J)	0.72
The fraction of mill volume filled by powder bed (f_c)	0.216
The fraction of the spaces between the balls at rest which is filled with powder (U)	0.75
Sample weight, g	203.3

2. Results and discussions

2.1. Grinding tests

The tests were initially conducted in conditions where no grinding aids were used. As a result of breaking the ionic bonds of the material due to a mechanical process, quite reactive positive and negative charges are created on the newly broken surfaces (Assaad et al., 2009). These charges enable the particles to agglomerate. As a result, these particles adhere to the mill surface and balls more easily. Following that, the tests were carried out at various dosages with two different types of grinding aids. Grinding aids can be classified into three types based on their structure: aliphatic amine-based, glycols-based and phenol-based (Hashem et al., 2019) The amine group Triethanolamine (TEA) and glycol group Ethylene glycol (EG) are used in this study (as given in Table 2).

Ethylene glycol is absorbed by the particles and the mill surface via hydroxyl groups, which neutralizes this electrostatic surface charge. Furthermore, the alkyl part of EG shields the surface charge of the particles, reducing adhesive forces and preventing powder aggregation and coating. This effect increases the mill's ability to produce finer particles. The increase in grinding index values caused by increasing EG dosage could be attributed to the solid surface's monolayer coverage. Unlike ethylene glycol, triethanolamine causes the formation of multimolecular layers on rigid surfaces, chiefly when used in high doses. The absence of any change in the grinding index values indicates the presence of this formation. Grinding aids, which tend to form multimolecular layers, should be used with caution as they can create capillary forces that favor agglomeration (Hashem et al., 2019).

The kinetic test program was implemented to observe the effect of grinding aids at different grinding times. Therefore, at each grinding aid dosages, the grinding was carried out for 30, 60, 90, and 120 minutes.

Table 2. *Test conditions at different grinding aid dosages*

Dosage (g/t)	TEA	EG
0	x	
1000	x	x
2000	x	x
4000	x	x

The size distributions of ground products with TEA and EG are presented in Figures 2 and 3, respectively. Size distribution data were utilized in the mathematical modelling of the mill.

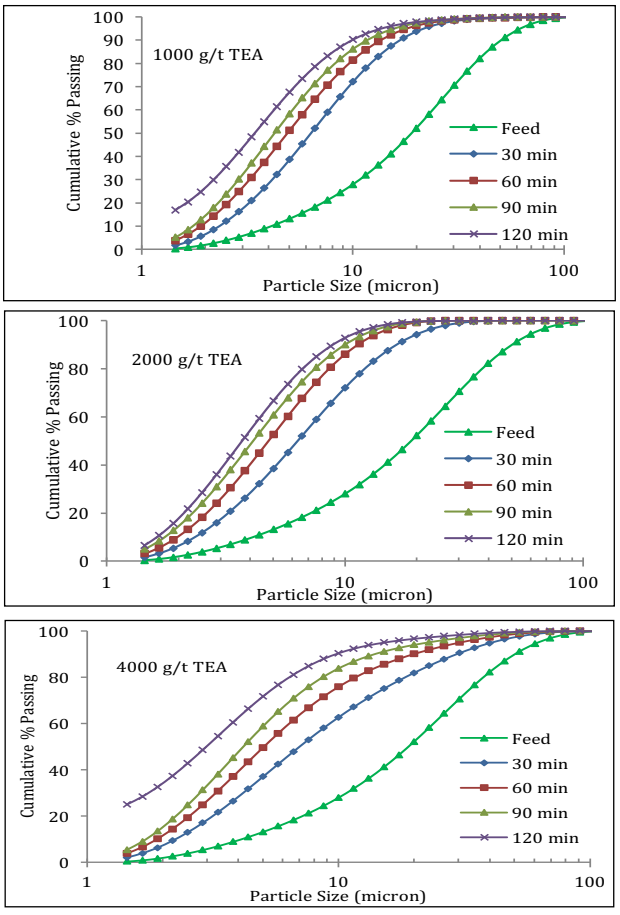

Figure 2. *Particle size distribution data with TEA grinding*

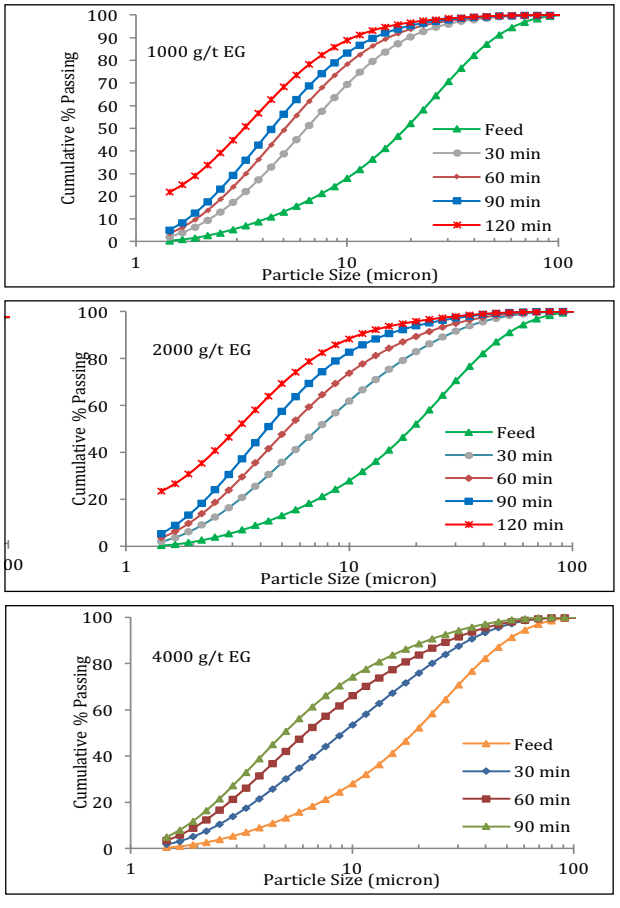

Figure 3. *Particle size distribution data with EG grinding*

2.2. Mathematical Modelling of Batch Stirred Milling

The size reduction in a comminution system is achieved by breaking the particles into smaller fragments. Reduction ratio in each size class is given by (Pi/Fi) and defined as the cumulative disappearance rate factor (Size vs ln(Pi/Fi)) and this behaviour can be mathematically expressed which can be used for modelling. The data obtained from the batch grinding tests performed without using grinding aids are used for modelling purposes. In order to figure out the disappearance rate of particles in each grinding test, the cumulative ratio change of the feed and product for each size fraction was sketched by size (Figure 4). Especially at coarser size ranges, the ratio was almost indicated similar behaviour for varying grinding times. The major difference was in the fine particle sizes as it could be expected.

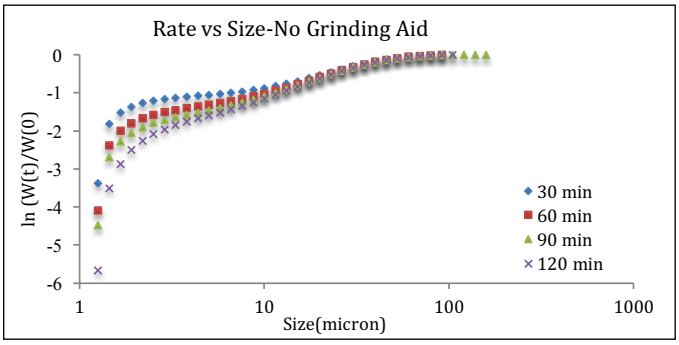

Figure 4. *Particle disappearance rate when no grinding aid was used*

The mathematical model of the batch grinding process is defined by deriving the mathematical expression for particle size versus the cumulative disappearance rate factor $\ln(W_i(t)/W_i(0))$. Farazdaghi-Harris approach (Eq.1) gave the best mathematical expression in terms of the data fitting (Farazdaghi and Harris, 1968).

$$y(x) = \sum_{i=0}^{N-1} \frac{1}{a_i + b_i x^{c_i}} \quad (1)$$

By using nonlinear Marquardt-Levenberg optimization technique or algorithm, the model parameters could be back-calculated (Marquardt, 1963). The model parameters *a, b* and *c* are constants, which reflect the grinding conditions and material properties. Specifically, b is related to the mill operating parameters such as ball size, tip speed and stirrer type and c is related to material properties. Parameter a is reflecting the mill rheology which is the grinding time (depending on fines generation), grinding aid type and dosage.

Model fitting studies have been conducted for each grinding time. As can be seen from the graphs given in Figure 5, there is a good agreement between the fitted and experimental results indicating that model structure represents the behaviour accurately.

For each data series, as mill operating conditions and the material are kept constant the calculated values of the Parameters b and c as constant numbers are -8.07E-04 and 2.362, respectively. The effect of grinding time is reflected in the Parameter *a*, which is presented in Figure 6. The change of Parameter a by grinding time indicates that as the grinding time increases, the increase in Parameter a reduces significantly. This behaviour is interpreted as the slowing down effect of grinding by time. As a result, the kinetic behaviour of the grinding action can be reflected on a single parameter while the other parameters are kept constant. These parameters are thought to be the controlling parameters for the grinding system and material properties. As the tests are conducted at the same system with the same material, no change has been observed on the related parameters.

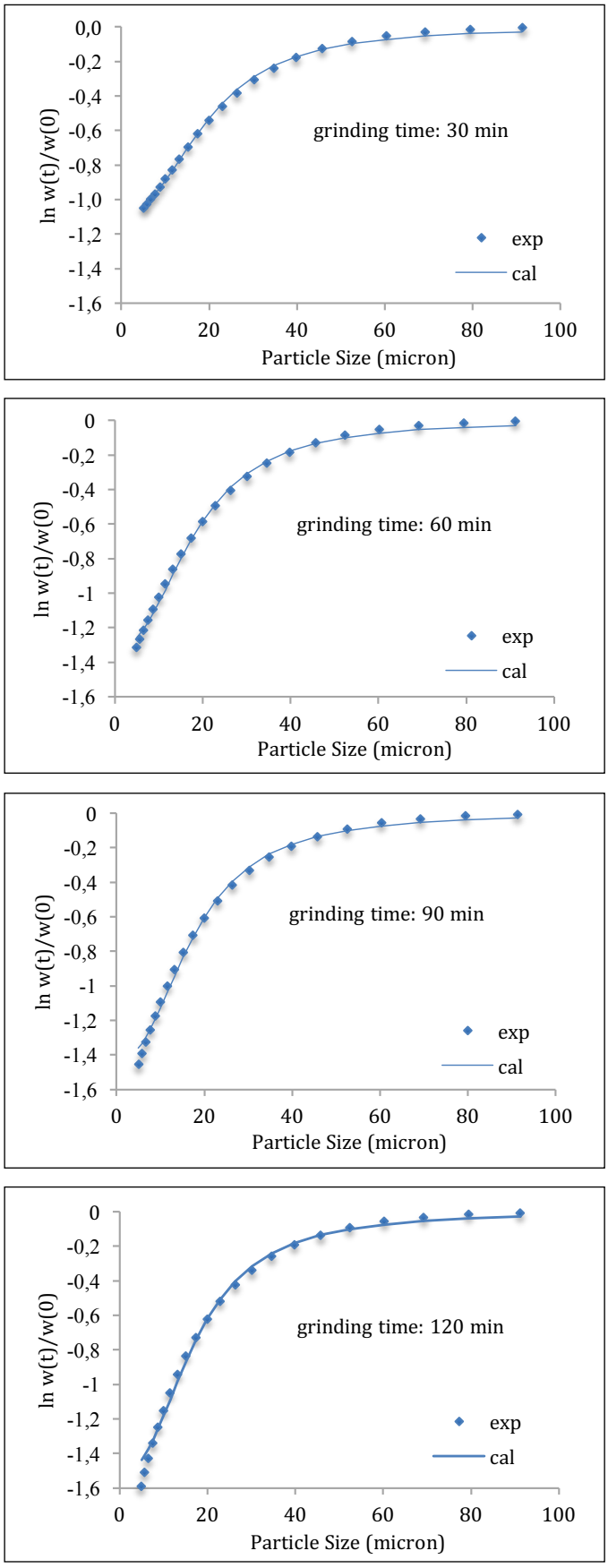

Figure 5. *Graphical representation of the fitted and experimental results for each grinding time*

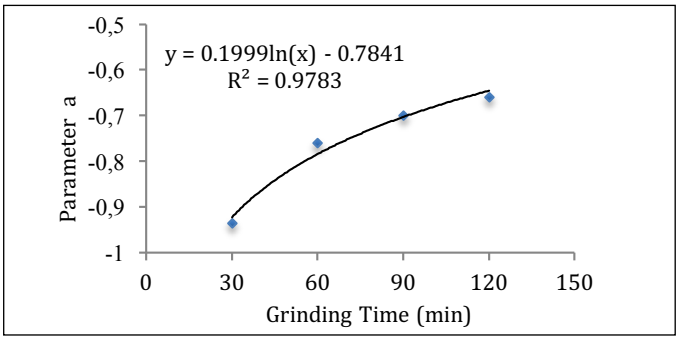

Figure 6. *Variation of "Parameter a" by time*

2.3. Comparing the grinding aid types and dosages during batch stirred milling

The structure of the model presented above can be used to provide a quantitative comparison of grinding aid types and dosages. The test results of TEA (Triethanolamine) and EG (ethylene glycol) have been analysed with the suggested model structure in order to prove this hypothesis.

The disappearance rate of material with varying dosages of TEA and EG at different grinding times are presented in Figure 7 and 8, respectively.

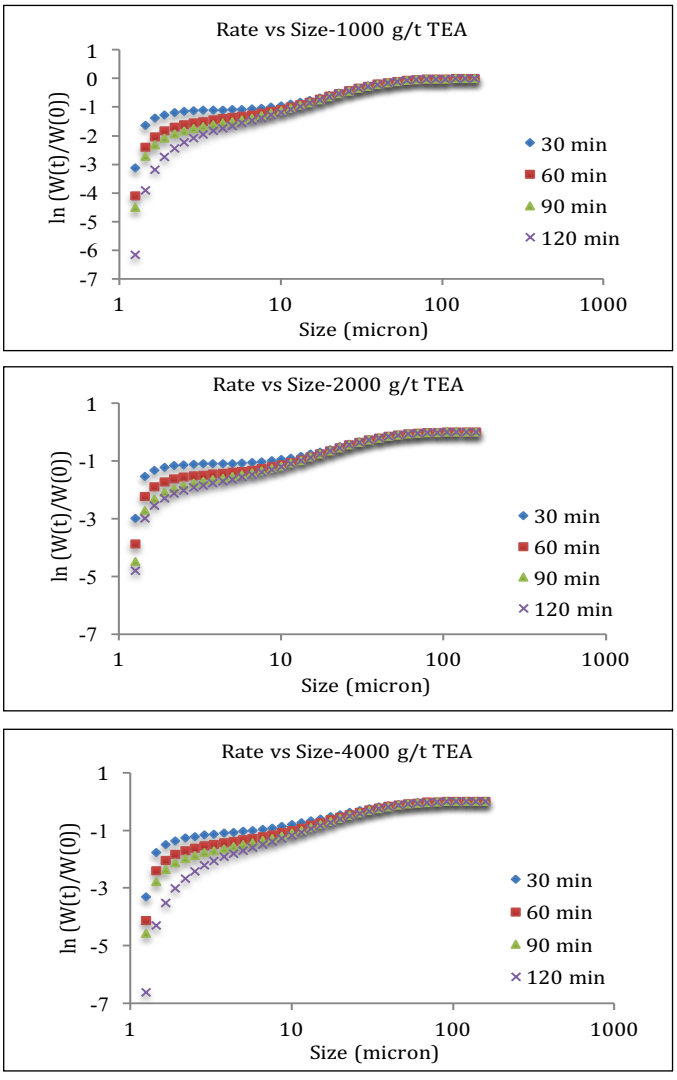

Figure 7. *Disappearance rate of material with TEA at varying dosages*

As can be seen from the graphs, a similar trend could be followed for varying grinding times, grinding aid types and dosages. In this experimental study the findings indicated that below 10 micron size the disappearance rate was increased. It is known that during grinding the ground particles may agglomerate, for that reason the dispersion effect of grinding aids on material is effective at very fine size ranges. Normally in a continuous milling operation this can be reflected on the discharge rate of the mill. But in a batch milling environment there is no transport from the mill. Therefore, at fixed milling operation conditions (ball size, ball load, tip speed) the dispersed fine particles can be ground more effectively. At shorter grinding times (in a batch grinding condition it is typically below 30 minutes), the higher the aid dosage, the more effective the grinding is. As the grinding times increase the fines generation increases but the increased grinding aid dosages does not improve the grinding efficiency. It can also be pointed out from the graphs for extended grinding time that the effect of grinding aid dosages on the grinding performance became stable.

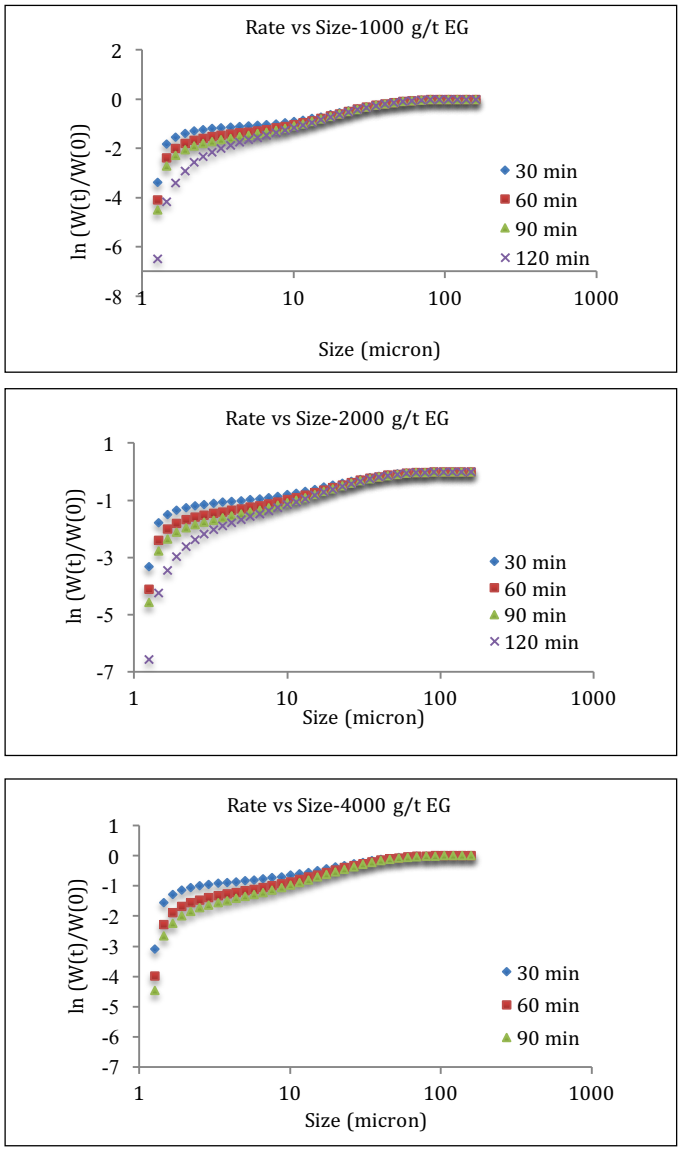

Figure 8. *Disappearance rate of material with EG at varying dosages*

The same model structure has been used in modelling studies for each grinding aid dosage. Model fitting studies addressed high accuracy in predictions as given in Figure 9. In order to simplify the illustrations only two sets of data from TEA and EG are presented as an example. In other test condition similar graphs have been obtained.

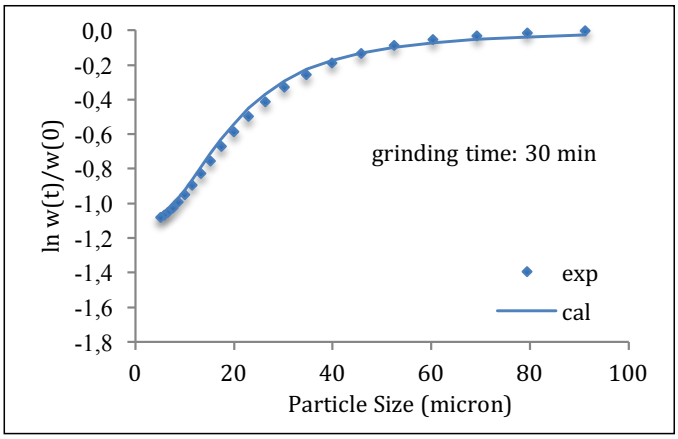

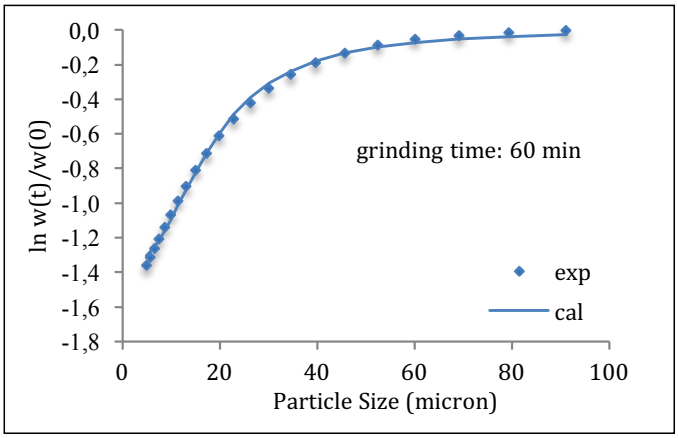

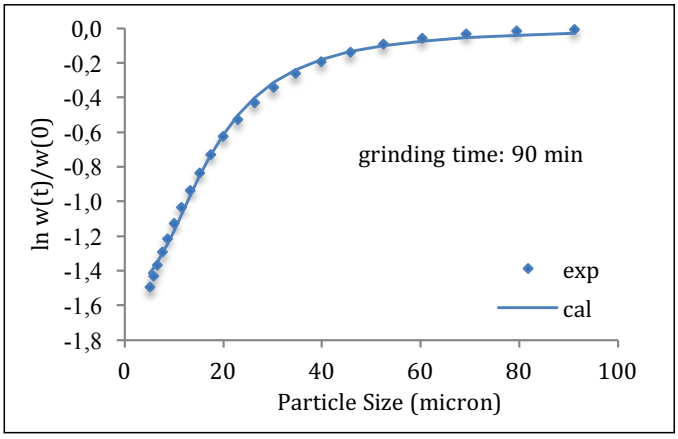

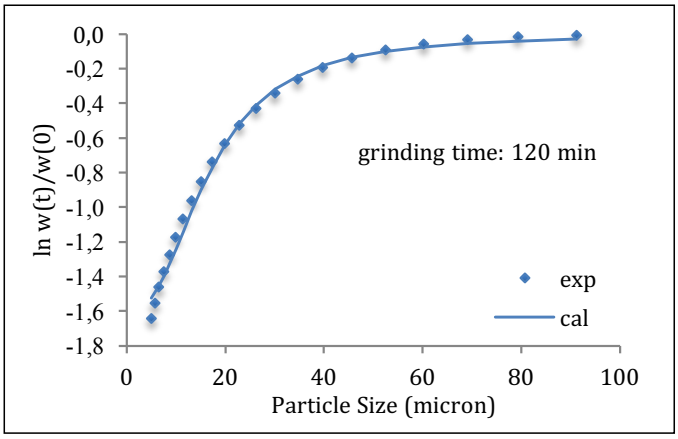

a: Results with TEA at 1000 ppm

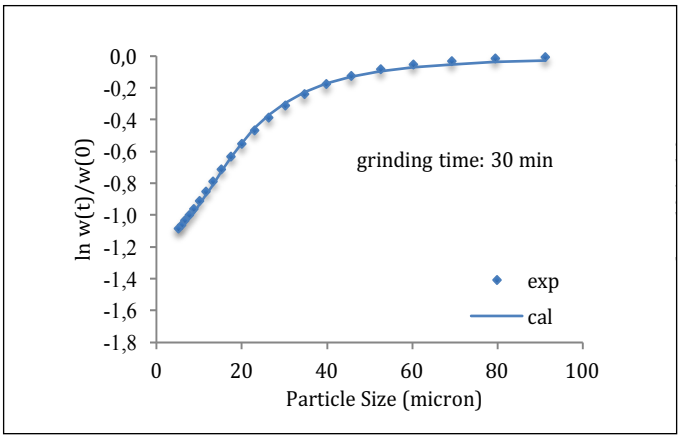

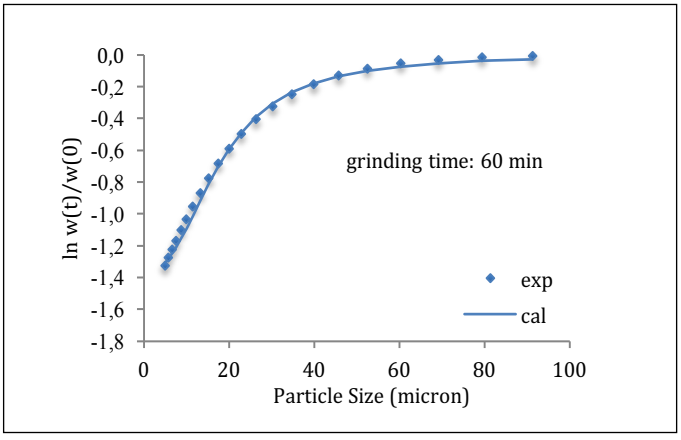

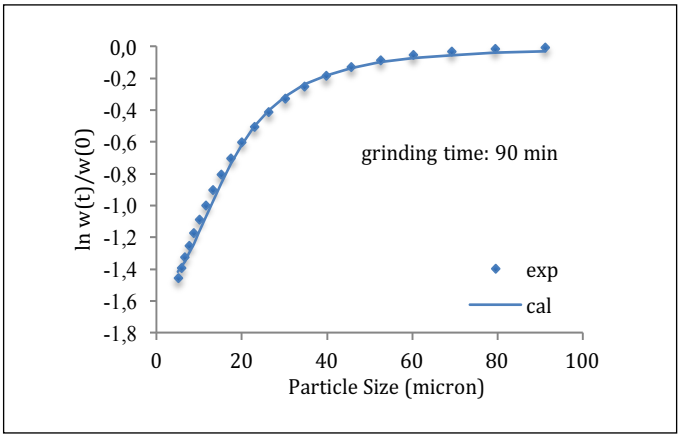

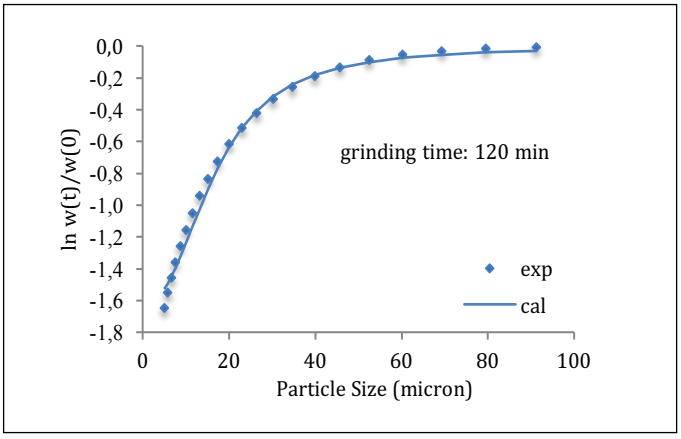

b: Results with EG at 1000 ppm

Figure 9. *Deviation of fitted data from experimental data set (a: TEA, b: EG*

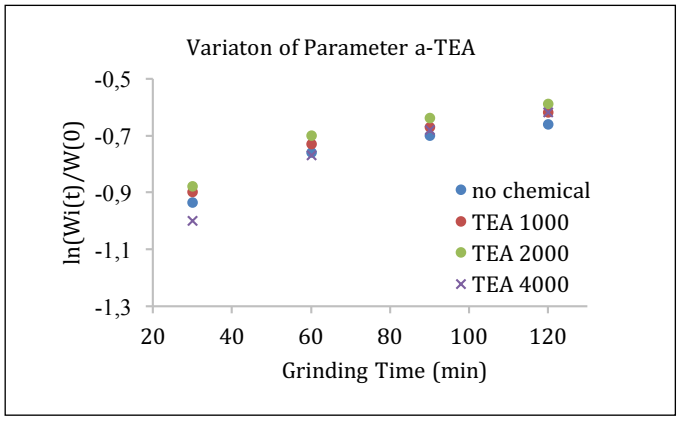

Figure 10. *Variation of Parameter a with TEA dosage*

During the calculations, as explained above the effect of different grinding aids and dosages could be reflected on the Parameter a. The effects of operational conditions on the model Parameter a were examined at different grinding times for TEA and EG at varying dosages, and the results are illustrated in Figures 10 and 11, respectively.

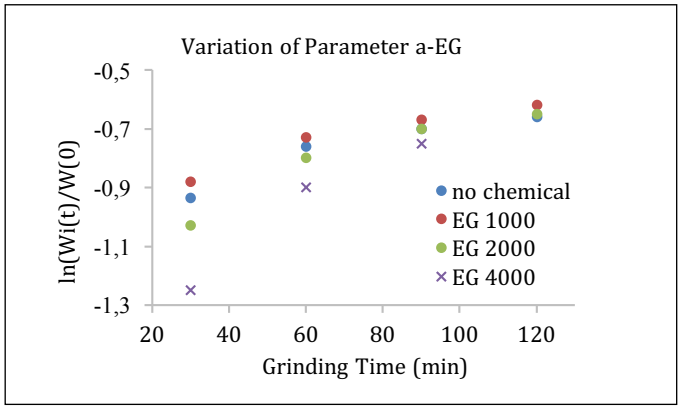

Figure 11. *Variation of Parameter a with EG dosage*

As can be followed from the graphs in Figures 10 and 11, the grinding rate seems to be slowing down as expected at increased grinding times. This can be explained as a cushioning effect or inefficient grinding in the existing conditions. In order to address the efficiency of grinding aid types, the comparison is given for different grinding aids at the very shortest and longest grind time of the tests. The data address that both TEA and EG are effective on grinding performance of potassium feldspar while the EG has created an adverse effect especially at higher dosages. The performance improvement of the grinding operation is quantified by calculating the A parameter. In this specific case, at higher dosages measured for TEA, the Parameter a varies 15 % compared to without grinding aid condition. A similar trend could be obtained for EG use as well. But as the grinding aid dosage reduces the improvement on grinding efficiency as reflected on Parameter a is limited to 8 % change (as a comparison to no grinding aid condition). However, high dosage use of EG indicates performance loss compared to the conditions without using grinding aids. This behaviour points out the critical concentration of grinding aids in the system and overdosing may end up in performance losses. This is related to the re-agglomeration behaviour of dispersed particles. Therefore, for each material type, grinding aid should be appropriately designed, and the dosage use has to be optimised by quantified test data. According to the test results, the modelling approach is useful to achieve this quantification process.

Conclusions

Batch vertical stirred mill can be modelled by relying on the rate disappearance factor by size. The Farazdaghi-Harris equation is well suited to express this situation mathematically.

The model parameters of the equation are thought to be representing the grinding conditions, the design of the system, and material properties. As the tests are conducted at the same system with the same material, no change has been observed on the related parameters. This allows reflecting the grind time and the effect of grinding aids on a single parameter (Parameter a).

Additionally, the grinding aid type is important for each material used. This phenomenon has been reported in many studies suggesting that GAs is solid-specific although there is no correlation of global surface chemical properties (such as functional groups, molar masses) with their effectiveness. From rheology studies, the observations can be attributed to the varying degree of flow properties such as flow index, bulk density, internal friction factor and shearing cohesion (Chipakwe et al., 2020). The specific formulation has to be implemented, and for each aid, an optimization study should be run for determining the best dosage conditions. Specifically, for comparative studies, the effect of the grinding aids and dosage can be quantified by calculating Parameter a by using the recommended model.

References

Altun, O., Benzer, H., Enderle, U. 2013. Effects of operating parameters on the efficiency of dry stirred milling. Minerals Engineering. 43-44, 58-66. doi: 10.1016/j.mineng.2012.08.003.

Altun, O., Benzer, H., Toprak, A., Enderle, U. 2015. Utilization of grinding aids in dry horizontal stirred milling. Powder technology. 286, 610-615. doi: 10.1016/j.powtec.2015.09.001.

Assaad, J. J., Asseily, S. E., Harb, J. 2009. Effect of specific energy consumption on fineness of portland cement incorporating amine or glycol-based grinding aids. Materials and structures. 42 (8), 1077-1087.

Chipakwe, V., Semsari, P., Karlkvist, T., Rosenkranz, J., Chelgani, S. C. 2020. A critical review on the mechanisms of chemical additives used in grinding and their effects on the downstream processes. Journal of Materials Research and Technology-Jmr&T. 9 (4), 8148-8162. doi: 10.1016/j.jmrt.2020.05.080.

Choi, H., Lee, W., Kim, S. 2009. Effect of grinding aids on the kinetics of fine grinding energy consumed of calcite powders by a stirred ball mill. Advanced Powder Technology. 20 (4), 350-354.

Farazdaghi, H., Harris, P. 1968. Plant competition and crop yield. Nature. 217(5125), 289.

Ferrara, G., Preti, U., Schena, G. 1987. Computer-aided use of a screening process model. APCOM 87. Proceeding of the Twentieth International Symposium on the Application of Computers and Mathematics in the Mineral Industries.

Fuerstenau, D. W. 1995. Grinding aids. KONA Powder and Particle Journal. 13, 5-18.

Gao, M. W., Forssberg, E. 1995. Prediction of product size distributions for a stirred ball mill. Powder technology. 84 (2), 101-106. doi: Doi 10.1016/0032-5910(95)02990-J.

Gokcen, H. S., Cayirli, S., Ucbas, Y., Kayaci, K. 2015. The effect of grinding aids on dry micro fine grinding of feldspar. International Journal of Mineral Processing. 136, 42-44. doi: 10.1016/j.minpro.2014.10.001.

Hashem, F., Hekal, E., Wahab, M. 2019. El The influence of Triethanol amine and ethylene glycol on the grindability, setting and hydration characteristics of Portland cement. Int. J. Petrochem. Sci. Eng. 4, 81-88.

Jankovic, A., Valery, W.,Davis, E. 2004. Cement grinding optimisation.

Minerals Engineering. 17(11-12), 1075-1081. doi: 10.1016/j.mineng.2004.06.031.

Jeknavorian, A. A., Barry, E. F., Serafin, F. 1998. Determination of grinding aids in Portland cement by pyrolysis gas chromatography mass spectrometry. Cement and Concrete Research. 28(9), 1335-1345. doi: Doi 10.1016/S0008-8846(98)00109-4.

Kwade, A. 1999. Wet comminution in stirred media mills - research and its practical application. Powder Technology. 105(1-3), 14-20. doi: 10.1016/S0032-5910(99)00113-8.

Kwade, A.,Schwedes, J. 1997. Wet comminution in stirred media mills. KONA Powder and Particle Journal. 15, 91-102.

Mannheim, V. 2007. Empirical modeling and determination of the grindability in stirred ball mills. Epitoanyag-Journal of Silicate Based and Composite Materials. 59 (2), 36-40.

Marquardt, D. W. 1963. An algorithm for least-squares estimation of nonlinear parameters. Journal of the Society for Industrial and Applied Mathematics. 11 (2), 431-441.

Ouattara, S., Frances, C. 2014. Grinding of calcite suspensions in a stirred media mill: Effect of operational parameters on the product quality and the specific energy. Powder Technology. 255, 89-97. doi: 10.1016/j.powtec.2013.11.025.

Paramasivam, R., Vedaraman, R. 1992. Effects of the physical-properties of liquid additives on dry grinding. Powder Technology. 70 (1), 43-50. doi: 10.1016/0032-5910(92)85052-W.

Prziwara, P., Breitung-Faes, S., Kwade, A. 2018. Impact of grinding aids on dry grinding performance, bulk properties and surface energy. Advanced Powder Technology. 29 (2), 416-425. doi: 10.1016/j.apt.2017.11.029.

Toprak, N. A., Altun, O., Benzer, A. H. 2018. The effects of grinding aids on modelling of air classification of cement. Construction and Building Materials. 160, 564-573. doi: 10.1016/j.conbuildmat.2017.11.088.

Toprak, N. A., Altun, O., Aydogan, N., Benzer, H. 2014. The influences and selection of grinding chemicals in cement grinding circuits. Construction and Building Materials. 68, 199-205. doi: 10.1016/j.conbuildmat.2014.06.079.

Valery, W., Jankovic, A. 2002. The future of comminution. Proceedings of 34th International Octobar Conference on Mining and Metalurgy. October.

Wang, Y.,Forssberg, E. 1995. Dispersants in stirred ball mill grinding. KONA Powder and Particle Journal. 13, 67-77.

Zheng, J., Harris, C. C., Somasundaran, P. 1996. A study on grinding and energy input in stirred media mills. Powder Technology. 86 (2), 171-178.<Go to ISI>://WOS:A1996TV87500005.

ISSN 2564-7024